ANALYSIS OF THE ENZYMES OLIGORIBONUCLEASE (ORN) AND RNA PYROPHOSPHOHYDROLASE (RPPH) IN ESCHERICHIA COLI K-12 RNA METABOLISM

by

NICHOLAS STACY WIESE

(Under the Direction of Sidney R. Kushner)

ABSTRACT

Degradation of mRNA and maturation of stable RNAs play vital roles in controlling gene expression at the post-transcriptional level. In *Escherichia coli* the enzymes RNA pyrophosphohydrolase (RppH) and oligoribonuclease (Orn) play unique roles in overall RNA metabolism by acting on disparate ends of RNA molecules. The work described in this dissertation further elucidates the functional and physiological role of these two enzymes.

We have analyzed the role of RppH in tRNA processing and show that the absence of RppH does not affect the processing of tRNAs by RNase E, contrary to long-held beliefs. We also show that RNase P processing is affected by RppH for a subset of tRNAs, and that this effect is mediated by the presence of the Rph-1 truncated protein.

We examined the role of RppH regulation on the entire transcriptome employing high-density tiling microarray analysis. We discovered that RppH is involved in regulating the entire flagellar gene regulatory network, and

hypermotility results in strains lacking RppH. As before however, we also observed that like RppH-dependent RNase P processing, hypermotility due to absence of RppH was dependent on the presence of the Rph-1 protein.

Lastly, we characterize how the absence of Orn affects cellular functions in *E. coli.* We constructed a full deletion of *orn* in a clean genetic background and controlled expression through tightly-regulated expression plasmids. Through numerous assays, we found that the absence of Orn alone does not cause a cessation in growth, but rather that cellular viability is dependent on the absence of either RNase T or PNPase in conjunction with Orn. These results are the first to implicate either RNase T or PNPase as a backup mechanism for oligoribonuclease activity. We also determined the true transcription start site of *orn*, and have identified the putative promoter sequence, contrary to what is currently annotated. These results suggest that *orn* regulation is more intricate than previously thought.

INDEX WORDS: RppH, Orn, RNase P, RNase T, Rph-1, mRNA decay, tRNA processing, nanoRNAs, *Escherichia coli*

# ANALYSIS OF THE ENZYMES OLIGORIBONUCLEASE (ORN) AND RNA PYROPHOSPHOHYDROLASE (RPPH) IN ESCHERICHIA COLI K-12 RNA METABOLISM

by

NICHOLAS STACY WIESE

B.S., University of Florida, 2006

A Dissertation Submitted to the Graduate Faculty of The University of Georgia in Partial Fulfillment of the Requirements for the Degree

DOCTOR OF PHILOSOPHY

ATHENS, GEORGIA

2015

# ANALYSIS OF THE ENZYMES OLIGORIBONUCLEASE (ORN) AND RNA PYROPHOSPHOHYDROLASE (RPPH) IN ESCHERICHIA COLI K-12 RNA METABOLISM

by

NICHOLAS STACY WIESE

| | |
|---|---|
| Major Professor: | Sidney R. Kushner |
| Committee: | Timothy Hoover |
| | Anna Glasgow Karls |
| | Robert Maier |

Electronic Version Approved:

Julie Coffield
Interim Dean of the Graduate School
The University of Georgia
May 2015

DEDICATION

To my parents, Jesper and Vicki Wiese, I would not be the man I am today without your love, guidance, and support. To my son, Alden, to show you anything is possible. To my wife, Laura, you are the (salted) butter to my bread, and breath to my life. I could not have made it out, without you.

ACKNOWLEDGEMENTS

My sincerest gratitude goes to Sidney R. Kushner, for providing me a home in his laboratory during my graduate studies. The knowledge, encouragement, humor, and great patience I received from him will be missed. It has been a pleasure to have Sidney as my graduate advisor, and I am grateful to have been lucky enough to work under his guidance.

I would also like to thank my committee members, who have provided constructive criticism and help direct my research. Special thanks are due to Bijoy Mohanty, for the expert advice and training. You taught me how to be a better scientist. To all members of the Kushner Lab, past and present, your commiseration, encouragement, camaraderie, and support through the past few years have been invaluable.

Most importantly, I would like to thank my entire family for their continuous support and encouragement. To my wife, Laura, your unwavering love and support made it possible for me to complete this work. To my son, Alden, you have been an endless source of joy and remind me on a daily basis that the most important part of life is not scientific. To Jim and Debbie, I could not have wished for better in-laws. To my parents, Jesper and Vicki, and brother, Kristoffer, you have always done everything in your power to make sure that I can achieve my dreams. Words have not been created to describe the amount of love I feel for all of you. I would not be here without any of you.

TABLE OF CONTENTS

Page

CHAPTER 1

# INTRODUCTION AND LITERATURE REVIEW

## INTRODUCTION

RNA degradation plays a vital role in overall RNA metabolism, by way of helping to control intracellular levels of certain RNA species such as messenger RNA (mRNA), transfer RNA (tRNA), and ribosomal RNA (rRNA). Especially for unstable RNA such as mRNA, decay plays an integral role in controlling expression of numerous genes by helping to control the steady-state level of transcripts (1), which can have half-lives ranging from 10 seconds to more than 30 minutes (2-4). Turnover of mRNA in the cell involves multiple pathways utilizing a series of ribonucleases (RNases) (1,5,6) that allow the cell to quickly adapt its metabolic and physiologic requirements to ever-changing environmental conditions (7).

Stable RNAs such as tRNA and rRNA are highly structured, exist for much longer periods of time, and are key components of the translational machinery inside the cell (6). These RNAs exist as larger precursor molecules that are functionally inactive and must be processed into their mature and functional forms. Examples of these include rRNAs and tRNAs within ribosomal RNA operons, tRNAs present in polycistronic transcripts, tRNAs associated with mRNA in multifunctional transcripts, and tRNAs encoded in monocistronic

transcripts (8,9). Initially, endonucleolytic cleavages yield smaller precursor molecules that undergo final processing through endonucleolytic and 3′→5′ exonucleolytic cleavages to yield 5S, 16S, and 23S rRNAs, as well as mature tRNAs (10,11).

Although many of the endoribonucleases have unique activities, there exists numerous functional overlaps among them regarding their roles in RNA metabolism. For instance, many of the endoribonucleases (RNase E, RNase P, RNase III, and RNase G) involved in maturation of the stable RNAs listed above also have a role in the degradation of mRNAs (12,13). Conversely, the exoribonucleases involved in mRNA degradation [polynucleotide phosphorylase (PNPase), RNase II, RNase R, and oligoribonuclease] (9,14) are distinct from those involved in stable RNA maturation (RNase D, RNase T, RNase BN, RNase PH) (15,16).

This reviews summarizes the notable features of ribonucleases and accessory proteins in *E. coli* involved in mRNA degradation, tRNA, and rRNA maturation, while highlighting the enzymes oligoribonuclease and RNA pyrophosphohydrolase because of their importance to the scope of this dissertation.

## RIBONUCLEASES

### Primary Endoribonucleases Involved in *E. coli* RNA Metabolism

As stated previously, endoribonucleases initiate the majority of processing of RNA transcripts by cleaving internal phosphodiester bonds by a hydrolytic

mechanism. The functional role and enzymatic features of the seven currently identified in *E. coli* are presented below.

## I. RIBONUCLEASE E (RNase E)

For many mRNAs, the initial step in their degradation is primarily believed to be cleavage by RNase E. RNase E, which is encoded by the *rne* gene, was first discovered by Apirion & Lassar (17) on the basis of a temperature sensitive mutant, and was subsequently shown to have a role in processing 9S rRNA into a 5S form (18). It has been shown that RNase E cleavage sites are A/U rich regions within mRNAs that contain little to no secondary structure (9,19). Although RNase E cleaves internally, binding has been shown to be 5′-end-dependent and requires at least four nucleotide single-stranded regions at the 5′ terminus of the mRNA transcript for efficient binding (12). Additionally, it is now known that RNase E has a significant preference for 5′-monophosphorylated ends over the typical 5′-triphosphorylated ends of primary transcripts (20).

More recent studies have concluded that RNase E is a major participant in the RNA turnover process, based on microarray and total-pulse labelled RNA analysis. Analysis of RNase E mutants revealed that mRNA decay was seriously deficient by impeding processing, as well as stabilization of bulk mRNA (21). However, even with a defective RNase E protein, cells were still able to turnover mRNAs, only at a much slower rate (1). These results suggest that other more specialized endonucleases such as RNase III, G, P, and Z may act in mRNA decay pathways even though RNase E is the major contributor to the

endonucleolytic initiation of mRNA decay (9,12).

## II. RIBONUCLEASE G (RNase G)

RNase G encoded by the *rng* gene, was originally identified as *cafA,* where overproduction caused the formation of cytoplasmic axion filaments among other morphological changes (22). CafA was later determined to have endoribonucleolytic activity and was later renamed RNase G (*cafA* to *rng*) (23,24). RNase G is 489 amino acids in length, with a predicted molecular mass of 55 kDa. Dimerization of the protein is required for full activity of RNase G (25). RNase G is primarily responsible for maturation of the 5′ terminus of 16S rRNA in *E. coli* (23,24), and to a lesser degree, 6S RNA (26), some tRNAs (27,28), and specific mRNA transcripts (29).

The RNase G protein is a paralogue to RNase E, sharing 34% sequence identity and 50% sequence similarity to the 470 amino acids near the N-terminal end of the RNase E protein (30,31). Unlike RNase E, RNase G is considered nonessential (23), and is found at levels 3% to that of RNase E (32). Despite its native low levels, when significantly overproduced in an *rne* mutant RNase G can partially complement the mutation (33), and more recently an *rng-219* allele has been shown to substitute for RNase E at normal levels (34).

## III. RIBONUCLEASE III (RNase III)

RNase III, encoded by the *rnc* gene, was first discovered in 1967 by Robertson et al. (35,36). It is unique from all other endoribonucleases in *E. coli* due to its

ability to cleave double-stranded RNA molecules (36,37), with a requirement of a dsRNA region of 15–20 base pairs (38). The RNase III protein is 226 amino acids in length with a molecular mass of 25.6 kDa and is active *in vivo* as a 50 kDa homodimer (39,40).

RNase III is primarily involved in the maturation of rRNAs. It cleaves the double-stranded regions bracketing both 16S and 23S rRNAs within the primary 30S transcript to produce shorter transcript intermediates that can be further processed into the mature 16s and 23s rRNAs (41,42). These cleavages generate a 2-nucleotide overhang on the 3′-end, with a 5′-monophosphate and 3′-hydroxyl terminus (43). Inactivation of RNase III results in atypical processing that yields incompletely processed 23S rRNA, however these species are still fully functional (41).

RNase III also participates in maturation of some tRNAs (38) as well as in mRNA decay (8). RNase III has been shown to be directly involved in controlling expression of itself and PNPase at the transcriptional level (44,45). Recent tiling microarrays have shown that approximately 12% of genes in *E. coli* were affected in an RNase III deletion strain, and the half-lives of total pulse-labeled RNA were not significantly affected in an RNase III deletion, indicating that RNase III plays a minor role in the mRNA decay pathway (46,47).

**IV. RIBONUCLEASE P (RNase P)**

RNase P, an essential endoribonuclease, was initially discovered upon investigation of tRNA maturation enzymes in extracts of *E. coli* (48). RNase P is

unique among the other endoribonucleases in *E. coli* in that it is made up of two components, a catalytic RNA subunit 377 nucleotides in length, known as the M1 RNA, encoded by the *rnpB* gene (49-51); and a protein component with a molecular mass of 13.8 kDa, known as C5, encoded by the *rnpA* gene (51,52). Previous research has shown that the M1 RNA can process tRNA precursors in the absence of the C5 protein, but the presence of the C5 protein greatly increases the efficiency of cleavage and is required for RNase P activity and cell viability *in vivo* (53,54).

RNase P is responsible for hydrolytically cleaving the 5′-leader sequences from tRNA precursors to produce the mature 5′-termini, which is essential for generating functional tRNAs (55,56). The enzyme is also involved in maturation of a number of other RNAs including the 5′-end of 4.5S RNA (57), tmRNA (58), small RNAs, tRNAs (27,28,59,60), as well as processing polycistronic mRNA transcripts (61). A global survey of RNase P activity identified cleavage sites within the intercistronic regions of numerous polycistronic operons, indicating that RNase P does play a small role in mRNA turnover (61).

**V. RIBONUCLEASE Z/BN (RNase Z/BN)**

RNase Z, encoded by the *rnz*/*elaC* gene in *E. coli*, is essential for the maturation of the 3′-end of tRNA precursors that lack the encoded –CCA determinant in eukaryotic organisms and some prokaryotes (62,63). RNase Z homologs are conserved in eukaryotes, archaea, and close to half of all sequenced bacterial

genomes (64). However, since all 86 tRNAs in *E. coli* contain chromosomally encoded CCA, the function of RNase Z in *E. coli* was not initially clear (65). More recent studies have proven that this enzyme is involved in mRNA decay. For example, it endonucleolytically cleaves the *rpsT* transcript at distinct sites but has no measureable activity on *E. coli* tRNA precursors (66).

A debate has existed as to whether or not RNase BN and RNase Z were the same enzyme. Ezraty et al. (65) claimed the *E. coli elaC* gene encodes RNase BN, an enzyme believed to be a 3′→5′ exoribonuclease (65). They reported however, that only limited exonucleotylic activity could be observed in conditions of high $Co^{2+}$ concentrations (0.2 mM) and microgram levels of protein, neither of which are biologically representative (65). In contrast to their data, Perwez et al. (66) reported that under ideal RNase BN activity conditions, RNase Z endonucleolytic activity was completely abolished (66). These results show that under native physiological conditions the enzyme functions as an endoribonuclease in mRNA degradation and therefore should be known as RNase Z.

## VI. RIBONUCLEASE LS (RNase LS)

RNase LS is encoded by the *rnlA* gene and is primarily involved in antagonism of bacteriophage T4 in *E. coli* and to a lesser degree mRNA decay (67-69). RNase LS mutants have been shown decrease the decay rate of the genes *rpsO* and *bla* when compared to a wild-type control (68). Additionally, RNase LS has been suggested to be involved in the degradation of stable RNA, specifically a

portion of 23S rRNA (68).

## VII. RIBONUCLEASE I (RNase I)

RNase I was the first endoribonuclease in *E. coli* to be identified. It is encoded by the *rna* gene, is a protein of 245 amino acids, and has a predicted molecular mass of 27.2 kDa (70,71). RNase I is nonspecific in action, generating a cyclic 2′,3′-nucleotide that is ultimately converted to a 3′-phosphate (72). Studies have reported that RNase I may be involved in stable RNA degradation under certain stress conditions (73,74).

## Exoribonucleases Involved in *E. coli* RNA Metabolism

Currently, 8 exoribonucleases have been discovered and characterized in *E. coli*. These exoribonucleases work exclusively in the 3′→5′ direction, cleaving one nucleotide at a time and are generally highly processive. To date, no exoribonucleases identified in *E. coli* act in the 5′→3′ direction. These enzymes release 5′-nucleoside monophosphates or nucleoside diphosphates by either hydrolytic cleavages or a phosphorolytic mechanism, respectively.

## I. POLYNUCLEOTIDE PHOSPHORYLASE (PNPase)

PNPase, encoded by the *pnp* gene, was first discovered in 1955 by Ochoa and Grunberg-Manago (75). PNPase catalyzes phosphorolytic degradation of RNA releasing 5′-nucleoside diphosphates. A 3′-overhang of approximately 7–10 ribonucleotides is required for PNPase to bind, and the enzyme is inhibited by

secondary structures (21). *In vivo,* PNPase is devoted to the processive degradation of RNA, but may also add heteropolymeric tails observed in *E. coli* (76). PNPase is regulated by the action of RNase E, RNase II, as well as PNPase itself. Experiments have shown that mutations in both RNase E and RNase II lead to an overall increase in PNPase levels (45,77,78).

**II. RIBONUCLEASE II (RNase II)**

RNase II, which is encoded by the *rnb* gene, is a sequence-independent hydrolytic ribonuclease that degrades RNA releasing 5′-nucleoside monophosphates, but cannot effectively degrade RNA substrates shorter than about 10–15 nucleotides in length (14). Similar to PNPase, RNase II activity is easily blocked by secondary structures, and its preferred substrate is homopolymeric poly(A) tails (21,79). RNase II activity is regulated at both the transcriptional and post-transcriptional levels. RNase E as well as PNPase directly degrade the *rnb* mRNA, whereas RNase III indirectly affects the *rnb* mRNA by affecting PNPase levels (78,80).

**III. RIBONUCLEASE R (RNase R)**

RNase R, which is encoded by the *rnr* gene, has been shown to be an important component in RNA metabolism (14). Like RNase II, RNase R is a sequence-independent hydrolytic ribonuclease that degrades RNA releasing 5′-nucleoside monophosphates. RNase R is unique in the fact that it is very efficient at degrading RNA with secondary structures. However, RNase R requires 7–12

nucleotide single-stranded regions in order to bind (81,82). RNase R is post-transcriptionally regulated by RNase E and G (83). It is also known that RNase R is a cold shock protein, whose levels are up-regulated 7–8-fold in response to a sudden temperature downshift (e.g., 37°–10°C), a condition which allows certain mRNAs to become more stable due to secondary structure formation (84).

## IV. RIBONUCLEASE D (RNase D)

RNase D, which is encoded by the *rnd* gene, is mainly active on tRNA substrates (85-87). It is a hydrolytic exoribonuclease with a molecular mass of 42.7 kDa (88). *In vitro* studies have shown RNase D is active on denatured or damaged tRNA molecules as well as certain tRNA precursors and other small structured RNAs (87,89). *In vivo* studies show that RNase D is involved in 3′-end maturation of tRNA precursors. However, strains lacking RNase D entirely do not exhibit a growth phenotype (90). Strains lacking RNase D do not become inviable until other exoribonucleases, RNase T, II, BN, and PH, are also eliminated from the cell (91). These data suggest that RNase D can function as a backup enzyme for tRNA maturation when the other primary exoribonucleases are missing (10).

## V. RIBONUCLEASE T (RNase T)

RNase T, which is encoded by the *rnt* gene, is unique from the other exoribonucleases because it is capable of removing residues close to a duplex structure without the need for unwinding the species (16). It is responsible in

end-turnover of tRNA, where the terminal AMP residue is removed from the –CCA determinant and subsequently added back by tRNA nucleotidyltransferase (92-94). It is also essential for generating the mature 3′-ends of 5S and 23S rRNA, in addition to the previously mentioned tRNA processing (95,96).

RNase T has a molecular mass of 23.5 kDa that is active as an $\alpha_2$ homodimer both *in vivo* and *in vitro* totaling ~50 kDa (97). The dimeric form is required for full activity *in vitro* and *in vivo*. RNase T can be purified from normally expressing cells and does not associate with other components in crude extracts (98).

RNase T has unusual substrate specificity in that the enzyme discriminates against pyrimidines, especially cytosine (16). A terminal C-residue can decrease RNase T activity for that substrate by 100-fold, and two consecutive C-residues essentially renders the enzyme inactive for the substrate (98). While oligoribonucleotides shorter than six residues are considered poor substrates, RNase T can act on these species (97). RNase T has also been reported to be able to digest single-stranded DNA molecules (99,100).

## VI. RIBONUCLEASE PH (RNase PH)

RNase PH, encoded by the *rph* gene, was first identified when extracts lacking RNase II, D, Z, and T were found to have mature 3′-termini of certain tRNA precursors (101). RNase PH catalyzes a Pi-dependent degradation of RNA that releases nucleoside diphosphates instead of monophosphates (102), and is responsible for 3′-end maturation of tRNAs and other small stable RNAs in *E.*

*coli* (11,103,104). Interestingly, like PNPase, under certain conditions RNase PH can act as a polymerizing enzyme by adding nucleoside diphosphates to the 3′-terminus of RNA molecules (105).

*E. coli* RNase PH has rather unique properties. The *rph* gene is 238 amino acids long with a predicted molecular mass of 25.5 kDa, however RNase PH migrates as a 30 kDa molecule on SDS-PAGE (102,106). Again, like PNPase, RNase PH forms a hexameric ring structure as a trimer of dimers (107).

Perhaps of most import is the presence of the *rph-1* allele that is found in various *E. coli* "wild-type" strains such as MG1655 and W3110. This allele contains a single GC base pair deletion, which causes a frameshift mutation resulting in the protein being 10 amino acids shorter than its wild-type counterpart (108). This mutation also has a polar effect on the downstream *pyrE* gene that causes pyrimidine starvation in minimal medium (108). The consequences of this mutation on RNA metabolism are just now beginning to be understood and are discussed further in this dissertation.

## VII. RIBONUCLEASE BN (RNase BN)

RNase BN has been renamed to RNase Z, which is an endoribonuclease. Its role and activity is discussed in the section on RNase Z.

## VIII. OLIGORIBONUCLEASE (Orn)

The end products of mRNA degradation by PNPase, RNase II, or RNase R are terminal digestion products approximately 2–7 nucleotides in length (1). In order

to completely degrade RNA to the mononucleotide level to promote the continued synthesis of new RNA transcripts, *E. coli* contains an enzyme known as oligoribonuclease. Orn is encoded by the *orn* gene and has been shown to be unique among the other exoribonucleases identified in *E. coli* because of its ability to degrade these 2–7 length oligoribonucleotides (109). Conversely the enzyme has no activity on oligoribonucleotides longer than 10 nucleotides in length.

**A. Protein Structure, Substrate Specificity, and Mechanism of Action**

Orn is a rather small protein, only 180 amino acids in length with a molecular mass of 20.7 kDa and exists in the cell as an $\alpha_2$ homodimer (110). Orn belongs to the DEDD family of exoribonucleases (110), is a homodimeric enzyme, and requires the presence of divalent cations ($Mg^{2+}$) as a cofactor (111). Similar to all other exoribonucleases, Orn is processive in the 3′→5′ direction and degrades one entire oligoribonucleotide at a time before moving to another molecule using a hydrolytic mechanism (112).

The enzyme's affinity is highest for 5–mer oligoribonucleotides and its reaction rate decreases as chain length increases. Secondary structure of the oligoribonucleotide chain has a marked inhibitory effect on the activity of Orn (112). The sequence of the oligoribonucleotide chain also effects the activity of Orn hydrolysis; highest rates are achieved with pyrimidine dinucleotides in decreasing order: CpC>UpU > CpU > UpC. Interestingly, the presence of guanosine at the 3′-end is severely inhibitory with reaction rates in decreasing

order as follows: CpG>UpG = ApG > GpG. This specificity is similar to what is seen with RNase T activity where consecutive cytosine residues are completely inhibitory to RNase T activity (98,112).

The enzyme requires a free 3′-OH end, and is not sensitive to 5′-phosphorylation of its substrate (111). It is also believed that Orn is inhibited by the nucleotide 3′-phosphoadenosine-5′-phosphate (pAp) (a product derived from numerous metabolic reactions) as well as 5′-ribonucleotides, the latter being more biologically significant since 5′-ribonucleotides are end products of Orn metabolism and likely contribute to modulation of Orn activity (113).

**B. Phylogenetic Distribution of Orn**

Orn is well conserved among numerous other organisms, and has orthologs with similar functions, providing further support for its proposed role within *E. coli*. Oligoribonuclease genes have been identified in the β and ɣ-Proteobacteria, such as *Neisseria meningitidis* and *Haemophilus influenzae*, respectively, in *Actinomycetes*, and *Saccharomyces cerevisiae* (110). Currently, no Orn-like protein has been identified in Archaea, Cyanobacteria, or the α-Proteobacteria (110). In contrast to prokaryotes, oligoribonuclease is found in all eukaryotic organisms ranging from *Drosophila melanogaster* to humans. The protein Sfn, which is present in humans, exhibits 3′→5′ exoribonuclease activity on small RNA oligomers as well as DNA oligomers (114). The enzyme is also highly conserved between all organisms, with the degree of identity of any oligoribonuclease from any organism ranging from 40–50%, suggesting a critical

conserved function (115).

Analogs of Orn have been identified within the Firmicutes, Bacteroidetes, Chlorobi, and δ-Proteobacteria. *Bacillus subtilis*, contains two Orn-like proteins, termed NrnA and NrnB (116). They have a similar mechanism of action, but show an *in vitro* preference for 3-mer substrates versus the 5-mer *E. coli* Orn preference (14). Orn is also found in *Streptomyces* spp. In this organism, mutations in *orn* have pleiotropic effects such as over production of pigmented antibiotic actinorhodin as well as differentiation in sporulation, raising the question of why the buildup of oligoribonucleotides and/or a lack of 5′-ribonucleotide monophosphates could have such an effect on the physiology (117).

**C. Orn and the mRNA Decay Pathway**

Although much is known about mRNA decay pathways, numerous questions still have yet to be answered. For example, Ghosh and Deutscher (118) have reported that Orn is essential to cell viability because of their inability to disrupt the chromosomal *orn* gene. In addition, successful interruption of *orn* was only accomplished in the presence of a low-copy, temperature-sensitive plasmid carrying a wild-type copy of the gene, but when this strain was shifted to the non-permissive temperature, the loss of the complementing plasmid resulted in slower cellular growth, which they hypothesized was due to the accumulation of small oligoribonucleotides (118). However, it could not be explained why Orn was essential to cell viability. Three possible explanations were proposed by

Ghosh and Deutscher (118).

First, in an Orn mutant cell, as oligoribonucleotides accumulate, there is an eventual depletion of the mononucleotide pool. The inherent instability of mRNAs allows a cell to rapidly adjust to changing conditions. However, without turnover of mRNAs to the mononucleotide level, depletion of the mononucleotide pool can have deleterious effects on the cell's ability to synthesize new transcripts.

Second, the accumulation of small oligoribonucleotides may also serve to inhibit essential enzymes thereby interfering with certain metabolic processes through either a negative feedback loop or allosteric inhibition. Small oligoribonucleotides may also interfere with gene expression in numerous ways. For instance, the protein Hfq is a small protein involved in mediating sRNA binding to target mRNAs. Its inactivation in the cell can cause pronounced pleiotropic phenotypes such as decreased growth rate or sensitivity to UV light (119). There exists the possibility that higher levels of small oligoribonucleotides may interfere with the binding of the sRNAs to Hfq thereby affecting gene expression through prevention of translation. It has also been shown that functional sRNAs, such as microRNAs, need to have at a minimum of 4–5 nucleotide 5′ homology with extensive 3′ homology or 8-nucleotide 5′ homology with no 3′ homology (120). Although microRNAs are found in eukaryotic systems, there may exist some features common in a prokaryotic organism such as *E. coli*. Accumulation of RNA oligomers 2–7 nucleotides in length in an *orn* mutant could inhibit sRNA–mRNA binding through formation of stable RNA

hybrids, potentially contributing to changes in gene expression. Recently, Goldman et al. (121) reported that an *orn* deletion strain in *Pseudomonas aeruginosa* gene expression had been altered through the presence of nanoRNAs by either altering transcript stability through incorporation of the nanoRNAs into newly formed transcripts, by priming transcription and changing the transcription start site, or by serving as "activators" of transcription initiation of promoters that would normally require high levels of the initiating NTP for initiation (121).

Last, there exists the possibility that Orn has a yet to be described function whose elimination may be responsible for the growth defects noted in the work conducted by Ghosh and Deutscher (118). The theory that Orn may be able to degrade short DNA oligonucleotides because of its 3′→5′ exonuclease activity, which includes proofreading domains inherent to all known DNA-dependent DNA polymerases, was shown to be true in the work conducted by Mechold et al. (113). It has also been shown that the human homolog of Orn, Sfn, displays this ability as well (114). This activity highlights the possibility that Orn may serve a function in DNA damage repair or recombination allowing for the recycling of nucleotides that may interfere in cellular processes. Thus, the DNase activity of Orn may have a more important functional role *in vivo*.

**Accessory Enzymes in RNA Metabolism Excluding Ribonucleases**

There are numerous proteins involved in RNA metabolism that are not exclusively ribonucleases. Two will be discussed below, both of which have the

unique characteristic of activating RNA molecules for degradation. This section however, will focus on RppH because of its role in this dissertation.

## I. POLY(A) POLYMERASE (PAP I)

Poly(A) polymerase, encoded by the *pcnB* gene, first identified in *E. coli* in 1962, is responsible for the addition of poly(A) residues onto the 3′-end of transcripts (122,123), a reaction currently hypothesized to mark transcripts for immediate degradation (124). The poly(A) tails are usually 10–40 nucleotides in length and are found on mRNA decay products as well as full-length transcripts with Rho-independent transcription terminators (125,126). A *pcnB* deletion strain was found to contain less than 10% of wild-type levels of poly(a) tails, suggesting that PAP I was responsible for the vast majority of polyadenylation *in vivo* (126).

## II. RNA PYROPHOSPHOHYDROLASE (RppH)

RppH, encoded by the *rppH* gene, belongs to the protein family of Nudix hydrolases (127,128). Nudix hydrolases are a group of enzymes found in over 250 species that hydrolyze a nucleoside diphosphate into another moiety, X (Nudix), and are involved in numerous cellular activities (129). Because of their large range of potential substrates, this family of proteins allows a cell to remove potentially harmful metabolites or biochemical intermediates that may build up during cellular processes (130).

**A. Protein Structure, Substrate Specificity, and Mechanism of Action**

*E. coli* RppH is a 20 kDa protein, that contains the typical nudix motif, a highly-conserved 23 amino acid sequence, found in other nudix family proteins (131,132). The crystal structure of the *Bdellovibrio bacteriovorus* RppH shows that the protein forms a dimer from two monomers and folds into a characteristic β-strand-loop-α-helix-loop (133,134). The enzyme requires the divalent cations $Mg^{2+}$ at an optimal concentration of 10 mM, as well as $Zn^{2+}$ and $Mn^{2+}$, but at lower concentrations (128).

While RppH falls into the Nudix hydrolase protein family, RppH proteins are also known as asymmetrically cleaving diadenosine tetraphosphate hydrolases. These enzymes catalyze the hydrolysis of an $Np_4N'$ to a nucleoside triphosphate (NTP or pppN) and a nucleoside monophosphate (N'MP or pN) (135). RppH has numerous potential substrates of $Np_4N$'s with varying nucleosides including mRNA 5′-cap analogs, nucleoside 5′-tetra-, penta-, and hexa- phosphates ($p_4N$, $p_5N$, $p_6N$), methylene and halomethylene analogues of $Ap_4A$, as well as 2′- (deoxy)adenylated $Ap_4A$s (136). Past experiments have shown that *E. coli* RppH has a hydrolysis rate for $Ap_5A$ of 100%, $Ap_6A$ at 92%, $Ap_4A$ at 14%, and almost no hydrolysis of $Ap_3A$ moieties (128,137). The end products of the hydrolysis reactions from $Ap_6A$ yields 2 ATP, $Ap_5A$ yields ATP and ADP, $Ap_4A$ yields ATP and AMP (128).

Debate still exists concerning what residue/s act as the catalytic base in the active site of *E. coli* RppH. In *E. coli*, *mutT,* the first Nudix hydrolase to be studied, and $Ap_4A$ pyrophosphatase, the second glutamic acid in the Nudix

motif acts as the catalytic base for the enzymes (138). The *B. bacteriovorus* RppH, however, has two potential catalytic bases at either the second glutamate of the Nudix motif or glutamate or histidine residue in the loop equivalent of the enzyme (134). Further research will have to be conducted on the *E. coli* RppH to determine the catalytic base.

**B. Phylogenetic Distribution of RppH**

*E. coli* RppH has homologs in numerous phyla of bacteria ranging from the Gram-positive Firmicutes to the Gram-negative Proteobacteria (β, ɣ, and δ) (134,137,139-142). The data concerning RppH homologs in the Firmicutes are limited to research in *Bacillus subtilis, Staphylococcus aureus,* and *Listeria monocytogenes*, whereas the data from the Proteobacteria have a wider range of bacterial organisms that have been studied. All of the RppH homologs, however, show similar cellular roles in removal of a pyrophosphate from the 5′-end of transcripts (decapping) and polyphosphatase activity.

*B. subtilis* RppH (BsRppH) has been shown to exhibit RNA pyrophosphohydrolase activity *in vitro*, and converts triphosphorylated transcripts to monophosphorylated RNA, similar to *E. coli* RppH (143). Unlike *E. coli* RppH which releases a pyrophosphate 85% of the time, BsRppH releases the ɣ and β phosphates as orthophosphate ions (127). This reaction allowed for a higher rate of degradation of transcripts from RNase J1 and RNase J1-J2 complexes, which is similar to eukaryotic mRNA degradation following 5′-end decapping (143).

*Rickettsia prowazekii*, the causative agent for epidemic typhus, contains an invasion gene *invA,* which has 37–44% homology to *E. coli* RppH (137). InvA is a Nudix hydrolase that encodes dinucleoside oligophosphate pyrophosphohydrolase activity on $Np_nN$ moieties where $n \geq 5$, which are considered to be signaling molecules (137). Similar to *E. coli* RppH, InvA produced ATP and ADP from the hydrolysis reaction (137).

*Legionella pneumophila,* which causes a specific type of pneumonia known as Legionnaires' disease, contains the protein NudA. This protein has been identified as another Nudix hydrolase that prefers $Ap_nA$ molecules as substrates, similar to that of *E. coli* RppH (141). Studies have shown that NudA is a virulence factor in *Legionella pneumophila* and that a *ΔnudA* mutant strain was incapable of invasion (141).

*B. bacteriovorus*, a Gram-negative bacterial parasite, was the first bacterial RNA pyrophosphohydrolase to have its structure determined (134,144). BdRppH was also the only other RppH, other than *E. coli* RppH, that was found to have both GTPase activity as well as decapping activity (134). Messing et al. (134) also showed that BdRppH could complement an *E. coli rppH* deletion strain, suggesting that the two enzymes have significant functional overlap (134).

### C. RppH in *E. coli*: Polyphosphate Regulation and mRNA Decapping

The presence of diadenosine polyphosphates $Ap_{4–6}A$, a byproduct of aminoacyl-tRNA synthetases, were originally discovered in 1966 (145). These polyphosphates have been implicated in numerous cellular processes such as

regulation of cell differentiation and apoptosis, cellular division, as well as inhibition of ATP-sensitive $K^+$ channels (146-148). *E. coli* RppH is enzymatically active on these polyphosphates and research has been conducted on how the presence of these polyphosphates affect *E. coli* activities, and what role *E. coli* RppH has in regulating these polyphosphates.

Numerous groups have investigated the accumulation of the $Ap_4A$ moiety in *E. coli*. For instance, Johnstone and Farr (149) studied what proteins actually bind to $Ap_4A$ moieties in different physiological conditions. Their results showed that $Ap_4A$ was bound to two known heat shock proteins, E89 and GroEL, as well as DnaK (this binding may have been facilitated by another protein), and that this binding inhibited those proteins from protecting the cell against heat shock (149). $Ap_4A$ is also responsible for controlling the timing of cellular division. High levels of $Ap_4A$ in a *cfcB1* mutant in *E. coli* were demonstrated to have an increased frequency of cellular division (148). Others have hypothesized that $Ap_4A$ may be synthesized in order to allow for increased time in DNA repair mechanisms (150).

Little is known about the role of $Ap_5A$ and $Ap_6A$ in *E. coli*, but research in higher organisms has been performed to elucidate their roles. For instance, $Ap_5A$ has been shown to inhibit adenylate kinase, an enzyme involved in maintenance of myocardial bioenergetics (151,152). Additionally, increased levels of $Ap_5A$ and $Ap_6A$ inhibit the opening of $K_{ATP}$ in pancreatic β-cells, where these channels are found in abundance (153,154).

All primary transcripts in *E. coli* contain a 5′-triphosphate. It has long been assumed that removal of the 5′-triphosphate was not necessary for initiation of mRNA decay, unlike the required removal of the 5′-methyl-G cap in eukaryotic mRNA decay initiation (155). Evidence for this hypothesis was derived from the knowledge that endonulceolytic cleavages from ribonucleases such as RNase E were the initiating step in mRNA decay and that RNase E was inhibited by the presence of a 5′-triphosphate, yet mRNA decay still occurs (6,20). Recent studies have shown that *E. coli* RppH removes a pyrophosphate from the 5′-end of primary transcripts, which stimulates RNase E dependent cleavages and therefore initiates the mRNA decay pathway (127,156).

Studies have also demonstrated that RNase P activity is dependent on the phosphorylation status of the 5′-leader of tRNA precursors. RNase P directly interacts with the 5′-leader of precursor tRNAs and its binding affinity is maintained in a leader-length dependent manner up to 4–6 nucleotides (157,158), with studies showing that as the leader length increases, the ability for RNase P to cleave at the +1 nucleotide of the precursor tRNA decreases (159). Therefore it is of import to discover how decapping activity from RppH could stimulate RNase P cleavages involved in 5′-end maturation of tRNA precursors.

## SUMMARY

The aim of my dissertation research has been to better understand the complex nature of post-transcriptional regulation in *E. coli*. As described in Chapter 2,

our data show that RNase E-mediated processing of primary tRNA transcripts was unaffected in an *rppHΔ754 rph-1* strain. However, in the absence of RppH, 5′-end maturation by RNase P was inhibited for the tRNAs *pheU, pheV,* and *ileX.* We also show that either inactivation of RNase E or presence of wild-type RNase PH abolishes the 5′ inhibition of processing by RNase P.

The work conducted in Chapter 3 shows, through the use of high-density tiling microarrays, the *in vivo* role of RppH on a transcriptome-wide scale. The data suggest that a *ΔrppH rph-1* mutant strain regulates the stability of the *flhDC* transcript, which encodes the master regulator of the flagellar network pathway. The *flhDC* transcript is up-regulated in a *ΔrppH rph-1* mutant which causes all downstream flagellar genes to be up-regulated, leading to increased cellular motility. However, in the presence or complete absence of RNase PH, this effect is abolished. These data suggest that while RppH has an effect on the transcriptome of *E. coli,* many of these effects are dependent on the Rph-1 truncated protein.

The work in Chapter 4 represents a solid beginning to the understanding of the physiological role that oligoribonuclease plays in the mRNA decay pathway in *E. coli.* Utilizing numerous mutagenesis strategies, we were able to construct a true *Δorn* strain in a clean genetic background and characterize its effects on the growth and cellular viability in *E. coli.* By constructing varying Orn expression plasmids, we were able to determine that *Δorn* confers a cold-sensitive phenotype and that complementation of Orn is temperature and copy-number dependent. We were also able to show through western blotting

analysis that Orn is produced at extremely low levels in wild-type *E. coli* and that our expression system provides tight control of Orn production. Additionally we also show that the currently annotated transcription start site is incorrect, and identified the putative promoter of *orn.* Lastly, we show that the enzyme RNase T has functional overlap to Orn and only when the cell is both RNase T and Orn deficient does the cell become inviable, which is contrary to current dogma.

## REFERENCES


1. Kushner, S.R. (2002) mRNA decay in *Escherichia coli* comes of age. *J. Bacteriol.*, **184**, 4658-4665; discussion 4657.
2. Goldenberg, D., Azar, I. and Oppenheim, A.B. (1996) Differential mRNA stability of the *cspA* gene in the cold-shock response of *Escherichia coli*. *Mol. Microbiol.*, **19**, 241-248.
3. Bäga, M., Gäransson, M., Normark, S. and Uhlin, B.E. (1988) Processed mRNA with differential stability in the regulation of *E. coli* pilin gene expression. *Cell*, **52**, 197-206.
4. Pedersen, S., Reeh, S. and Friesen, J.D. (1978) Functional mRNA half-lives in *E. coli*. *Molecular Genetics and Genomics*, **166**, 329-336.
5. Cannistraro, V.J. and Kennell, D. (1993) The 5' ends of RNA oligonucleotides in *Escherichia coli* and mRNA degradation. *Eur. J. Biochem.*, **213**, 285-293.

6. Carpousis, A.J., Luisi, B.F. and McDowall, K.J. (2009) Endonucleolytic initiation of mRNA decay in *Escherichia coli*. *Prog. Mol. Biol. Transl. Sci.*, **85**, 91-135.

7. Nilsson, G., Belasco, J.G., Cohen, S.N. and von Gabain, A. (1984) Growth-rate dependent regulation of mRNA stability in *Escherichia coli*. *Nature*, **312**, 75-77.

8. Nicholson, A.W. (1999) Function, mechanism and regulation of bacterial ribonucleases. *FEMS Microbiol. Rev.*, **23**, 371-390.

9. Deutscher, M.P. (2006) Degradation of RNA in bacteria: comparison of mRNA and stable RNA. *Nucleic Acids Res.*, **34**, 659-666.

10. Li, Z. and Deutscher, M.P. (1996) Maturation pathways for *E.coli* tRNA precursors: a random multienzyme process *in vivo*. *Cell*, **86**, 503-512.

11. Li, Z., Pandit, S. and Deutscher, M.P. (1998) 3' exoribonucleolytic trimming is a common feature of the maturation of small, stable RNAs in *Escherichia coli*. *Proc. Natl. Acad. Sci. USA*, **95**, 2856-2861.

12. Condon, C. (2007) Maturation and degradation of RNA in bacteria. *Curr. Opin. Microbiol.*, **10**, 271-278.

13. Kushner, S.R. (1996) In Neidhardt, F. C., Curtiss III, R., Ingraham, J. L., Lin, E. C. C., Low, J., K.B., Magasanik, B., Reznikoff, W. S., Riley, M., Schaechter, M. and Umbarger, H. E. (eds.), *Escherichia coli and Salmonella: Cellular and Molecular Biology, Second Edition*. ASM Press, Washington, DC, Vol. 1, pp. 849-860.

14. Andrade, J.M., Pobre, V., Silva, I.J., Domingues, S. and Arraiano, C.M. (2009) The role of 3'-5' exoribonucleases in RNA degradation. *Prog. Mol. Biol. Transl. Sci.*, **85**, 187-229.

15. Reuven, N.B. and Deutscher, M.P. (1993) Multiple exoribonucleases are required for the 3' processing of *Escherichia coli* tRNA precursors *in vivo*. *FASEB J.*, **7**, 143-148.

16. Zuo, Y. and Deutscher, M.P. (2002) The physiological role of RNase T can be explained by its unusual substrate specificity. *J. Biol. Chem.*, **277**, 29654-29661.

17. Apirion, D. and Lasser, A.B. (1978) A conditional lethal mutant of *Escherichia coli* which affects the processing of ribosomal RNA. *J. Biol. Chem.*, **253**, 1738-1742.

18. Ghora, B.K. and Apirion, D. (1978) Structural analysis and *in vitro* processing to p5 rRNA of a 9S RNA molecule isolated from an *rne* mutant of *E. coli*. *Cell*, **15**, 1055-1066.

19. Coburn, G.A. and Mackie, G.A. (1999) Degradation of mRNA in *Escherichia coli*: An old problem with some new twists. *Prog. Nucleic Acid Res. Mol. Biol.*, **62**, 55-108.

20. Mackie, G.A. (1998) Ribonuclease E is a 5'-end-dependent endonuclease. *Nature*, **395**, 720-723.

21. Arraiano, C.M., Andrade, J.M., Domingues, S., Guinote, I.B., Malecki, M., Matos, R.G., Moreira, R.N., Pobre, V., Reis, F.P., Saramago, M. *et al.*

(2010) The critical role of RNA processing and degradation in the control of gene expression. *FEMS Microbiol. Rev.*, **34**, 883-923.

22. Okada, Y., Wachi, M., Hirata, A., Suzuki, K., Nagai, K. and Matsuhashi, M. (1994) Cytoplasmic axial filaments in *Escherichia coli* cells: possible function in the mechanism of chromosome segregation and cell division. *J. Bacteriol.*, **176**, 917-922.

23. Wachi, M., Umitsuki, G., Shimizu, M., Takada, A. and Nagai, K. (1999) *Escherichia coli cafA* gene encodes a novel RNase, designated as RNase G, involved in processing of the 5' end of 16S rRNA. *Biochemical and Biophysical Research Communications*, **259**, 483-488.

24. Li, Z., Pandit, S. and Deutscher, M.P. (1999) RNase G (CafA protein) and RNase E are both required for the 5' maturation of 16S ribosomal RNA. *EMBO J.*, **18**, 2878-2885.

25. Briant, D.J., Hankins, J.S., Cook, M.A. and Mackie, G.A. (2003) The quartenary structure of RNase G from *Escherichia coli*. *Mol. Microbiol.*, **50**, 1381-1390.

26. Kim, K.S. and Lee, Y. (2004) Regulation of 6S RNA biogenesis by switching utilization of both sigma factors and endoribonucleases. *Nucleic Acids Res.*, **32**, 6057-6068.

27. Mohanty, B.K. and Kushner, S.R. (2008) Rho-independent transcription terminators inhibit RNase P processing of the *secG leuU* and *metT* tRNA

polycistronic transcripts in *Escherichia coli*. *Nucleic Acids Res.*, **36**, 364-375.

28. Mohanty, B.K. and Kushner, S.R. (2007) Ribonuclease P processes polycistronic tRNA transcripts in *Escherichia coli* independent of ribonuclease E. *Nucleic Acids Res.*, **35**, 7614-7625.

29. Kaga, N., Umitsuki, G., Nagai, K. and Wachi, M. (2002) RNase G-dependent degradation of the *eno* mRNA encoding a glycolysis enzyme enolase in *Escherichia coli*. *Biosci. Biotechn. and Biochem.*, **66**, 2216-2220.

30. McDowall, K.J. and Cohen, S.N. (1996) The N-terminal domain of the *rne* gene product has RNase E activity and is non-overlapping with the arginine-rich RNA-binding motif. *J. Mol. Biol.*, **255**, 349-355.

31. Taraseviciene, L., Bjork, G.R. and Uhlin, B.E. (1995) Evidence for a RNA binding region in the *Escherichia coli* processing endoribonuclease RNase E. *J. Biol. Chem.*, **270**, 26391-26398.

32. Lee, K., Bernstein, J.A. and Cohen, S.N. (2002) RNase G complementation of *rne* null mutation identified functional interrelationships with RNase E in *Escherichia coli*. *Mol. Microbiol.*, **43**, 1445-1456.

33. Ow, M.C., Perwez, T. and Kushner, S.R. (2003) RNase G of *Escherichia coli* exhibits only limited functional overlap with its essential homologue, RNase E. *Mol. Microbiol.*, **49**, 607-622.

34. Chung, D.-H., Min, Z., Wang, B.-C. and Kushner, S.R. (2010) Single amino acid changes in the predicted RNase H domain of *E. coli* RNase G lead to the complementation of RNase E mutants. *RNA*, **16**, 1371-1385.

35. Robertson, H.D., Webster, R.E. and Zinder, N.D. (1967) A nuclease specific for double-stranded RNA. *Virology*, **12**, 718-719.

36. Robertson, H.D., Webster, R.E. and Zinder, N.D. (1968) Purification and properties of ribonuclease III from *Escherichia coli*. *J. Biol. Chem.*, **243**, 82-91.

37. Conrad, C. and Rauhut, R. (2002) Ribonuclease III: new sense from nuisance. *Int. J. Biochem. Cell Biol.*, **34**, 116-129.

38. Court, D. (1993) In Belasco, J. and Brawerman, G. (eds.), *Control of messenger RNA stability*. Academic Press, New York, pp. 71-117.

39. Dunn, J.J. (1976) RNase III cleavage of single-stranded RNA. Effect of ionic strength on the fideltiy of cleavage. *J. Biol. Chem.*, **251**, 3807-3814.

40. Nashimoto, H. and Uchida, H. (1985) DNA sequencing of the *Escherichia coli* ribonuclease III gene and its mutations. *Molecular and General Genetics*, **201**, 25-29.

41. King, T.C., Sirdeshmukh, R. and Schlessinger, D. (1984) RNase III cleavage is obligate for maturation but not for function of *Escherichia coli* pre-23S rRNA. *Proc. Natl. Acad. Sci. USA*, **81**, 185-188.

42. Babitzke, P., Granger, L., Olszewski, J. and Kushner, S.R. (1993) Analysis of mRNA decay and rRNA processing in *Escherichia coli* multiple mutants carrying a deletion in RNase III. *J. Bacteriol.*, **175**, 229-239.

43. Meng, W. and Nicholson, A.W. (2008) Heterodimer-based analysis of subunit and domain contributions to double-stranded RNA processing by *Escherichia coli* RNase III *in vitro*. *Biochem. J.*, **410**, 39-48.

44. Bardwell, J.C.A., Regnier, P., Chen, S.-M., Nakamura, Y., Grunberg-Manago, M. and Court, D.L. (1989) Autoregulation of RNase III operon by mRNA processing. *EMBO J.*, **8**, 3401-3407.

45. Portier, C., Dondon, L., Grunberg-Manago, M. and Regnier, P. (1987) The first step in the functional inactivation of the *Escherichia coli* polynucleotide phosphorylase messenger is ribonuclease III processing at the 5' end. *EMBO J.*, **6**, 2165-2170.

46. Wilson, H.R., Yu, D., Peters, H.K., 3rd, Zhou, J.G. and Court, D.L. (2002) The global regulator RNase III modulates translation repression by the transcription elongation factor N. *EMBO J.*, **21**, 4154-4161.

47. Stead, M.B., Marshburn, S., Mohanty, B.K., Mitra, J., Pena Castillo, L., Ray, D., van Bakel, H., Hughes, T.R. and Kushner, S.R. (2011) Analysis of *Escherichia coli* RNase E and RNase III activity *in vivo* using tiling microarrays. *Nucleic Acids Res.*, **39**, 3188-3203.

48. Robertson, H.D., Altman, S. and Smith, J.D. (1972) Purification and properties of a specific *Escherichia coli* ribonuclease which cleaves a

tyrosine transfer ribonucleic acid presursor. *J. Biol. Chem.*, **247**, 5243-5251.

49. Guerrier-Takada, C., Gardiner, K., Marsh, T., Pace, N. and Altman, S. (1983) The RNA moiety of ribonuclease P is the catalytic subunit of the enzyme. *Cell*, **35**, 849-857.

50. Stark, B.C., Kole, R., Bowman, E.J. and Altman, S. (1977) Ribonuclease P: an enzyme with an essential RNA component. *Proc. Natl. Acad. Sci. USA*, **75**, 3719-3721.

51. Rudd, K.E. (1998) Linkage map of *Escherichia coli* K-12, Edition 10: the physical map. *Microbiol. Mol. Biol. Rev.*, **62**, 985-1019.

52. Brown, J.W. (1998) The ribonuclease P database. *Nucleic Acids Res.*, **26**, 351-352.

53. Altman, S. (1990) Ribonuclease P. Postscript. *The Journal of Biological Chemistry*, **265**, 20053-20056.

54. Pace, N.R. and Smith, D. (1990) Ribonuclease P: function and variation. *J. Biol. Chem.*, **265**, 3587-3590.

55. Frank, D.N. and Pace, N.R. (1998) Ribonuclease P: unity and diversity in a tRNA processing ribozyme. *Annu. Rev. Biochem.*, **67**, 153-180.

56. Altman, S., Kirsebom, L. and Talbot, S. (1995) In Soll, D. and RajBhandary (eds.), *tRNA: Structure and Function*. American Society for Microbiology Press, Washington, DC, pp. 67-78.

57. Peck-Miller, K.A. and Altman, S. (1991) Kinetics of the processing of the precursor to 4.5S RNA, a naturally occurring substrate for RNase P from *Escherichia coli*. *J. Mol. Biol.*, **221**, 1-5.

58. Komine, Y., Kitabatake, M., Yokigawa, T., Nishikawa, K. and Inokuchi, H. (1994) A tRNA-like structure is present in 10Sa RNA, a small stable RNA from *Escherichia coli*. *Proc. Natl. Acad. Sci. USA*, **91**, 9223-9227.

59. Agrawal, A., Mohanty, B.K. and Kushner, S.R. (2014) Processing of the seven valine tRNAs in *Escherichia coli* involves novel features of RNase P. *Nucleic Acids Res.*, **42**, 11166-11179.

60. Nomura, T. and Ishihama, A. (1988) A novel function of RNase P from *Escherichia coli*: processing of a suppressor tRNA precursor. *EMBO J.*, **7**, 3539-3545.

61. Li, Y. and Altman, S. (2003) A specific endoribonuclease, RNase P, affects gene expression of polycistronic operon mRNAs. *Proc. Natl. Acad. Sci. USA*, **100**, 13213-13218.

62. Pellegrini, O., Nezzar, J., Marchfelder, A., Putzer, H. and Condon, C. (2003) Endonucleolytic processing of CCA-less tRNA precursors by RNase E in *Bacillus subtilis*. *EMBO J.*, **22**, 4534-4543.

63. Rudd, K.E. (2000) EcoGene: a genome sequence database for *Escherichia coli* K-12. *Nucleic Acids Res.*, **28**, 60-64.

64. Li de la Sierra-Gallay, I., Pellegrini, O. and Condon, C. (2005) Structural basis for substrate binding, cleavage and allostery in the tRNA maturase RNase Z. *Nature*, **433**, 657-661.

65. Ezraty, B., Dahlgren, B. and Deutscher, M.P. (2005) The RNase Z homologue encoded by *Escherichia coli elaC* gene is RNase BN. *J. Biol. Chem.*, **280**, 16542-16545.

66. Perwez, T. and Kushner, S.R. (2006) RNase Z in *Escherichia coli* plays a significant role in mRNA decay. *Mol. Microbiol.*, **60**, 723-737.

67. Yamanishi, H. and Yonesaki, T. (2005) RNA cleavage linked with ribosomal action. *Genetics*, **171**, 419-425.

68. Otsuka, Y. and Yonesaki, T. (2005) A novel endoribonuclease, RNase LS, in *Escherichia coli*. *Genetics*, **169**, 13-20.

69. Otsuka, Y., Ueno, H. and Yonesaki, T. (2003) *Escherichia coli* endoribonucleases involved in cleavage of bacteriophage T4 mRNAs. *J. Bacteriol.*, **185**, 983-990.

70. Meador III, J., Cannon, B., Cannistraro, V.J. and Kennell, D. (1990) Purification and characterization of *Escherichia coli* RNase I. Comparisons with RNase M. *Eur. J. Biochem.*, **187**, 549-553.

71. Subbarayan, P.R. and Deutscher, M.P. (2002) *Escherichia coli* RNase M is a multiply altered form of RNase I. *RNA*, **7**, 1702-1707.

72. Shen, V. and Schlessinger, D. (1982) In Boyer, P. D. (ed.), *The Enzymes*. Academic, New York, Vol. 15, pp. 501–515.

73. Kaplan, R. and Apirion, D. (1974) The involvement of ribonuclease I, ribonuclease II, and polynucleotide phosphorylase in the degradation of stable ribonucleic acid during carbon starvation in *E. coli*. *J. Biol. Chem.*, **249**, 149-151.

74. Ito, R. and Ohnishi, Y. (1983) The roles of RNA polymerase and RNAase I in stable RNA degradation in *Escherichia coli* carrying the *srnB*+ gene. *Biochim. Biophys. Acta*, **739**, 27-34.

75. Grunberg-Manago, M., Ortiz, P.J. and Ochoa, S. (1955) Enzymatic synthesis of nucleic acidlike polynucleotides. *Science*, **122**, 907-910.

76. Mohanty, B.K. and Kushner, S.R. (2000) Polynucleotide phosphorylase functions both as a 3' - 5' exonuclease and a poly(A) polymerase in *Escherichia coli*. *Proc. Natl. Acad. Sci. USA*, **97**, 11966-11971.

77. Robert-Le Meur, M. and Portier, C. (1992) *Escherichia coli* polynucleotide phosphorylase expression is autoregulated through an RNase III-dependent mechanism. *EMBO J.*, **11**, 2633-2641.

78. Zilhao, R., Cairrao, R., Régnier, P. and Arraiano, C.M. (1996) PNPase modulates RNase II expression in *Escherichia coli*: Implications for mRNA decay and cell metabolism. *Mol. Microbiol.*, **20**, 1033-1042.

79. Spickler, C. and Mackie, G.A. (2000) Action of RNase II and polynucleotide phosphorylase against RNAs containing stem-loops of defined structure. *J. Bacteriol.*, **182**, 2422-2427.

80. Zilhao, R., Cairrao, F., Régnier, P. and Arraiano, C.M. (1995) Precise physical mapping of the *Escherichia coli rnb* gene, encoding ribonuclease II. *Molecular Genetics and Genomics*, **248**, 242-246.

81. Cheng, Z.F. and Deutscher, M.P. (2002) Purification and characterization of the *Escherichia coli* exoribonuclease RNase R. Comparison with RNase II. *J. Biol. Chem.*, **277**, 21624-21649.

82. Vincent, H.A. and Deutscher, M.P. (2006) Substrate recognition and catalysis by the exoribonuclease RNase R. *J. Biol. Chem.*, **281**, 29769-29775.

83. Cairrao, F. and Arraiano, C.M. (2006) The role of endoribonucleases in the regulation of RNase R. *Biochem. Biophys. Res. Commun.*, **343**, 731-737.

84. Cairrao, F., Cruz, A., Mori, H. and Arraiano, C.M. (2003) Cold shock induction of RNase R and its role in the maturation of the quality control mediator SsrA/tmRNA. *Mol. Microbiol.*, **50**, 1349-1360.

85. Cudny, H. and Deutscher, M.P. (1980) Apparent involvement of ribonuclease D in the 3' processing of tRNA precursors. *Proc. Natl. Acad. Sci. USA*, **77**, 837-841.

86. Cudny, H., Zaniewski, R. and Deutscher, M.P. (1981) *Escherichia coli* RNase D. Purification and structural characterization of a putative processing nuclease. *J. Biol. Chem.*, **256**, 5627-5632.

87. Cudny, H., Zaniewski, R. and Deutscher, M.P. (1981) *Escherichia coli* RNase D. Catalytic properties and substrate specificity. *J. Biol. Chem.*, **256**, 5633-5637.

88. Zhang, J. and Deutscher, M.P. (1988) *Escherichia coli* RNase D: sequencing of the *rnd* structural gene and purification of the overexpressed protein. *Nucleic Acids Res.*, **16**, 6265-6278.

89. Ghosh, R.K. and Deutscher, M.P. (1978) Identification of an *Escherichia coli* nuclease acting on structurally altered transfer RNA molecules. *J. Biol. Chem.*, **253**, 997-1000.

90. Blouin, R.T., Zaniewski, R. and Deutscher, M.P. (1983) Ribonuclease D is not essential for the normal growth of *Escherichia coli* or bacteriophage T4 or for the biosynthesis of a T4 suppressor tRNA. *J. Biol. Chem.*, **258**, 1423-1426.

91. Kelly, K.O. and Deutscher, M.P. (1992) The presence of only one of five exoribonucleases is sufficient to support the growth of *Escherichia coli*. *J. Bacteriol.*, **174**, 6682-6684.

92. Deutscher, M.P. (1990) Ribonucleases, tRNA nucleotidyltransferase, and the 3' processing of tRNA. *Prog. Nucleic Acid Res. Mol. Biol.*, **39**, 209-240.

93. Deutscher, M.P., Marlor, C.W. and Zaniewski, R. (1985) RNase T is responsible for the end-turnover of tRNA in *Escherichia coli*. *Proc. Natl. Acad. Sci. USA*, **82**, 6427-6430.

94. Deutscher, M.P., Marlor, C.W. and Zaniewski, R. (1984) Ribonuclease T: new exoribonuclease possibly involved in end-turnover of tRNA. *Proc. Natl. Acad. Sci. USA*, **81**, 4290-4293.

95. Li, Z. and Deutscher, M.P. (1995) The tRNA processing enzyme RNase T is essential for maturation of 5S RNA. *Proc. Natl. Acad. Sci. USA*, **92**, 6883-6886.

96. Li, Z., Pandit, S. and Deutscher, M.P. (1999) Maturation of 23S ribosomal RNA requires the exoribonuclease RNase T. *RNA*, **5**, 139-146.

97. Huang, S. and Deutscher, M.P. (1992) Sequence and transcriptional analysis of the *Escherichia coli* rnt gene encoding RNase T. *J. Biol. Chem.*, **267**, 25609-25613.

98. Deutscher, M.P. and Marlor, C.W. (1985) Purification and characterization of *Escherichia coli* RNase T. *J. Biol. Chem.*, **260**, 7067-7071.

99. Zuo, Y. and Deutscher, M.P. (1999) The DNase activity of RNase T and its application to DNA cloning. *Nucleic Acids Res.*, **27**, 4077-4082.

100. Viswanathan, M., Lanjuin, A. and Lovett, S.T. (1999) Identification of RNase T as a high-copy suppressor of the UV sensitivity associated with single-strand DNA exonuclease deficiency in *Escherichia coli*. *Genetics*, **151**, 929-934.

101. Cudny, H. and Deutscher, M.P. (1988) 3' Processing of tRNA precursors in ribonuclease-deficient *Escherichia coli*. *J. Biol. Chem.*, **263**, 1518-1523.

102. Kelly, K.O. and Deutscher, M.P. (1992) Characterization of *Escherichia coli* RNase PH. *J. Biol. Chem.*, **267**, 17153-17158.

103. Deutscher, M.P., Marshall, G.T. and Cudny, H. (1988) RNase PH: A new phosphate-dependent nuclease distinct from polynucleotide phosphorylase. *Proc. Natl. Acad. Sci. USA*, **85**, 4710-4714.

104. Li, Z. and Deutscher, M.P. (1994) The role of individual exoribonucleases in processing at the 3' end of *Escherichia coli* tRNA precursors. *J. Biol. Chem.*, **269**, 6064-6071.

105. Ost, K.A. and Deutscher, M.P. (1990) RNase PH catalyzes a synthetic reaction, the addition of nucleotides to the 3' end of RNA. *Biochimie*, **72**, 813-818.

106. Jensen, K.F., Andersen, J.T. and Poulsen, P. (1992) Overexpression and rapid purification of the *orfE/rph* gene product, RNase PH of *Escherichia coli*. *J. Biol. Chem.*, **267**, 17147-17152.

107. Symmons, M.F., Williams, M.G., Luisi, B.F., Jones, G.H. and Carpousis, A.J. (2002) Running rings around RNA: a superfamily of phosphate-dependent RNases. *Trends Biochem. Sci.*, **27**, 11-18.

108. Jensen, K.G. (1993) The *Escherichia coli* K-12 "wild types" W3110 and MG1655 have an *rph* frameshift mutation that leads to pyrimidine starvation due to low *pyrE* expression levels. *J. Bacteriol.*, **175**, 3401-3407.

109. Yu, D. and Deutscher, M.P. (1995) Oligoribonuclease is distinct from the other known exoribonucleases of *Escherichia coli*. *J. Bacteriol.*, **177**, 4137-4139.

110. Zhang, X., Zhu, L. and Deutscher, M.P. (1998) Oligoribonuclease is encoded by a highly conserved gene in the 3'-5' exonuclease superfamily. *J. Bacteriol.*, **180**, 2779-2781.

111. Niyogi, S.K. and Datta, A.K. (1975) A novel oligoribonuclease of *Escherichia coli* I. Isolation and properties. *J. Biol. Chem.*, **250**, 7307-7312.

112. Datta, A.K. and Niyogi, K. (1975) A novel oligoribonuclease of *Escherichia coli*. II. Mechanism of action. *J. Biol. Chem.*, **250**, 7313-7319.

113. Mechold, U., Ogryzko, V., Ngo, S. and Danchin, A. (2006) Oligoribonuclease is a common downstream target of lithium-induced pAp accumulation in *Escherichia coli* and human cells. *Nucleic Acids Res.*, **34**, 2364-2373.

114. Nguyen, L.H., Erzberger, J.P., Root, J. and Wilson, D.M., 3rd. (2000) The human homolog of *Escherichia coli* Orn degrades small single-stranded RNA and DNA oligomers. *J. Biol. Chem.*, **275**, 25900-25906.

115. Koonin, E.V. (1997) A conserved ancient domain joins the growing superfamily of 3'-5' exonucleases. *Curr. Biol.*, **7**, R604-606.

116. Fang, M., Zeisberg, W.M., Condon, C., Ogryzko, V., Danchin, A. and Mechold, U. (2009) Degradation of nanoRNA is performed by multiple redundant RNases in *Bacillus subtilis*. *Nucleic Acids Res.*, **37**, 5114-5125.

117. Sello, J.K. and Buttner, M.J. (2008) The oligoribonuclease gene in *Streptomyces coelicolor* is not transcriptionally or translationally coupled to *adpA*, a key *bldA* target. *FEMS Microbiol. Lett.*, **286**, 60-65.

118. Ghosh, S. and Deutscher, M.P. (1999) Oligoribonuclease is an essential component of the mRNA decay pathway. *Proc. Natl. Acad. Sci. USA*, **96**, 4372-4377.

119. Moller, T., Franch, T., Hojrup, P., Keene, D.R., Bachinger, H.P., Brennan, R.G. and Valentin-Hansen, P. (2002) Hfq: a bacterial Sm-like protein that mediates RNA-RNA interaction. *Mol. Cell*, **9**, 23-30.

120. Brennecke, J., Stark, A., Russell, R.B. and Cohen, S.M. (2005) Principles of microRNA-target recognition. *PLoS Biology*, **3**, e85.

121. Goldman, S.R., Sharp, J.S., Vvedenskaya, I.O., Livny, J., Dove, S.L. and Nickels, B.E. (2011) NanoRNAs prime transcription initiation *in vivo*. *Mol. Cell*, **42**, 817-825.

122. August, J., Ortiz, P.J. and Hurwitz, J. (1962) Ribonucleic acid-dependent ribonucleotide incorporation. I. Purification and properties of the enzyme. *J. Biol. Chem.*, **237**, 3786-3793.

123. Cao, G.-J. and Sarkar, N. (1992) Identification of the gene for an *Escherichia coli* poly(A) polymerase. *Proc. Natl. Acad. Sci. USA*, **89**, 10380-10384.

124. Li, Z., Pandit, S. and Deutscher, M.P. (1998) Polyadenylation of stable RNA precursors *in vivo*. *Proc. Natl. Acad. Sci. USA*, **95**, 12158-12162.

125. O'Hara, E.B., Chekanova, J.A., Ingle, C.A., Kushner, Z.R., Peters, E. and Kushner, S.R. (1995) Polyadenylylation helps regulate mRNA decay in *Escherichia coli*. *Proc. Natl. Acad. Sci. USA*, **92**, 1807-1811.

126. Mohanty, B.K. and Kushner, S.R. (1999) Analysis of the function of *Escherichia coli* poly(A) polymerase I in RNA metabolism. *Mol. Microbiol.*, **34**, 1094-1108.

127. Deana, A., Celesnik, H. and Belasco, J.G. (2008) The bacterial enzyme RppH triggers messenger RNA degradation by 5' pyrophosphate removal. *Nature*, **451**, 355-358.

128. Bessman, M.J., Walsh, J.D., Dunn, C.A., Swaminathan, J., Weldon, J.E. and Shen, J. (2001) The gene ygdP, associated with the invasiveness of *Escherichia coli* K1, designates a Nudix hydrolase, Orf176, active on adenosine (5')-pentaphospho-(5')-adenosine (Ap5A). *J. Biol. Chem.*, **276**, 37834-37838.

129. Bessman, M.J., Frick, D.N. and O'Handley, S.F. (1996) The MutT proteins of "Nudix" hydrolases, a family of versatile, widely distributed "housecleaning enzymes. *J. Biol. Chem.*, **271**, 25059-25062.

130. McLennan, A.G. (2006) The Nudix hydrolase superfamily. *Cell Mol. Life Sci.*, **63**, 123-143.

131. Mejean, V., Salles, C., Bullions, L.C., Bessman, M.J. and Claverys, J.P. (1994) Characterization of the mutX gene of Streptococcus pneumoniae as a homologue of *Escherichia coli* mutT, and tentative definition of a catalytic domain of the dGTP pyrophosphohydrolases. *Mol. Microbiol.*, **11**, 323-330.

132. Zheng, Q.C., Li, Z.S., Sun, M., Zhang, Y. and Sun, C.C. (2005) Homology modeling and substrate binding study of Nudix hydrolase Ndx1 from *Thermos thermophilus* HB8. *Biochem. Biophys. Res. Commun.*, **333**, 881-887.

133. Gabelli, S.B., Bianchet, M.A., Bessman, M.J. and Amzel, L.M. (2001) The structure of ADP-ribose pyrophosphatase reveals the structural basis for the versatility of the Nudix family. *Nat. Struct. Biol.*, **8**, 467-472.

134. Messing, S.A., Gabelli, S.B., Liu, Q., Celesnik, H., Belasco, J.G., Pineiro, S.A. and Amzel, L.M. (2009) Structure and biological function of the RNA pyrophosphohydrolase BdRppH from *Bdellovibrio bacteriovorus*. *Structure*, **17**, 472-481.

135. Warner, A.H. and Finamore, F.J. (1965) Isolation, purification, and characterization of P1,P4-diguanosine 5'-tetraphosphate asymmetrical-pyrophosphohydrolase from brine shrimp eggs. *Biochemistry*, **4**, 1568-1575.

136. Guranowski, A. (2000) Specific and nonspecific enzymes involved in the catabolism of mononucleoside and dinucleoside polyphosphates. *Pharmacol. Ther.*, **87**, 117-139.

137. Gaywee, J., Xu, W., Radulovic, S., Bessman, M.J. and Azad, A.F. (2002) The *Rickettsia prowazekii* invasion gene homolog (*invA*) encodes a Nudix hydrolase active on adenosine (5')-pentaphospho-(5')-adenosine. *Mol. Cell Proteomics*, **1**, 179-185.

138. Mildvan, A.S., Xia, Z., Azurmendi, H.F., Saraswat, V., Legler, P.M., Massiah, M.A., Gabelli, S.B., Bianchet, M.A., Kang, L.W. and Amzel, L.M. (2005) Structures and mechanisms of Nudix hydrolases. *Arch. Biochem. Biophys.*, **433**, 129-143.

139. Jester, B.C., Romby, P. and Lioliou, E. (2012) When ribonucleases come into play in pathogens: a survey of Gram-positive bacteria. *Int. J. Microbiol.*, **2012**, 592196.

140. Conyers, G.B. and Bessman, M.J. (1999) The gene, *ialA*, associated with the invasion of human erythrocytes by *Bartonella bacilliformis*, designates a nudix hydrolase active on dinucleoside 5'-polyphosphates. *J. Biol. Chem.*, **274**, 1203-1206.

141. Edelstein, P.H., Hu, B., Shinzato, T., Edelstein, M.A., Xu, W. and Bessman, M.J. (2005) *Legionella pneumophila* NudA Is a Nudix hydrolase and virulence factor. *Infect. Immun.*, **73**, 6567-6576.

142. Ismail, T.M., Hart, C.A. and McLennan, A.G. (2003) Regulation of dinucleoside polyphosphate pools by the YgdP and ApaH hydrolases is essential for the ability of Salmonella enterica serovar typhimurium to invade cultured mammalian cells. *J. Biol. Chem.*, **278**, 32602-32607.

143. Richards, J., Liu, Q., Pellegrini, O., Celesnik, H., Yao, S., Bechhofer, D.H., Condon, C. and Belasco, J.G. (2011) An RNA pyrophosphohydrolase triggers 5'-exonucleolytic degradation of mRNA in *Bacillus subtilis*. *Mol. Cell*, **43**, 940-949.

144. Rendulic, S., Jagtap, P., Rosinus, A., Eppinger, M., Baar, C., Lanz, C., Keller, H., Lambert, C., Evans, K.J., Goesmann, A. *et al.* (2004) A predator unmasked: life cycle of *Bdellovibrio bacteriovorus* from a genomic perspective. *Science*, **303**, 689-692.

145. Zamecnik, P.C., Stephenson, M.L., Janeway, C.M. and Randerath, K. (1966) Enzymatic synthesis of diadenosine tetraphosphate and diadenosine triphosphate with a purified lysyl-sRNA synthetase. *Biochem. Biophys. Res. Commun.*, **24**, 91-97.

146. Jovanovic, A. and Terzic, A. (1996) Diadenosine tetraphosphate-induced inhibition of ATP-sensitive K+ channels in patches excised from ventricular myocytes. *Br. J. Pharmacol.*, **117**, 233-235.

147. Vartanian, A., Prudovsky, I., Suzuki, H., Dal Pra, I. and Kisselev, L. (1997) Opposite effects of cell differentiation and apoptosis on Ap3A/Ap4A ratio in human cell cultures. *FEBS Lett.*, **415**, 160-162.

148. Nishimura, A., Moriya, S., Ukai, H., Nagai, K., Wachi, M. and Yamada, Y. (1997) Diadenosine 5',5'''-P1,P4-tetraphosphate (Ap4A) controls the timing of cell division in *Escherichia coli*. *Genes Cells*, **2**, 401-413.

149. Johnstone, D.B. and Farr, S.B. (1991) AppppA binds to several proteins in *Escherichia coli*, including the heat shock and oxidative stress proteins DnaK, GroEL, E89, C45 and C40. *EMBO J.*, **10**, 3897-3904.

150. Varshavsky, A. (1983) Do stalled replication forks synthesize a specific alarmone? *J. Theor. Biol.*, **105**, 707-714.

151. Lienhard, G.E. and Secemski, II. (1973) P 1 ,P 5 -Di(adenosine-5')pentaphosphate, a potent multisubstrate inhibitor of adenylate kinase. *J. Biol. Chem.*, **248**, 1121-1123.

152. Dzeja, P.P., Vitkevicius, K.T., Redfield, M.M., Burnett, J.C. and Terzic, A. (1999) Adenylate kinase-catalyzed phosphotransfer in the myocardium : increased contribution in heart failure. *Circ. Res.*, **84**, 1137-1143.

153. Jovanovic, A., Alekseev, A.E. and Terzic, A. (1997) Intracellular diadenosine polyphosphates: a novel family of inhibitory ligands of the ATP-sensitive K+ channel. *Biochem. Pharmacol.*, **54**, 219-225.

154. Ripoll, C., Martin, F., Manuel Rovira, J., Pintor, J., Miras-Portugal, M.T. and Soria, B. (1996) Diadenosine polyphosphates. A novel class of glucose-induced intracellular messengers in the pancreatic beta-cell. *Diabetes*, **45**, 1431-1434.

155. Coller, J. and Parker, R. (2004) Eukaryotic mRNA decapping. *Annu. Rev. Biochem.*, **73**, 861-890.

156. Celesnik, H., Deana, A. and Belasco, J.G. (2007) Initiation of RNA decay in *Escherichia coli* by 5' pyrophosphate removal. *Mol. Cell*, **27**, 79-90.

157. Niranjanakumari, S., Stams, T., Crary, S.M., Christianson, D.W. and Fierke, C.A. (1998) Protein component of the ribozyme ribonuclease P alters substrate recognition by directly contacting precursor tRNA. *Proc. Natl. Acad. Sci. USA*, **95**, 15212-15217.

158. Koutmou, K.S., Zahler, N.H., Kurz, J.C., Campbell, F.E., Harris, M.E. and Fierke, C.A. (2010) Protein-precursor tRNA contact leads to sequence-specific recognition of 5' leaders by bacterial ribonuclease P. *J. Mol. Biol.*, **396**, 195-208.

159. Brannvall, M., Mattsson, J.G., Svard, S.G. and Kirsebom, L.A. (1998) RNase P RNA structure and cleavage reflect the primary structure of tRNA genes. *J. Mol. Biol.*, **283**, 771-783.

# CHAPTER 2

# ANALYSIS OF THE ROLE OF RNA PYROPHOSPHOHYDROLASE (RPPH) IN TRNA PROCESSING IN *ESCHERICHIA COLI*[1]

[1]Wiese, N.S., Bowden, K.E., Mohanty, B.K., and Kushner, S.R. To be submitted to *RNA*.

**ABSTRACT**

RNase E, a 5′-end dependent endoribonuclease in *Escherichia coli*, rapidly processes many mono- and polycistronic primary tRNA transcripts into pre-tRNAs that are further matured into functional tRNAs that can be aminoacylated. Since the ability of RNase E to interact with many RNA substrates is inhibited by the presence of a 5′-triphosphate, it was predicted that inactivation of RNA pyrophosphohydrolase (encoded by *rppH*) might interfere with the processing of many tRNA species. Surprisingly, although an *rppHΔ754 rph-1* mutant showed a small growth defect, RNase E-mediated tRNA processing was unaffected. However, in the absence of RppH, the 5′-end maturation of a subset of tRNAs (*pheU, pheV*, and *ileX*) by RNase P was significantly inhibited. Specifically, primary tRNA transcripts with 5′ leaders less than 5 nucleotides in length were not processed by RNase P in an *rppHΔ754 rph-1* double mutant. Surprisingly, the inhibition of 5′ processing was suppressed by either inactivation of RNase E or the presence of the 3′→5′ exonuclease RNase PH (*rph*). In fact, we demonstrate that the *rph-1* allele, a single base pair frameshift in the carboxy terminus, encodes a truncated protein that lacks exonuclease activity but interferes with the ability of RNase P to process the *pheU*, *pheV* and *ileX* precursor tRNAs.

## INTRODUCTION

In all organisms, tRNAs are synthesized as precursors that are rapidly processed by a series of ribonucleases to generate functional forms that can be charged with their corresponding amino acids. In the case of polycistronic tRNA transcripts in *E. coli*, endonucleolytic cleavages by either RNase E and/or RNase P separate the pre-tRNAs (1-5). Subsequently, the mature 5′ termini are generated by the action of RNase P (6), while exonucleolytic processing at the 3′ termini by a combination of exoribonucleases, including RNase T, RNase PH, RNase D, RNase BN, and RNase II leads to the exposure of the encoded CCA determinants (7-9). In the case of monocistronic tRNA transcripts, Rho-independent transcription terminators are generally removed by a combination of RNase E, RNase G, RNase P, or PNPase (1,4,10), while Rho-dependent transcripts have their 3′ extensions initially processed initially by a combination of RNase II and PNPase (3). Previous studies have also shown that the ability of RNase P to effectively generate a mature 5′-terminus is partially dependent on prior 3′ processing of the pre-tRNA by RNase E (1).

A potential complication in the processing of primary tRNA transcripts arises from the fact that RNase E, the endonuclease involved in separating many polycistronic tRNA transcripts (1,2), has been shown to be inhibited by the presence of a 5′-triphosphate (11-13). The 5′-triphosphorylated RNA substrates can be converted to a 5′-monophosphorylated form by the *rppH* encoded RNA pyrophosphohydrolase and that this so-called “decapping” can stimulate the further processing of certain mRNA species by RNase E (11,13-16). Based on

these observations, it seemed possible that the phosphorylation state of the 5′-terminus might play a role in the processing of primary tRNA transcripts.

In addition, numerous studies have presented evidence that RNase P also has preference for certain nucleotides and leader lengths (the region upstream of +1 nucleotide of the mature tRNA sequence) at the 5′-termini of RNA substrates (17-25). Other experiments have shown that the RNase P holoenzyme directly interacts with the 5′-leader of precursor tRNAs and the subsequent binding affinity is maintained in a leader-length dependent manner up to 4-6 nucleotides (18,19,22,25). With longer leader regions, binding affinity is maintained in a leader-length independent manner due to structural dynamics (18). *In vitro* cleavage assays have also shown that as the leader length increases, the ability of RNase P to properly cleave at +1 nucleotide of the precursor tRNA decreases (21). Taken together, these studies indicated an intricate relationship between the status of the 5'-leader of the precursor tRNA and the ability of RNase P to properly bind and cleave the pre-tRNA. Thus it appeared that 5'-end decapping by RppH could play a role in the ability of both RNase E and RNase P to properly process tRNA precursors.

Here we show that the presence of a 5′-triphosphate on primary tRNA transcripts (either polycistronic or monocistronic) does not affect the ability of RNase E to initiate their processing. In contrast, the 5′-triphosphate on short 5′-leaders significantly inhibits RNase P activity, particularly if RNase E has already processed the 3′-terminus. For example, the *pheU* and *pheV* tRNAs are monocistronic transcripts that contain Rho-independent transcription

terminators and 5′-leaders of 3-4 nt. Inactivation of RppH significantly inhibited the ability of RNase P to generate mature 5′-termini. However, the inhibition of RNase P activity was not observed if the 3′ Rho-independent transcription terminator was not removed from the primary transcript. Longer 5′-leader regions (>5 nt) were not affected by the presence of a 5′-terminal triphosphate. Furthermore, the presence of a 5′- triphosphate did not inhibit the ability of RNase P to separate polycistronic transcripts such as *valV valW* and *leuQ leuP leuV*. Surprisingly, the inhibition of RNase P processing was suppressed either by the presence of a functional RNase PH protein or if the *rph* gene were completely deleted.

## MATERIALS AND METHODS

### Bacterial strains and plasmids

The *E. coli* strains used in this study were all derived from MG1693 (*rph-1 thyA715*) (*E. coli* Genetic Stock Center, Yale University) and are listed in Table 1. This strain contains no RNase PH activity and shows reduced expression of *pyrE* due to the single nucleotide frameshift in the *rph* gene (26). An *rph*$^+$ derivative (SK10153) was constructed as previously described (8). The *rne-1* and *rnpA49* alleles encode temperature-sensitive RNase E and RNase P proteins, respectively, which are unable to support cell viability at 44°C (8,27-29). The construction of SK2525 (1), SK2534 (1), and SK5665 (29) have been previously described. SK3564 [*rneΔ1018::bla thyA715 rph-1 recA56 srlD::*Tn*10*/pDHK30(*rng-219* Sm$^r$/Sp$^r$)/pWSK219(Km$^r$)] is an RNase E deletion

strain that contains a mutant RNase G (*rng-219*) protein synthesized from a single copy plasmid that supports cell viability (30). The *rng::cat* allele is an insertion/deletion of a chloramphenicol resistance cassette into the gene encoding RNase G (31). The construction of SK2541 (32) and SK5704 has been previously described (33).

For this study, a P1 lysate grown on JW2798 (*ΔrppH::kan* Keio Collection, Japan) was used to transduce MG1693, SK2525 (*rnpA49*), SK5665 (*rne-1*), and SK2534 (*rne-1 rnpA49*) to construct SK4390 (*ΔrppH::kan*), SK4395 (*ΔrppH::kan rnpA49*), SK4394 (*ΔrppH::kan rne-1*), and SK4397 (*ΔrppH::kan rne-1 rnpA49*), respectively. SK10751 was constructed by transducing P1 lysate grown on JW3618 (*Δrph::kan* Keio Collection, Japan) into MG1693 (*rph-1 thyA715*). Plasmid pCP20 was then transformed into the cell in order to remove the kanamycin resistance cassette as previously described (34). SK10752 was constructed by transducing P1 lysate grown on JW2798 (*ΔrppH::kan* Keio Collection, Japan) into SK10751. Strains SK10755, SK10756, SK10757, SK10758 were constructed by transforming pNWK18 into MG1693 (*rph-1 thyA715*), SK4390 (*ΔrppH::kan*), SK10751, and SK10752 respectively. Plasmid pNWK18 (*rph-1*/$Cm^R$) was constructed by cloning the *rph-1* coding sequence containing its own promoter into a $Cm^R$ resistance derivative of the 6–8 copy vector pSBK29 (32) using *Pst*I-*Bam*HI sites. A PCR fragment containing the *rph-1* coding sequence was amplified using primer pairs RPH-PST and RPH-1291 and Q5™ high- fidelity DNA polymerase (NEB). pNWK18 plasmid DNA was sequenced to confirm the presence of the *rph-1* allele.

**Growth curves**

Cultures were grown with shaking in Luria broth containing thymine (50 µg/mL) and kanamycin (25 µg/mL) (when *ΔrppH::kan* was present) at 37°C until they reached 20 Klett units above background (No. 42 green filter). Subsequently, the cultures were shifted to 44°C to inactivate the temperature sensitive RNase E and RNase P proteins. Cell densities were recorded every 30 min and the cultures were maintained in mid-exponential phase (80 Klett units) by diluting with fresh pre-warmed medium. The Klett values (Fig. 1) were adjusted to reflect the appropriate dilution factors. The growth curves for MG1693 (*rph-1*) and SK10153 (*rph*$^{+}$) were carried out at 37°C and the cultures were maintained at 80 Klett units above by diluting with fresh prewarmed medium.

**Growth of bacterial strains and isolation of total RNA**

Bacterial strains were grown with shaking in at 37°C in Luria broth as described above a cell density of 20 Klett units above background (~5.0 x $10^7$ cells/ml). Cultures were then shifted to 44°C for two hours and maintained at 80 Klett units above background by diluting, if necessary, with fresh prewarmed medium. Unless otherwise noted, RNA was extracted using the method described by Stead *et al.* (35). RNA was quantified on a NanoDrop™ 2000c (Thermo Scientific) apparatus. Five hundred ng of each RNA sample were run on a 1% Agarose-Tris-acetate-EDTA gel and visualized with ethidium bromide to ensure satisfactory quality prior to further analysis.

RNA to be used in primer extensions, RT-PCR cloning, and sequencing experiments was further treated with the DNA-free kit™ (Ambion) to remove any contaminating DNA. In some cases the RNA used in the initial RT-PCR cloning experiments was isolated using the Trizol® Reagent (Invitrogen) as described by the manufacturer. Subsequently, RNA isolated by both methods was directly compared in a series of Northern analyses and PCR cloning and sequencing experiments that demonstrated the comparability of both methods (data not shown).

**Northern analysis**

Northern analysis was performed as previously described in O'Hara *et al.* (33). Five µg of total RNA were run on either 6% or 8% polyacrylamide-8.3 M urea gels and transferred to a positively charged nylon membrane (Nytran® SPC, Whatman®) for 2.5 hours at 20 volts followed 45 minutes at 40 volts. Northern blots were probed with $^{32}$P-5'-end-labeled oligonucleotides (36) specific to the mature sequence of each tRNA being tested. The probe sequences are available on request. Each blot was scanned with a PhosphorImager (Storm™ 840, GE Healthcare) and the data were quantified using ImageQuant TL 5.2 software (GE Healthcare).

**Primer extension analysis**

Primer extension analysis of various tRNA transcripts was carried out as previously described (3). The sequences were analyzed on a 6% PAGE containing 8 M urea.

**RT-PCR cloning and sequencing of 5'-3' self-ligated transcripts**

The 5′ and 3′-ends of the *pheU, pheV* and *ileX* transcripts were identified by cloning and sequencing the RT-PCR products obtained from 5′→3′ end-ligated circular RNAs following the methods previously described (4). The 5′–3′ junctions of the cDNAs were amplified with pairs of gene-specific primers using Q5™ high- fidelity DNA polymerase (NEB).

**Immunoprecipitation analysis**

Strains were grown at 37°C with shaking at 255 rpm to Klett 80 in Luria broth supplemented with thymine (50 µg/mL) and antibiotic, where appropriate. Cell cultures (50 mL) were collected for protein isolation and quantified as described previously (17). Immunoprecipitations were performed at 4°C by mixing one mg of total protein and RNase PH antibody cross-linked to Pierce Protein A/G magnetic beads (Thermo Scientific; 25 µl) for 1 hour in a shaker. The protein-bead complexes were washed three times with RIPA buffer (150mM NaCl, 50 mM Tris-HCl pH 8, 1.0% Nonidet P-40, 0.5% DOC, 0.1% SDS). The immunocomplexes were subsequently eluted from the beads in 40 µl of the SDS-PAGE loading buffer after heating at 55°C for 15 min, followed by boiling

for 5 min. Co-immunoprecipitation samples were separated on 12% (for RNase PH and RppH) SDS-PAGE gels and transferred to PVDF membranes (Immobilon TM-P; Millipore) using a Bio-Rad Mini-Protean 3 electrophoretic apparatus. The membranes were probed with either RNase PH antibody (1:10,000 dilution) or RppH antibody (1:5,000 dilution) using the ECL PlusTM Western Blotting Detection Kit (GE Healthcare) per manufacturer instructions. The RNase PH and RppH MAP antibodies were raised against RNase PH and RppH-specific peptides, respectively, by GenScript USA Inc, NJ.

## RESULTS

### Physiological properties of *ΔrppH* strains

In order to examine the phenotypic properties of strains defective in converting 5′-terminal triphosphates into 5′-phosphomonoesters, we constructed an isogenic set of strains in the MG1693 (*rph-1 thyA715*) genetic background using a complete deletion/insertion of the structural gene for RNA pyrophosphohydrolase (*rppHΔ754::kan*) and temperature sensitive alleles for both RNase E [*rne-1*(37)] and RNase P [*rnpA49* (27)] as described in the Materials and Methods. Since both RNase E and RNase P have been shown to play a major role in the processing of primary tRNA transcripts (1-4,10) and previous work by Deana et al. (15) showed that the conversion of the 5′-triphosphate to a 5′-monophosphoester by RppH stimulated RNase E-mediated mRNA decay, we hypothesized that strains carrying the *ΔrppH* allele would have growth defects. In fact, there was a significant growth defect in the *rppHΔ754*

*rph-1* strain compared to the *rph-1* control at 44°C (Fig. 1). Furthermore, in the *rppHΔ754 rne-1 rph-1* and *rppHΔ754 rnpA49 rph-1* multiple mutants, deletion of RppH exacerbated the conditional lethality associated with the inactivation of either RNase E or RNase P (Fig. 1). Thus, as seen previously, the *rne-1* single mutant continued to grow for several hours after the shift to 44°C as did the *rnpA49* single mutant (29), but both double mutants showed a more dramatic secession of growth and reduced final cell densities (Fig. 1). The most striking phenotype was observed in the *rne-1 rnpA49 rppHΔ754 rph-1* quadruple mutant, where growth ceased within 30 min after the shift to the nonpermissive temperature (Fig. 1).

**Failure to remove the 5'-terminal triphosphate does not inhibit RNase E processing of primary polycistronic tRNA transcripts**

It has been shown previously that RNase E is responsible for separating a significant number of polycistronic transcripts (*glyW cysT leuZ*, *argX hisR leuT proM*) into pre-tRNAs that can be further processed into mature species (1,2). Since most tRNA precursors are processed very rapidly, with half-lives estimated to be <30 seconds (1) and it has been shown that RNase E is a 5′-end-dependent endonuclease that is inhibited by a 5′-triphosphate (11-15), we expected to see an inhibition of processing of these primary transcripts in the *rppHΔ754 rph-1* mutant. However, as shown in Fig. 2 (lane 4), deletion of RppH did not alter the processing of the *argX hisR leuT proM* primary transcript. In contrast, inactivation of RNase E led to the appearance of the primary transcript

as well as a number of partially processed intermediates (Fig. 2B, lane 3). Furthermore, inactivation of RNase P led to the expected accumulation of a histidine pre-tRNA that retained its 5′ leader sequences (Fig. 2B, lane 2). The processing of the transcript in the *rne-1 rppHΔ754 rph-1* triple mutant was very similar to what was observed in the *rne-1 rph-1* double mutant (Fig. 2B, lanes 3 & 5). Comparable results were observed for the *glyW cysT leuZ* transcript (data not shown).

**Inactivation of RppH does not affect the processing of polycistronic tRNA transcripts by RNase P**

Recently it has been shown that a number of primary polycistronic tRNA transcripts, including *valV valW, leuQ leuP leuV*, the *valU,* and *lysT* operons, are separated into pre-tRNAs exclusively by RNase P (3-5). Accordingly, we tested to see if failure to remove the 5′-terminal triphosphate might affect the processing of polycistronic transcripts by RNase P. As shown previously, the *valV valW* operon is rapidly processed in an RNase P-dependent fashion (Fig. 3, lanes 1 & 2) that does not involve the activity of RNase E (Fig. 3, lane 3). Significantly, inactivation of RppH did not affect the processing of the *valV valW* transcript (Fig. 3, lane 4). Furthermore, the processing profile was also not changed in the *rppHΔ754 rnpA49 rph-1* triple mutant (Fig. 3, lane 5). Similar results were observed with the *leuQ leuP leuV* operon (data not shown).

**RppH does not affect the maturation of monocistronic tRNA precursors with 5′-leaders >8-10 nucleotides**

Since the failure to convert the terminal triphosphate to a monophosphate by RppH had no effect on the processing of polycistronic tRNA transcripts, we also examined the processing of several monocistronic tRNA transcripts. Initially we tested the *leuX* transcript, which has been shown to have a 22 nucleotide 5′-leader that is removed by RNase P, and a Rho-independent transcription terminator that is processed primarily by the 3′→5′ exonuclease polynucleotide phosphorylase (PNPase) (10). As observed with the polycistronic transcripts (Figs. 2, 3), inactivation of RppH did not affect the processing of the *leuX* primary transcript (Fig. 4, lane 4). In addition, the processing profile in the *rppHΔ754 rnpA49 rph-1* triple mutant was identical to what was observed with the *rnpA49 rph-1 double* mutant (Fig. 4, lanes 4 & 5).

Subsequently, we tested the processing of the four *asn* tRNA precursors (*asnT, asnU, asnV*, and *asnW*), which have been shown to have ~9-10 nucleotide 5′-leaders that are removed by RNase P (1). Removal of the 3′ Rho-independent transcription terminators is partially dependent on RNase E (1). In the case of these four monocistronic transcripts, we expected to see precursors accumulate in the presence of a 5′-triphosphate that inhibited either RNase E or RNase P activity. However, as shown in Fig. 5 (lane 2), inactivation of RppH had no effect on *asn* tRNA processing. In contrast, inactivation of RNase P led to the accumulation of precursor species that retained their 5′-leader sequences (Fig. 5, lane 4), while inactivation of RNase E led to the appearance of transcripts

that retained their Rho-independent transcription terminators (Fig. 5, lane 3). The most significant change in the processing of the four *asn* tRNAs transcripts occurred in the *rppHΔ754 rne-1 rnpA49 rph-1* quadruple mutant (Fig. 5, lane 7).

**Inactivation of RppH inhibits the 5′-end maturation of the *pheU* and *pheV* primary transcripts**

Based on the data presented in Figs. 2-5, it appeared that the presence of a 5′-triphosphate on primary tRNA transcripts did not interfere with their processing by either RNase E or RNase P. However, as previously mentioned, the RNase P holoenzyme interacts with the 5′-leader and proper cleavage is dependent on its length (18,19,21,25). Accordingly, we hypothesized that primary tRNA transcripts with 5′-leaders of less than five nucleotides might demonstrate an RppH effect. Accordingly, we focused on the *pheU* and *pheV* transcripts, which have predicted 5′-leaders of less than five nucleotides (1). Both are monocistronic transcripts that have the same mature tRNA sequence and use RNase P and RNase E to process their 5′- and 3′-termini, respectively [Fig. 6A, (1)]. Since the presence of a 5′-triphosphate did not affect RNase E-dependent 3′-maturation of other monocistronic tRNA precursors (Fig. 4, 5), we were not surprised that this observation also held true for the *pheU* and *pheV* transcripts, where no full-length transcripts were observed in the absence of RppH (Fig. 6B, lane 2). These results contrasted to what was observed in the *rne-1* strain, where we saw a small amount of full-length transcript in addition to the mature species (Fig. 6B, lane 4), in agreement with previously published results (1).

However, in the absence of RppH we observed a processing intermediate that was several nucleotides longer than the mature species (Fig. 6B, lane 2) and appeared to be comparable to the species observed in an *rnpA49 rph-1* double mutant (Fig. 6B, lane 3). Surprisingly, in the *rppHΔ754 rne-1 rph-1* triple mutant, the processing intermediate disappeared (Fig. 6B, lane 5). Furthermore, while the combination of *rppHΔ754 rnpA49 rph-1* alleles gave the same processing profile as the *rnpA49 rph-1* double mutant (Fig. 6B, lanes 3 & 6), the further inactivation of RNase E significantly changed the processing profile (Fig. 6B, lane 7).

**The 5′-leaders of the *pheU* and *pheV* transcripts are not processed in the absence of RppH**

Since the longer intermediates observed in the absence of RppH could have arisen from a failure to process properly either at the 5′- or 3′-terminus, we carried out primer extension analysis using RNA isolated from wild type *rppHΔ754 rph-1* and *rnpA49 rph-1* strains (Fig. 7). Although it has been reported that the transcription start sites of both *pheU* and *pheV* are only one nucleotide upstream of the mature 5′-terminus (38), our data clearly demonstrated that transcription starts at two sites, either 3 or 4 nucleotides upstream of the mature 5′-terminus (Fig. 7). As expected, in the absence of RNase P, almost all of the *pheU* and *pheV* tRNAs retained their 5′ leaders and there appeared to be almost equal amounts of the two transcription products (Fig. 7, lanes 5 & 6). Although inactivation of RppH did not completely block 5′-

end maturation by RNase P, the majority of the *pheU* and *pheV* species retained their primary 5′ sequences (Fig. 7, lanes 3 & 4). It should also be noted that in the *rph-1* control strain, approximately 20% of the mature *pheU* and *pheV* tRNAs contained an extra nucleotide at the 5' terminus.

**Analysis of the 5′- and 3′-termini of the *pheU* and *pheV* transcripts using RNA ligation and RT-PCR**

We have previously used an RNA self-ligation procedure to map the 5′- and 3′-ends of specific tRNA transcripts in various genetic backgrounds (4,8,10). In the case of the *pheU* and *pheV* transcripts, differences in the 3′ downstream sequences made it possible for us to distinguish between the two primary sequences (Fig. 8). Initially, we examined tRNAs isolated from MG1693 (*rph-1*). As shown in Fig. 8A in MG1693, 86% of the clones had mature 5′-termini. The other clones had anywhere from 1-4 extra nucleotides at the 5′-terminus. Interestingly, only a small fraction of the clones had mature 3′-termini, with many having 1-3 downstream nucleotides, supporting previous data suggesting that RNase E cleaves several nucleotides downstream of the mature CCA terminus (1). A higher percentage of mature 3′-termini were observed in SK10153 (wild type) indicating that RNase PH plays a significant role in the final maturation of the *pheU* and *pheV* transcripts (data not shown).

Since both the northern analysis (Fig. 6) and primer extension data (Fig. 7) suggested that most of the *pheU* and *pheV* transcripts had immature 5′-termini, we next examined RNA isolated from an *rnpA49* mutant that had been shifted to

44°C to inactivate RNase P. Of the 21 independent clones sequenced, only one had a mature 5′-terminus (Fig. 8C). The remainder of the clones had 2-4 extra nucleotides at their 5′-ends. In addition, 52% of the clones had mature 3′-termini compared to 11% in the *rph-1* single mutant.

When we analyzed the RNA isolated from the *rppHΔ754 rph-1* mutant, the data again confirmed the results shown in Figs. 6-7. Specifically, 52% of the clones had 3 extra nucleotides at their 5′-termini (Fig. 8B). The data from the 3′-terminus was comparable to what was seen with the *rnpA49 rph-1* double mutant. It should also be noted that a small fraction (between 8-14%) of the clones in the various genetic backgrounds had short poly(A) tails added to immature 3′-termini, in agreement with previously reported results (8).

After identifying that the *rph-1* allele produces a truncated protein, we examined the 5′- and 3′-termini of the *pheU* and *pheV* transcripts in both a *Δrph* and *Δrph Δrpph* background in order to ascertain whether or not the Rph-1 truncation could have an effect on processing. In the *Δrph Δrpph* mutant, the overwhelming majority of clones (93%) contained the mature 5′-terminus (Fig. 8D) in stark contrast to the *rppHΔ754 rph-1* mutant (48%) (Fig. 8C) as corroborated by the northern analysis (Fig. 6C, lanes 3 & 6). Analysis of the 3′-termini in the *Δrph Δrpph* mutant yielded comparable results (Fig. 8E) to the processing profile observed in the *rppHΔ754 rph-1* mutant (Fig. 8B).

**Inactivation of RNase E suppresses the inhibition of RNase P activity on the *pheU* and *pheV* transcripts in the absence of RppH**

As previously seen in the northern analysis of the *pheU* and *pheV* transcripts, inactivation of RNase E appears to suppress the effect of the *rppHΔ754* allele on the 5′-end maturation of the transcripts (Fig. 6B, lane 5). Of the 40 clones obtained from an *rne-1 rph-1* strain, 70% had mature 5′-termini (data not shown). In addition, as expected a few contained the entire Rho-independent transcription terminator (date not shown). In the *rppHΔ754 rne-1 rph-1 triple mutant,* 78% (23/30) of the clones had mature 5′-termini compared to 46% (18/41) in the *rppHΔ754 rph-1* double mutant (data not shown).

**RppH affects the processing of the monocistronic *ileX* transcript**

Since inactivation of RppH inhibited the 5′-end processing of the *pheU* and *pheV* primary transcripts (Fig. 6), we also examined the *ileX* transcript, which has a predicted leader of a single nucleotide (38). Northern analysis suggested that all of the strains retained a much longer *ileX* transcript, which most likely contained the Rho-independent transcription terminator as well as a slightly longer species than the mature transcript in the *rph-1*, *Δrpph rph-1, Δrph, Δrph ΔrppH,* and *rnpA49 rph-1* strains (Fig. 9, lanes 1, 3, 5–7). Since the difference in the electrophoretic mobility between the various species in the above mentioned strains was very small, we used the RNA self-ligation assay described above to

determine the 5′- and 3′-termini of the *ileX* transcripts isolated from the various strains.

In the *rph-1* single mutant, the bulk of the clones had mature 5′-termini, with only 12% of the clones having 1-2 extra nucleotides at the 5′-terminus (Fig. 10A). Interestingly, a number of the clones retained the complete Rho-independent transcription terminator. In contrast, in the absence of RppH, most of the clones (86%) had immature 5′-termini that contained 1-4 extra nucleotides (Fig. 10B). Similar results were seen in the *rnpA49 rph-1* double mutant (Fig. 10C). Surprisingly, in both the *rppHΔ754 rph-1* and *rnpA49 rph-1* mutants, many of the clones had truncated 3′-termini (Fig. 10B & C). These results were not observed for the *pheU* and *pheV* transcripts (Fig. 8) or with the previously published data from *leuX* (10).

In the *Δrph* single mutant only 40% of clones had mature 5′-termini, with the remainder (60%) having 1–3 extra nucleotides at the 5′-terminus (Fig. 10D), counter to the results seen in the *rph-1* (Fig. 10A) strain, and more similar to the results observed in the *Δrpph Δrph* double mutant (Fig. 10E). Upon analyzing the 3′-termini of the transcript of the *Δrph* single mutant, 71% of the clones had immature 3′-termini containing 1–3 extra nucleotides downstream of the CCA determinant (Fig. 10D). As observed in the *rph-1* strain, 29% of the clones in the *Δrph* single mutant retained a portion of the Rho-independent transcription terminator (Fig. 10D).

Lastly, we analyzed the ligation products of the *Δrpph Δrph* double mutant. Approximately 44% of the clones sequenced contained the mature 5′-

termini and the remainder (54%) of the clones contained 2 or 3 extra nucleotides at the 5′-termini (Fig. 10E). A little less than half of the clones sequenced contained mature 3′-termini (44%) and 39% contained 1–2 extra nucleotides downstream. As observed in the northern blot (Fig. 9) and supported by the sequence data, 16% of the clones isolated in the *Δrpph Δrph* double mutant retained the complete Rho-independent transcription terminator (in addition to other strains sequenced), providing further evidence that the *ileX* transcript is not processed as efficiently as other tRNA transcripts.

**The presence of the *rph-1* allele inhibits RNase P activity on the *pheU* and *pheV* pre-tRNAs**

As shown in Fig. 6 and confirmed in Fig. 8A, RNase PH plays an important role particularly in the final maturation of the *pheV* pre-tRNA. Accordingly, we reexamined the maturation of the *pheU* and *pheV* tRNAs in strains encoding wild type RNase PH. The presence of a functional RNase PH protein led to the disappearance of the slightly larger mature transcript (Fig. 6C, lane 2). However, to our surprise in the *rppHΔ754 rph*$^{+}$ as well as the *rppHΔ754 Δrph* strain, RNase P processing of the 5′-termini was no longer inhibited (Fig. 6C, lanes 3–6).

**The *rph-1* allele encodes a truncated protein**

For many years, the analysis of RNA metabolism in *E. coli* has used derivatives of MG1655 as their control “wild-type” strain. However, in reality MG1655

contains a single base pair deletion in the structural gene for RNase PH (26) known as *rph-1*. It is commonly believed that the *rph-1* allele has no enzymatic activity and produces no noticeable levels of RNase PH (26). However, numerous western blots conducted in our laboratory suggested the presence of a possible truncated protein (data not shown). In order to rule out the possibility that the band observed in an *rph-1* background was due to non-specific hybridization from the RNase PH antibody, a *Δrph* allele was transduced into MG1693. As shown in Fig. 12, the band in an *rph-1* background (lanes 1 & 2), which is ~2–3 kD smaller in size than wild-type RNase PH (lanes 3 & 4), disappeared in a *Δrph* strain (lanes 5 & 6).

**RNase PH and RppH do not appear to physically interact**

After verifying that the *rph-1* allele produces a truncated protein, we hypothesized that the Rph-1 protein might retain some residual exonuclease activity or could play a structural role in conjunction with RppH that would affect RNase P processing at the 5′-end of *pheU* and *pheV* transcripts. Therefore co-immunoprecipitation experiments were performed in order to discover any potential protein-protein interactions. However, we observed no interactions between RNase PH and RppH (Fig. 11, lanes 2 & 5).

**Overexpression of Rph-1 does not exacerbate *pheU* and *pheV* processing**

Since the *rph-1* allele leads to a low level of truncated protein, we hypothesized that overexpression of Rph-1 from a plasmid might result in increased inhibition

of RNase P activity on the *pheU* and *pheV* pre-tRNAs. Accordingly, the *rph-1* allele under the control of its native promoter was cloned into a 6–8 copy number plasmid as described in methods and transformed to make strains SK10755, SK10756, SK10757, and SK10758. These strains were ran alongside their parent strains on a western blot and every lane where Rph-1 was being overexpressed (Fig. 13, lanes 2, 4, 6 & 8) showed at least a 10-fold increase in protein level. However, as shown in Fig. 6D, increased expression of the Rph-1 protein did not lead to further inhibition of RNase P processing at the 5′-termini of the *pheU* and *pheV* pre-tRNAs.

**DISCUSSION**

Previous work has confirmed that the conversion of the 5′-triphosphate to a 5′-monophosphate by RppH triggers RNase E activity in the mRNA decay pathway (11,13-15). Here we report that this is not the case for its interactions with tRNA transcripts. We also present evidence that presence of the 5′-triphosphate does not inhibit processing of polycistronic operons that are RNase E and RNase P dependent as well as in monocistronic operons where the 5′-leader length is greater than 8–10 nucleotides (Figs. 2–6). Additionally we also show that 5′-leader removal by RNase P is inhibited by the presence of the 5′-triphosphate when the leader is less than 5 nucleotides, but only when the Rph-1 truncated protein is present in the cell.

Evidence supporting these claims can be observed through the analysis of the growth properties of the various mutant strains. Initially we expected the

*ΔrppH rne-1 rph-1* triple mutant to grow much more slowly than the *ΔrppH rnpA49 rph-1* triple mutant given the fact that RNase E activity is dependent on 5′-triphosphate removal by RppH (15). Our results, however, failed to validate this hypothesis. In fact, the *ΔrppH rne-1 rph-1* triple mutant grew better than the *ΔrppH rnpA49 rph-1* triple mutant (Fig. 1), perhaps due to the fact that $tRNA^{phe}$ processing is significantly inhibited in the triple mutant strain.

We observed no dependence of 5′-triphosphate removal for RNase E to function in tRNA maturation. For polycistronic operons, processing by RNase E in the *ΔrppH* mutant proceeded normally; no full-length tRNA precursors were observed (Figs. 2 & 3). These results also held true for monocistronic tRNA precursors with Rho-independent transcription terminators that are normally removed by RNase E (Figs. 4 & 5). Surprisingly, however, was the trend that the *rne-1* mutation suppressed the *ΔrppH* mutation (Fig. 6). These data indicate that RNase E may cleave internally when the 5′-triphosphate is present on the leader. Further experimentation will have to be conducted to verify if this scenario is accurate.

When analyzing the processing of the *pheU* and *pheV* monocistronic operons, we observed an intermediate effect in the *ΔrppH rph-1* double mutant when compared to the *rnpA49 rph-1* mutant (Figs. 6, 7, & 8). Interestingly, this observation was only apparent in the presence of the Rph-1 truncated protein (Fig. 6B & C). When RNase PH was either present or completely absent in the cell, RNase P processing of *pheU* and *pheV* was not inhibited (Fig. 6C). We also showed that even in the presence of excess Rph-1 (Fig. 6D) there was no

exacerbation of the phenotype observed in the *ΔrppH rph- 1* mutant (Fig. 6B & C). Removing the RNase PH truncated protein somehow allowed RNase P to process the 5′-end of the *pheU* and *pheV* transcripts more efficiently, even in the absence of RppH. We also provided evidence that Rph-1 and RppH may not physically interact (Fig. 11), which could have provided an explanation as to the presence of the processing intermediate. Our data suggest that Rph-1 may bind tightly to the 3′-end of the transcripts and prevent 3′-end processing, which could have an effect on processing by RNase P as evidenced by the knowledge that RNase P activity is dependent on 3′-end processing (1).

**ACKNOWLEDGEMENTS**

This work was supported in part by a grant from the National Institutes of Health (GM081544) to S.R.K.

**REFERENCES**

1. Ow, M.C. and Kushner, S.R. (2002) Initiation of tRNA maturation by RNase E is essential for cell viability in *E. coli*. *Genes Dev.*, **16**, 1102-1115.
2. Li, Z. and Deutscher, M.P. (2002) RNase E plays an essential role in the maturation of *Escherichia coli* tRNA precursors. *RNA*, **8**, 97-109.
3. Mohanty, B.K. and Kushner, S.R. (2007) Ribonuclease P processes polycistronic tRNA transcripts in *Escherichia coli* independent of ribonuclease E. *Nucleic Acids Res.*, **35**, 7614-7625.

4. Mohanty, B.K. and Kushner, S.R. (2008) Rho-independent transcription terminators inhibit RNase P processing of the *secG leuU* and *metT* tRNA polycistronic transcripts in *Escherichia coli*. *Nucleic Acids Res.*, **36**, 364-375.

5. Agrawal, A., Mohanty, B.K. and Kushner, S.R. (2014) Processing of the seven valine tRNAs in *Escherichia coli* involves novel features of RNase P. *Nucleic Acids Res.*, **42**, 11166-11179.

6. Lundberg, U. and Altman, S. (1995) Processing of the precursor to the catalytic RNA subunit of RNase P from *Escherichia coli*. *RNA*, **1**, 327-334.

7. Reuven, N.B. and Deutscher, M.P. (1993) Multiple exoribonucleases are required for the 3' processing of *Escherichia coli* tRNA precursors *in vivo*. *FASEB J.*, **7**, 143-148.

8. Mohanty, B.K., Maples, V.F. and Kushner, S.R. (2012) Polyadenylation helps regulate functional tRNA levels in *Escherichia coli*. *Nucleic Acids Res.*, **40**, 4589-4603.

9. Li, Z. and Deutscher, M.P. (1996) Maturation pathways for *E. coli* tRNA precursors: a random multienzyme process *in vivo*. *Cell*, **86**, 503-512.

10. Mohanty, B.K. and Kushner, S.R. (2010) Processing of the *Escherichia coli leuX* tRNA transcript, encoding $tRNA^{leu5}$, requires either the 3'-5' exoribonuclease polynucleotide phosphorylase or RNase P to remove the Rho-independent transcription terminator. *Nucleic Acids Res.*, **38**, 5306-5318.

11. Mackie, G.A. (1998) Ribonuclease E is a 5'-end-dependent endonuclease. *Nature*, **395**, 720-723.

12. Mackie, G.A. (2000) Stabilization of circular *rpsT* mRNA demonstrates the 5'-end dependence of RNase E action *in vivo*. *J. Biol. Chem.*, **275**, 25069-25072.

13. Jiang, X. and Belasco, J.G. (2004) Catalytic activation of multimeric RNase E and RNase G by 5'-monophosphorylated RNA. *Proc. Natl. Acad. Sci. USA*, **101**, 9211-9216.

14. Celesnik, H., Deana, A. and Belasco, J.G. (2007) Initiation of RNA decay in *Escherichia coli* by 5' pyrophosphate removal. *Mol. Cell*, **27**, 79-90.

15. Deana, A., Celesnik, H. and Belasco, J.G. (2008) The bacterial enzyme RppH triggers messenger RNA degradation by 5' pyrophosphate removal. *Nature*, **451**, 355-358.

16. Foley, P.L., Hsieh, P.K., Luciano, D.J. and Belasco, J.G. (2015) Specificity and Evolutionary Conservation of the *Escherichia coli* RNA Pyrophosphohydrolase RppH. *J. Biol. Chem.*

17. Kazantsev, A.V., Krivenko, A.A. and Pace, N.R. (2009) Mapping metal-binding sites in the catalytic domain of bacterial RNase P RNA. *RNA*, **15**, 266-276.

18. Rueda, D., Hsieh, J., Day-Storms, J.J., Fierke, C.A. and Walter, N.G. (2005) The 5' leader of precursor tRNAAsp bound to the *Bacillus subtilis*

RNase P holoenzyme has an extended conformation. *Biochem.*, **44**, 16130-16139.

19. Niranjanakumari, S., Stams, T., Crary, S.M., Christianson, D.W. and Fierke, C.A. (1998) Protein component of the ribozyme ribonuclease P alters substrate recognition by directly contacting precursor tRNA. *Proc. Natl. Acad. Sci. USA*, **95**, 15212-15217.
20. Guerrier-Takada, C. and Altman, S. (1993) A physical assay for and kinetic analysis of the interactions between M1 RNA and tRNA precursor substrates. *Biochem.*, **32**, 7152-7161.
21. Brannvall, M., Mattsson, J.G., Svard, S.G. and Kirsebom, L.A. (1998) RNase P RNA structure and cleavage reflect the primary structure of tRNA genes. *J. Mol. Biol.*, **283**, 771-783.
22. McClain, W.H., Lai, L.B. and Gopalan, V. (2010) Trials, travails and triumphs: an account of RNA catalysis in RNase P. *J. Mol. Biol.*, **397**, 627-646.
23. Li, H. (2007) Complexes of tRNA and maturation enzymes: shaping up for translation. *Curr. Opin. Struct. Biol.*, **17**, 293-301.
24. Hartmann, R.K., Gossringer, M., Spath, B., Fischer, S. and Marchfelder, A. (2009) The making of tRNAs and more - RNase P and tRNase Z. *Prog. Mol. Biol. Transl. Sci.*, **85**, 319-368.
25. Koutmou, K.S., Zahler, N.H., Kurz, J.C., Campbell, F.E., Harris, M.E. and Fierke, C.A. (2010) Protein-precursor tRNA contact leads to sequence-

specific recognition of 5' leaders by bacterial ribonuclease P. *J. Mol. Biol.*, **396**, 195-208.

26. Jensen, K.G. (1993) The *Escherichia coli* K-12 "wild types" W3110 and MG1655 have an *rph* frameshift mutation that leads to pyrimidine starvation due to low *pyrE* expression levels. *J. Bacteriol.*, **175**, 3401-3407.

27. Schedl, P. and Primakoff, P. (1973) Mutants of *Escherichia coli* thermosensitive for the synthesis of transfer RNA. *Proc. Natl. Acad. Sci. USA*, **70**, 2091-2095.

28. Ono, M. and Kuwano, M. (1979) A conditional lethal mutation in an *Escherichia coli* strain with a longer chemical lifetime of mRNA. *J. Mol. Biol.*, **129**, 343-357.

29. Arraiano, C.M., Yancey, S.D. and Kushner, S.R. (1988) Stabilization of discrete mRNA breakdown products in *ams pnp rnb* multiple mutants of *Escherichia coli* K-12. *J. Bacteriol.*, **170**, 4625-4633.

30. Chung, D.-H., Min, Z., Wang, B.-C. and Kushner, S.R. (2010) Single amino acid changes in the predicted RNase H domain of *E. coli* RNase G lead to the complementation of RNase E mutants. *RNA*, **16**, 1371-1385.

31. Wachi, M., Umitsuki, G. and Nagai, K. (1997) Functional relationship between *Escherichia coli* RNase E and the CafA protein. *Molecular Genetics and Genomics*, **253**, 515-519.

32. Ow, M.C., Perwez, T. and Kushner, S.R. (2003) RNase G of *Escherichia coli* exhibits only limited functional overlap with its essential homologue, RNase E. *Mol. Microbiol.*, **49**, 607-622.

33. O'Hara, E.B., Chekanova, J.A., Ingle, C.A., Kushner, Z.R., Peters, E. and Kushner, S.R. (1995) Polyadenylylation helps regulate mRNA decay in *Escherichia coli*. *Proc. Natl. Acad. Sci. USA*, **92**, 1807-1811.

34. Cherepanov, P.P. and Wackernagel, W. (1995) Gene disruption in *Escherichia coli*: TcR and KmR cassettes with the option of Flp-catalyzed excision of the antibiotic-resistance determinant. *Gene*, **158**, 9-14.

35. Stead, M.B., Agrawal, A., Bowden, K.E., Nasir, R., Mohanty, B.K., Meagher, R.B. and Kushner, S.R. (2012) RNA*snap*: a rapid, quantitative and inexpensive, method for isolating total RNA from bacteria. *Nucleic Acids Res.*, **40**, e156.

36. Mohanty, B.K., Giladi, H., Maples, V.F. and Kushner, S.R. (2008) Analysis of RNA decay, processing, and polyadenylation in *Escherichia coli* and other prokaryotes. *Methods Enzymol.*, **447**, 3-29.

37. Babitzke, P. and Kushner, S.R. (1991) The Ams (altered mRNA stability) protein and ribonuclease E are encoded by the same structural gene of *Escherichia coli*. *Proc. Natl. Acad. Sci. USA*, **88**, 1-5.

38. Keseler, I.M., Bonavides-Martinez, C., Collado-Vides, J., Gama-Castro, S., Gunsalus, R.P., Johnson, D.A., Krummenacker, M., Nolan, L.M.,

Paley, S., Paulsen, I.T. *et al.* (2009) EcoCyc: a comprehensive view of *Escherichia coli* biology. *Nucleic Acids Res.*, **37**, D464-470.

Table 1. Bacterial strains used in this work.

| Strains | Genotype | Reference/source |
|---|---|---|
| MG1693 | *thyA715 rph-1* | *E. coli* Genetic Stock Center |
| SK10153 | *thyA715 rph*$^{+}$ | (8) |
| SK2525 | *rnpA49 thyA715 rph-1 rbsD296::*Tn*10* Tc$^{r}$ | (1) |
| SK2534 | *rne-1 rnpA49 thyA715 rph-1 rbsD296::*Tn*10* Tc$^{r}$ | (1) |
| SK2541 | *rne-1 rng::cat thyA715 rph-1* Km$^{r}$ | (32) |
| SK3564 | *rneΔ1018::bla thyA715 rph-1 recA56 srlD::*Tn*10*/pDHK30(*rng219* Sm$^{r}$/Sp$^{r}$)/ pWSK219(Km$^{r}$) | (30) |
| SK4390 | *ΔrppH::kan thyA715 rph-1* | This study |
| SK4394 | *ΔrppH::kan rne-1 thyA715 rph-1* | This study |
| SK4395 | *ΔrppH::kan rnpA49 thyA715 rph-1 rbsD296::*Tn*10* Km$^{r}$/Tc$^{r}$ | This study |
| SK4397 | *ΔrppH::kan rne-1 rnpA49 thyA715 rph-1 rbsD296::*Tn*10* Km$^{r}$/Tc$^{r}$ | This study |
| SK5665 | *rne-1 thyA715 rph-1* | (29) |
| SK10751 | *Δrph thyA715* | This study |
| SK10752 | *Δrph ΔrppH::kan thyA715* | This study |
| SK10755 | *thyA715 rph-1*/pNWK18 (*rph-1*/Cm$^{R}$) | This study |

| | | |
|---|---|---|
| SK10756 | *ΔrppH::kan thyA715 rph*-1/pNWK18 (*rph-1*/$Cm^R$) | This study |
| SK10757 | *Δrph thyA715*/pNWK18 (*rph-1*/$Cm^R$) | This study |
| SK10758 | *Δrph ΔrppH::kan thyA715*/pNWK18 (*rph-1*/$Cm^R$) | This study |

Figure 1. Growth curves of strain carrying the *rphΔ754, rne-1* and *rnpA49* alleles.

Growth curves were conducted as described in Materials and Methods. The legend identifying each strain is located within the growth curve.

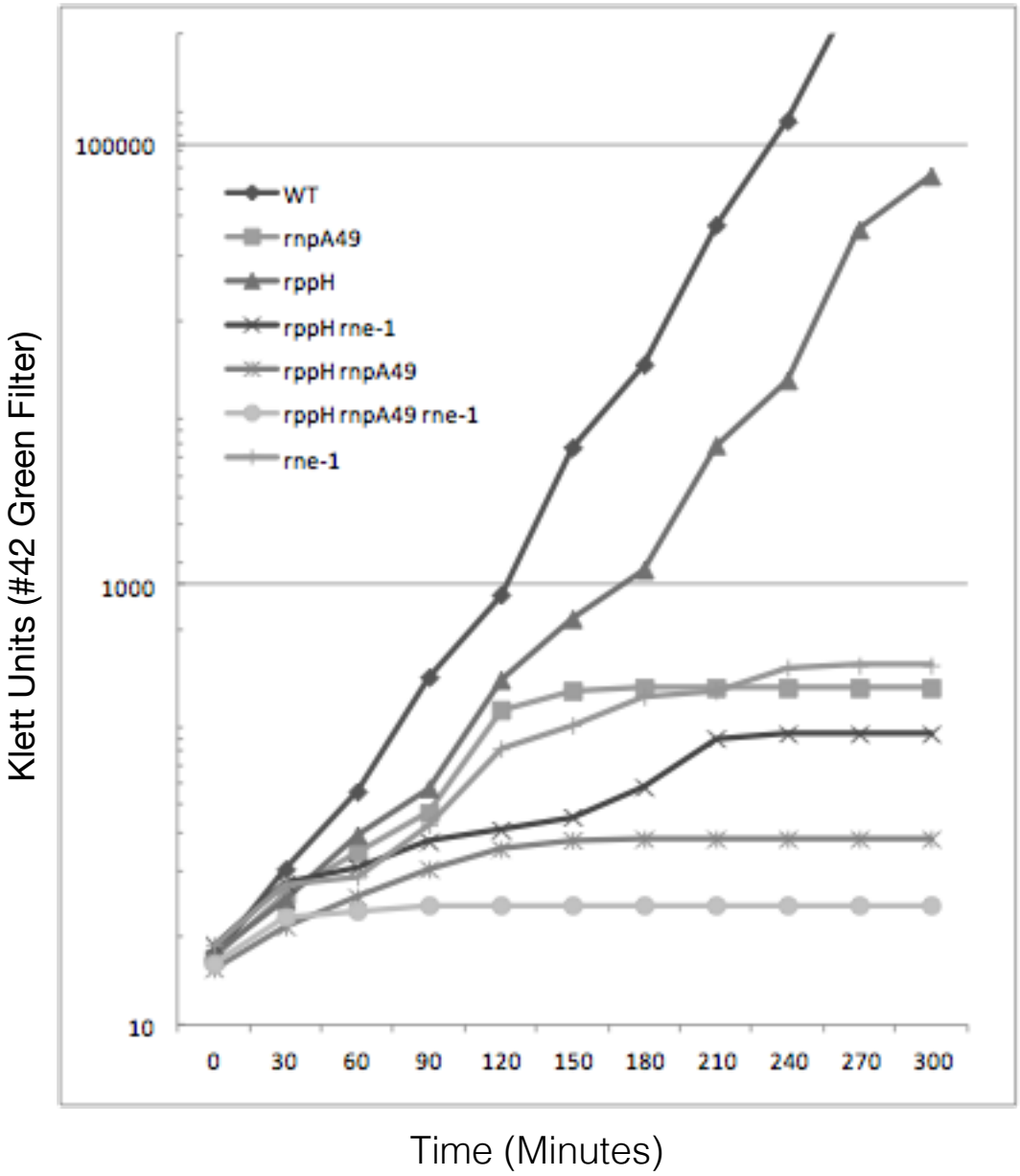
Klett Units (#42 Green Filter)
100000
1000
10
WT
rnpA49
rppH
rppH rne-1
rppH rnpA49
rppH rnpA49 rne-1
rne-1
0
30
60
90
120
150
180
210
240
270
300
Time (Minutes)

Figure 2. Processing of the *argX hisR leuT proM* polycistronic operon in the *rppHΔ754 rph-1*, *rne-1 rph-1*, and *rnpA49 rph-1* mutant backgrounds.

Northern analysis was conducted as described in Materials and Methods. (A) Schematic of the *argX hisR leuT proM* transcript. Downward arrows labeled "P" and "E" indicate RNase P and RNase E cleavage sites, respectively. Left-handed arrow indicates the oligonucleotide probe. The diagram is not drawn to scale. (B) Northern analysis of *argX hisR leuT proM* transcript with the use of the *hisR* oligonucleotide probe. Processing intermediates of the transcript are indicated on the right-hand side of the northern blot.

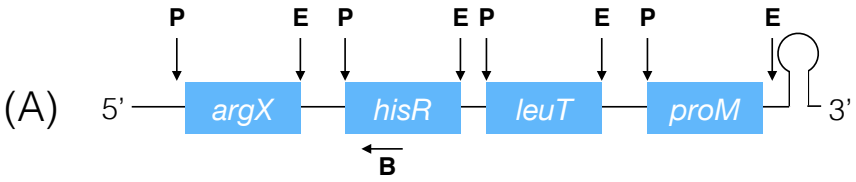
(A)
P
E
P
E
P
E
P
E
5'
argX
hisR
leuT
proM
3'
B

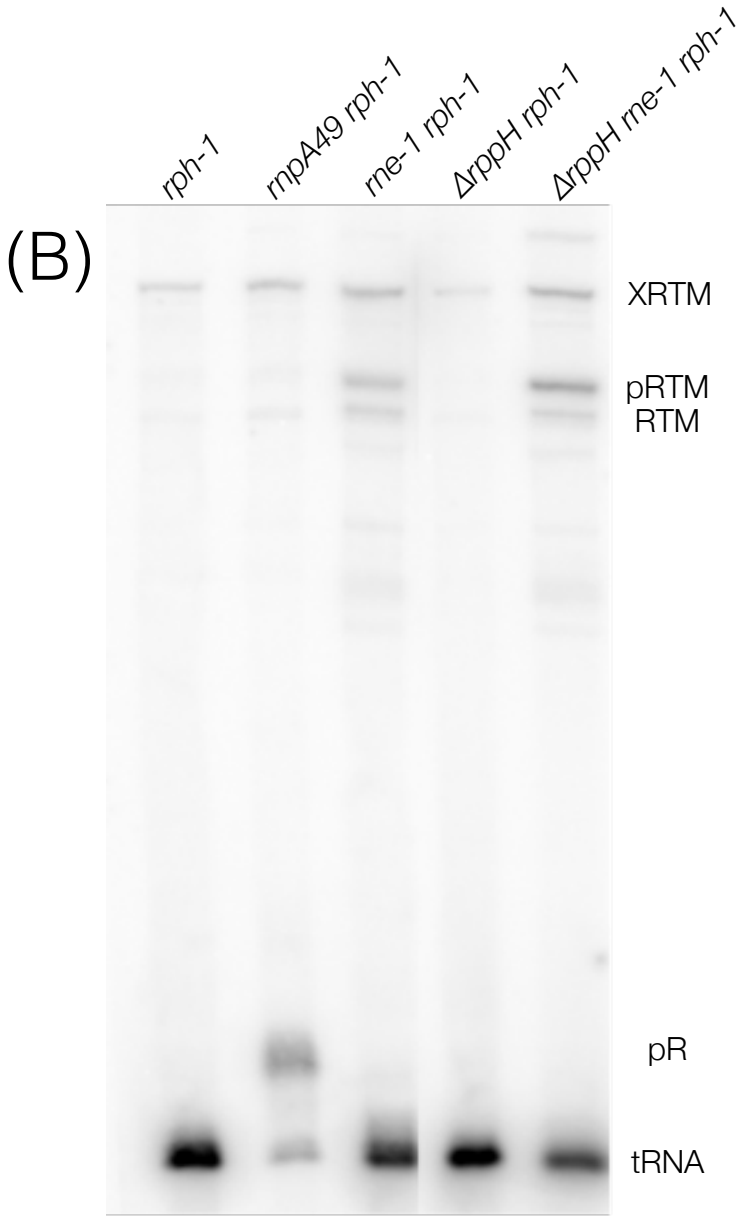
(B)
rph-1
rnpA49 rph-1
rne-1 rph-1
ΔrppH rph-1
ΔrppH rne-1 rph-1
XRTM
pRTM
RTM
pR
tRNA

Figure 3. Processing of the *valV valW* polycistronic operon in the *rppHΔ754 rph-1*, *rne-1 rph-1*, and *rnpA49 rph-1* mutant backgrounds.

Northern analysis was conducted as described in Materials and Methods. (A) Schematic of the *valV valW* transcript. Downward arrows labeled “P” indicates RNase P cleavage site. The diagram is not drawn to scale. (B) Northern analysis of the *valV valW* transcript with the use of the *valW* oligonucleotide probe, which hybridizes to both the *valV* and *valW* mature sequences. Processing intermediates of the transcript are indicated on the right-hand side of the northern blot.


(A)
P
P
5'
valV
valW
3'

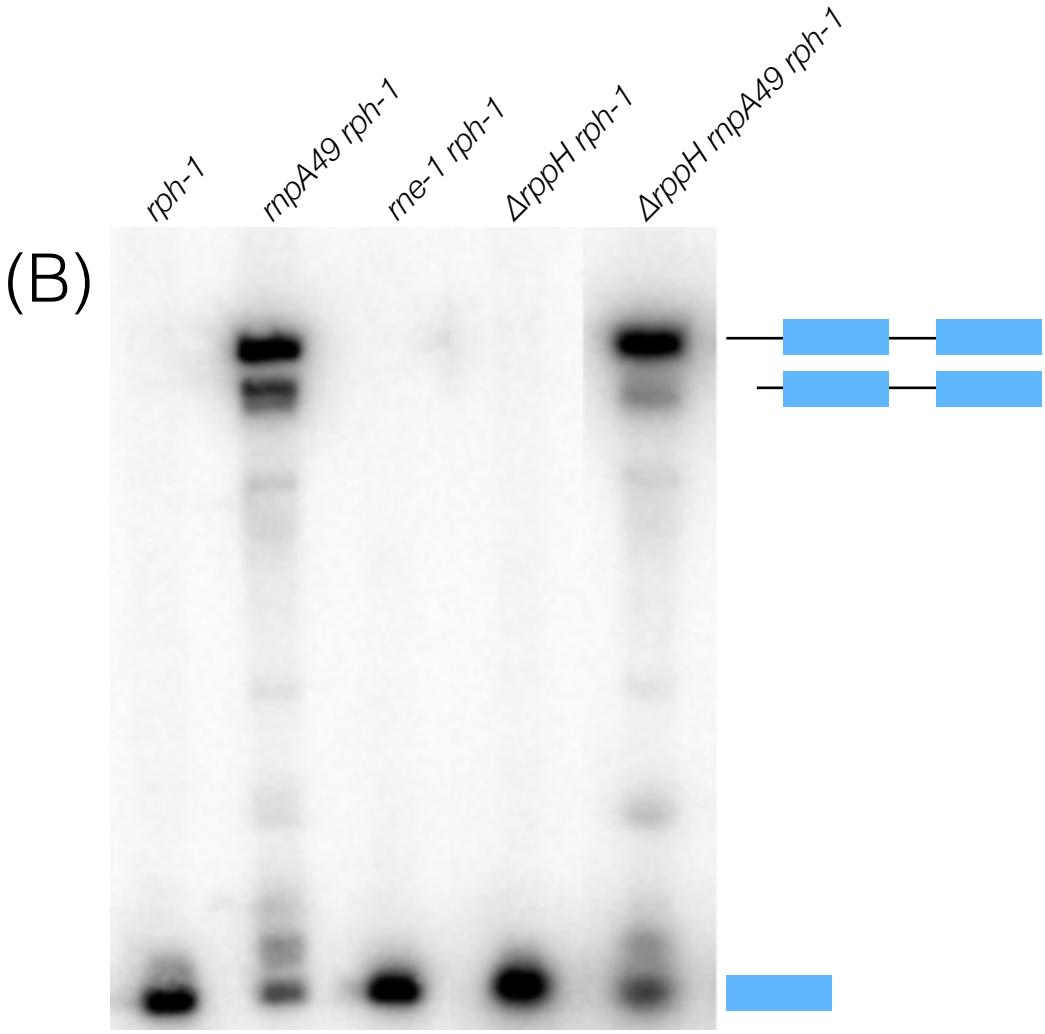
(B)
rph-1
rnpA49 rph-1
rne-1 rph-1
ΔrppH rph-1
ΔrppH rnpA49 rph-1

Figure 4. Processing of the *leuX* monocistronic operon in the *rppHΔ754 rph-1*, *rne-1 rph-1*, and *rnpA49 rph-1* mutant backgrounds.

Northern analysis was conducted as described in Materials and Methods. (A) Schematic of the *leuX* transcript. Numbers (nt) indicate the size of the 5'-leader of $tRNA^{leuX}$. Downward arrows labeled "P" indicate RNase P cleavage sites. The diagram is not drawn to scale. (B) Northern analysis of the *leuX* transcript with the use of the *leuX* oligonucleotide probe, which hybridizes to the mature sequence of *leuX*. Processing intermediates of the transcript are indicated on the right-hand side of the northern blot.

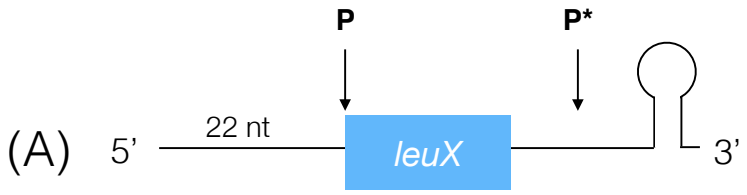
(A)
5’
22 nt
P
P*
leuX
3’

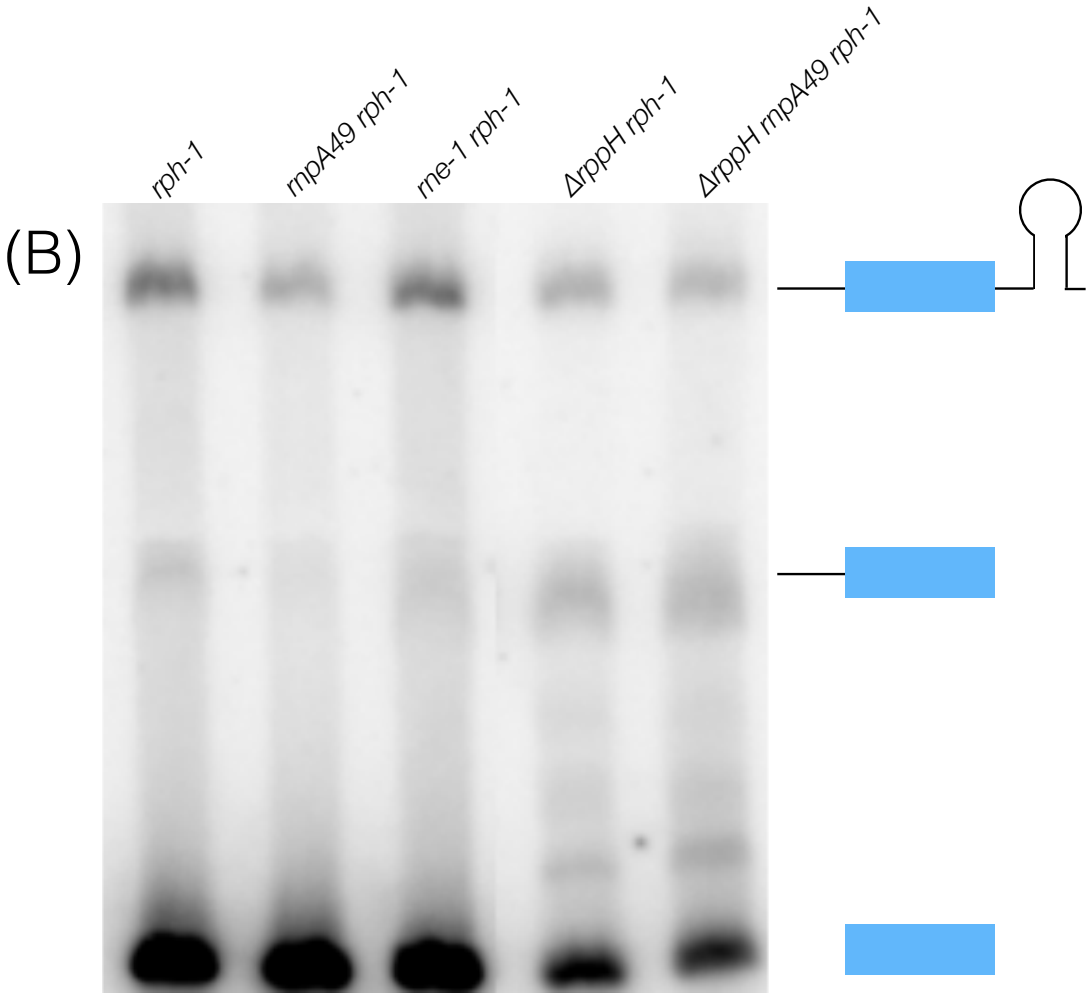
(B)
rph-1
rnpA49 rph-1
rne-1 rph-1
ΔrppH rph-1
ΔrppH rnpA49 rph-1

Figure 5. Processing of the *asnT, asnU, asnV, asnW* monocistronic operons in the *rppHΔ754 rph-1*, *rne-1 rph-1*, and *rnpA49 rph-1* mutant backgrounds.

Northern analysis was conducted as described in Materials and Methods. (A) Schematic of the four *asn* transcripts. Numbers (nt) indicate the size of the 5'-leader of $tRNA^{asn}$. Downward arrows labeled "P" and "E" indicate RNase P and RNase E cleavage sites, respectively. The diagram is not drawn to scale. (B) Northern analysis of the *asn* transcripts with the use of the *asn* oligonucleotide probe, which hybridizes to the mature sequence of all *asn* monocistronic precursors. Processing intermediates of the transcript are indicated on the right-hand side of the northern blot.

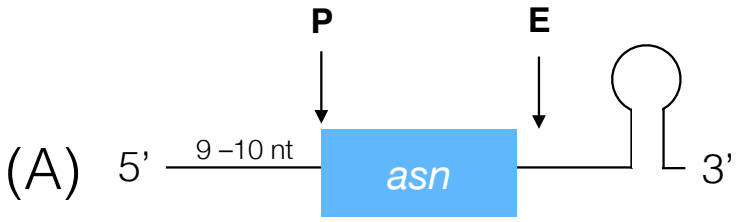
(A)
P
E
5’
9 –10 nt
asn
3’

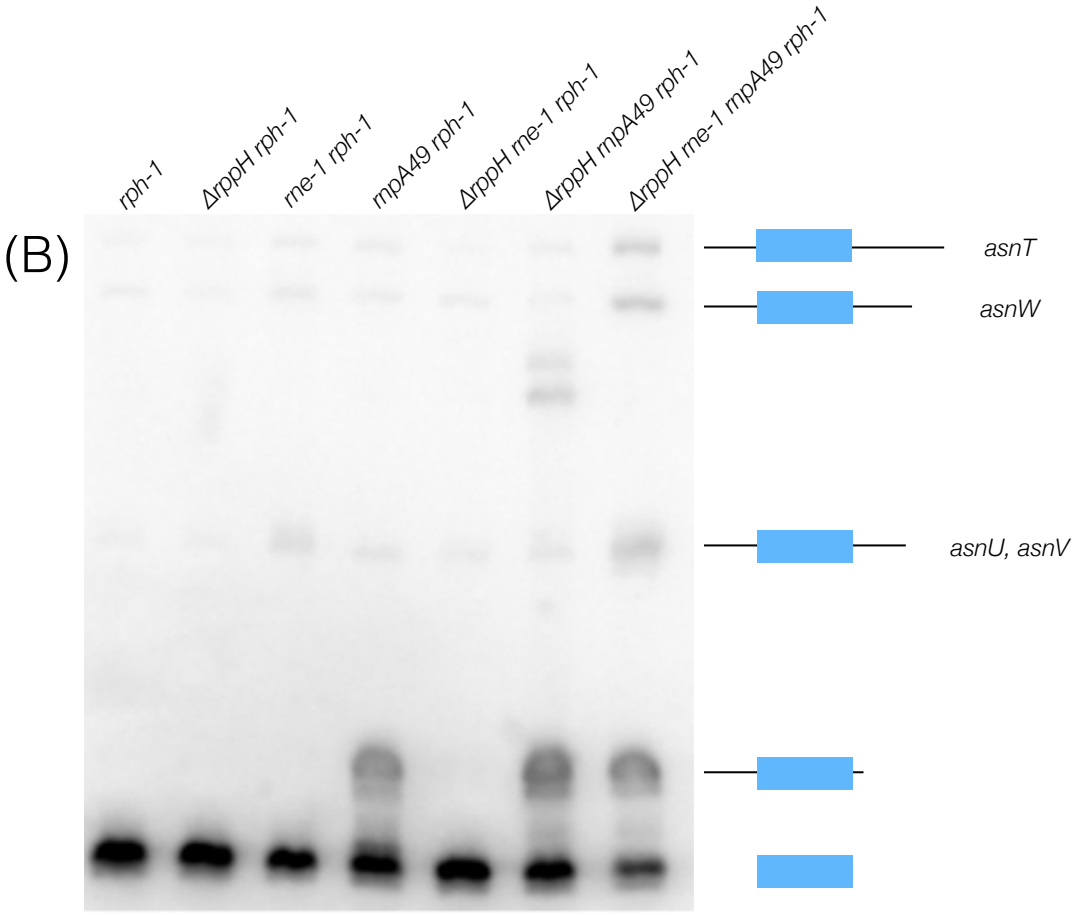
(B)
rph-1
ΔrppH rph-1
rne-1 rph-1
mpA49 rph-1
ΔrppH rne-1 rph-1
ΔrppH mpA49 rph-1
ΔrppH rne-1 mpA49 rph-1
asnT
asnW
asnU, asnV

Figure 6. Processing of the *pheU* and *pheV* monocistronic operons in the *rph-1, rph*$^{+}$*, ΔrppH, rne-1,* and *rnpA49* mutant backgrounds.

Northern analysis was conducted as described in Materials and Methods. (A) Schematic of the *phe* transcripts. Numbers (nt) indicate the size of the 5'-leader of tRNA$^{Phe}$. Downward arrows labeled "P" and "E" indicate RNase P and RNase E cleavage sites, respectively. The diagram is not drawn to scale. (B, C & D) Northern analysis of the *phe* transcripts with the use of the *phe* oligonucleotide probe, indicated by the black bar in (A), hybridizes to the mature sequences of both the *pheU* and *pheV* transcripts. Processing intermediates of the transcript are indicated on the right-hand side of the northern blot.

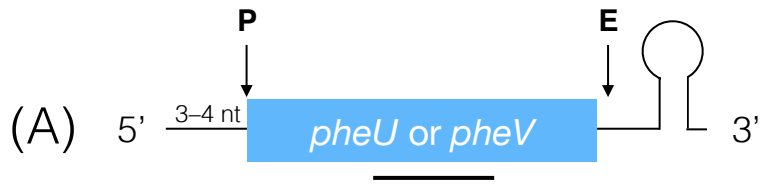
(A)
P
E
5’
3–4 nt
pheU or pheV
3’

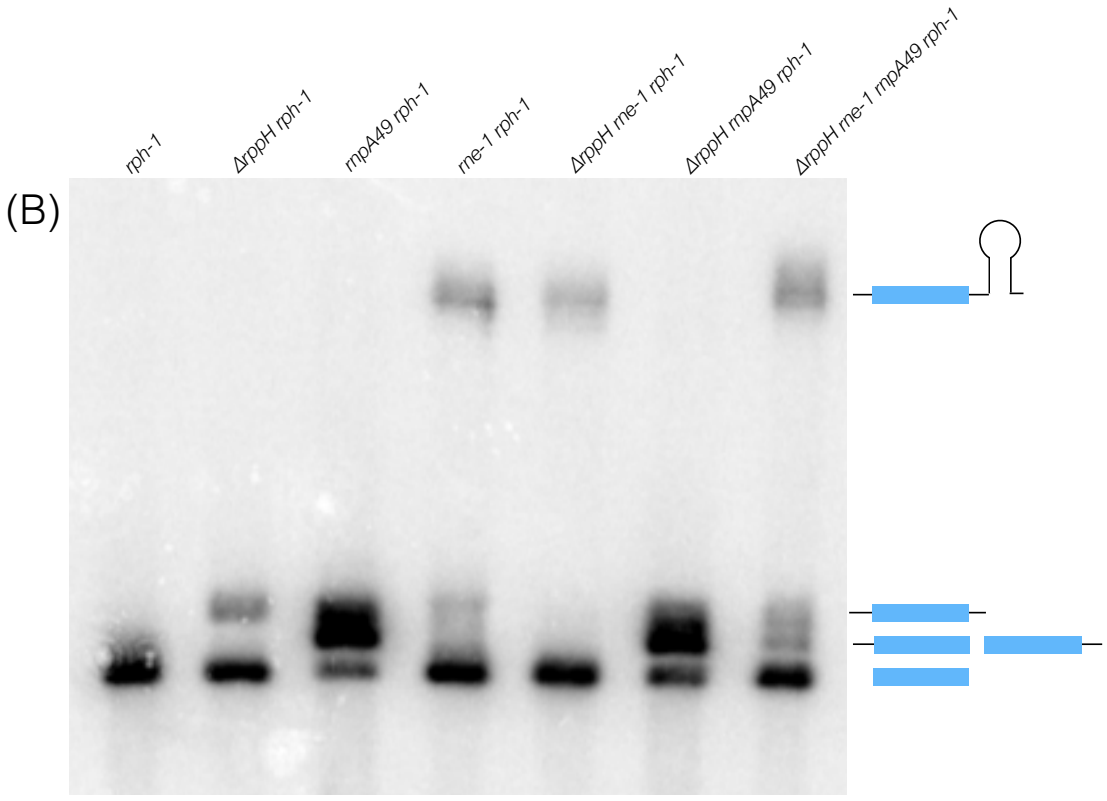
(B)
rph-1
ΔrppH rph-1
rnpA49 rph-1
rne-1 rph-1
ΔrppH rne-1 rph-1
ΔrppH rnpA49 rph-1
ΔrppH rne-1 rnpA49 rph-1

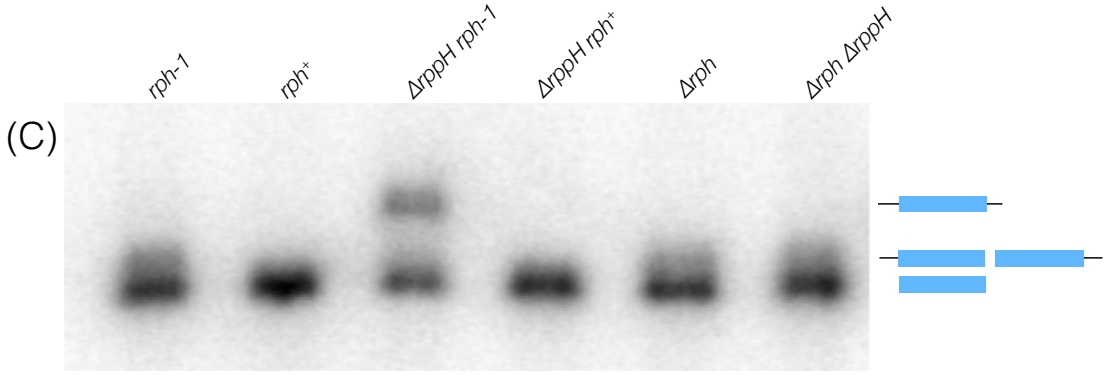
(C)
rph-1
rph+
ΔrppH rph-1
ΔrppH rph+
Δrph
Δrph ΔrppH

(D)

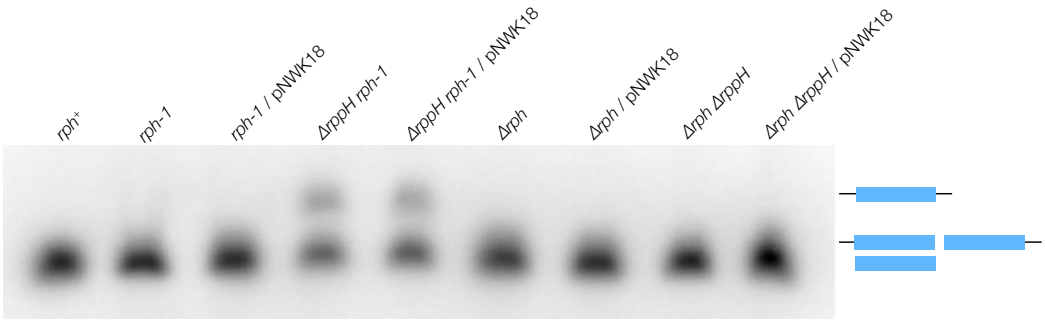
rph+
rph-1
rph-1 / pNWK18
ΔrppH rph-1
ΔrppH rph-1 / pNWK18
Δrph
Δrph / pNWK18
Δrph ΔrppH
Δrph ΔrppH / pNWK18

Figure 7. Analysis of the 5′-termini of *pheU* and *pheV* in the *rppHΔ754 rph-1* and *rnpA49 rph-1* mutant backgrounds.

Primer extension analysis was conducted as described in Materials and Methods. A black bracket indicates the transcription start sites of *pheU* and *pheV*. Arrows indicate the mature 5′-termini of *pheU* and *pheV*, with the orange arrow indicating the major transcription start site, and the blue arrow indicating the minor transcription start site. The expanded sequence is shown to the left and at bottom of the figure. The schematic below the figure indicates the mature sequence with a blue box.

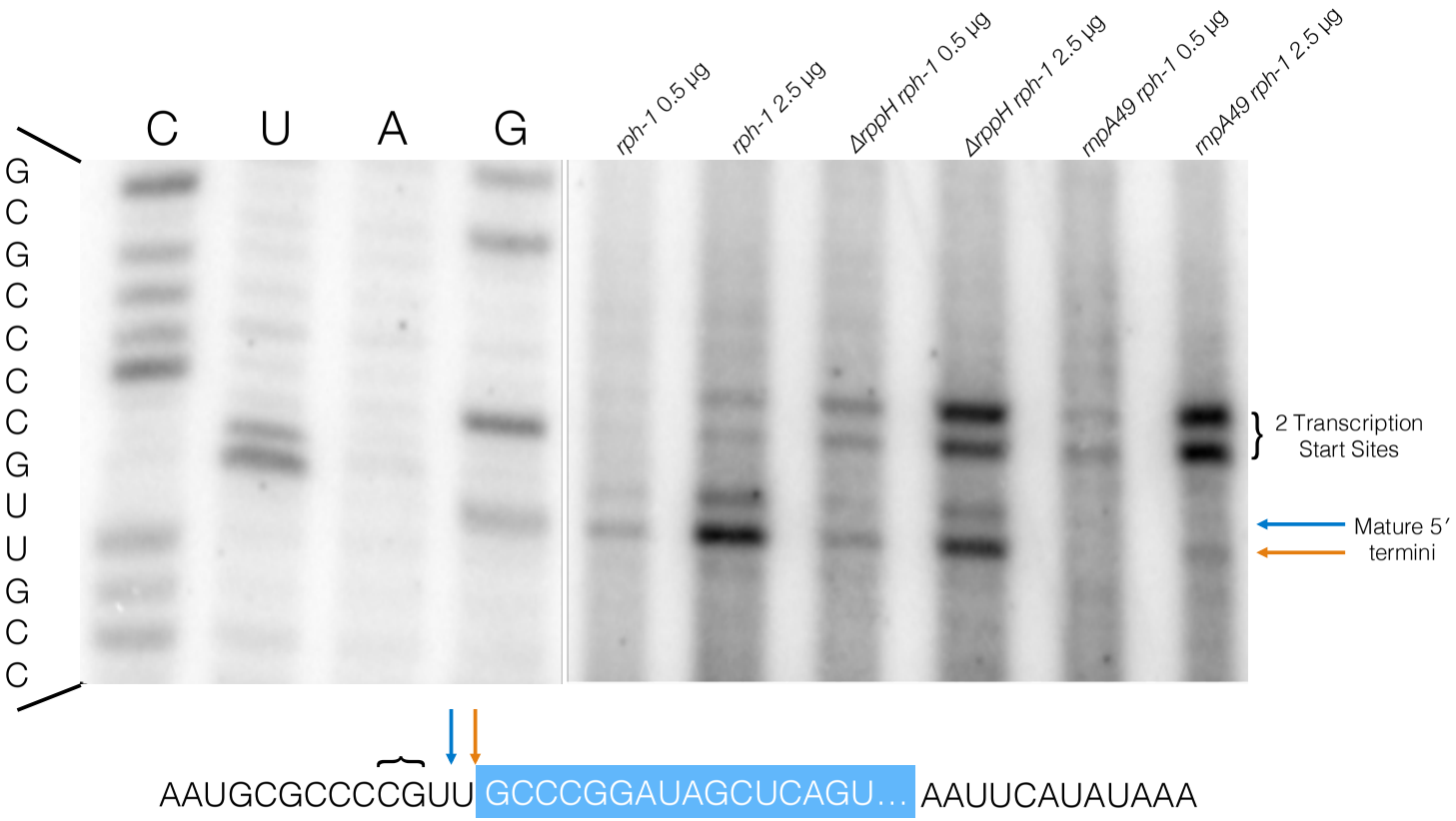
C
U
A
G
G
C
G
C
C
C
C
G
U
U
G
C
C
rph-1 0.5 µg
rph-1 2.5 µg
ΔrppH rph-1 0.5 µg
ΔrppH rph-1 2.5 µg
rnpA49 rph-1 0.5 µg
rnpA49 rph-1 2.5 µg
2 Transcription Start Sites
Mature 5′ termini
AAUGCGCCCCGUU GCCCGGAUAGCUCAGU… AAUUCAUAUAAA

Figure 8. Analysis of the 5′- and 3′-termini of *pheU* and *pheV* monocistronic operons in various mutant backgrounds.

RNA self-ligation and RT-PCR was conducted as described in Materials and Methods. The 5′-leader and mature sequence, indicated by the blue bar, is identical for both *pheU* and *pheV,* whereas the 3′-termini are highly variable. Arrows to the left of the blue bar indicate 5′-termini, while arrows to the right of the blue bar indicate 3′-termini. Numbers above the arrows indicate number of clones that ligated at that nucleotide, and "n" indicates the number of clones sequenced. (A) Ligation products of *pheU* and *pheV* in the *rph-1* background with TAP. (B) Ligation products of *pheU* and *pheV* in the *ΔrppH rph-1* background with TAP. (C) Ligation products of *pheU* and *pheV* in the *rnpA49 rph-1* background without TAP. (D) Ligation products of *pheU* and *pheV* in the *ΔrppH Δrph* background with TAP.

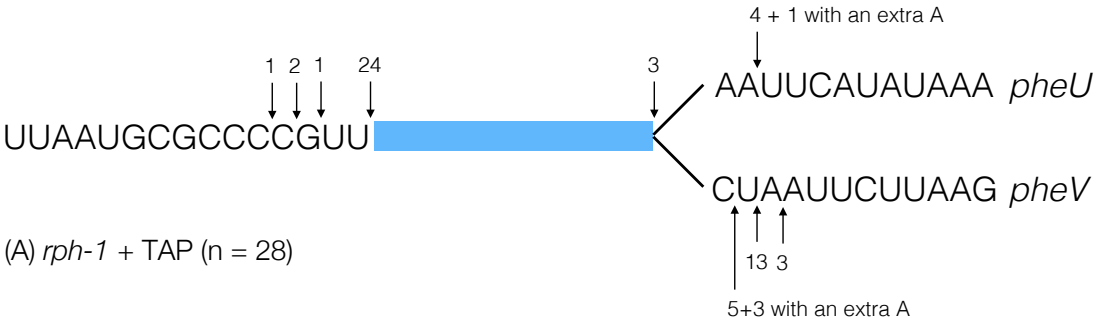


(A) *rph-1* + TAP (n = 28)

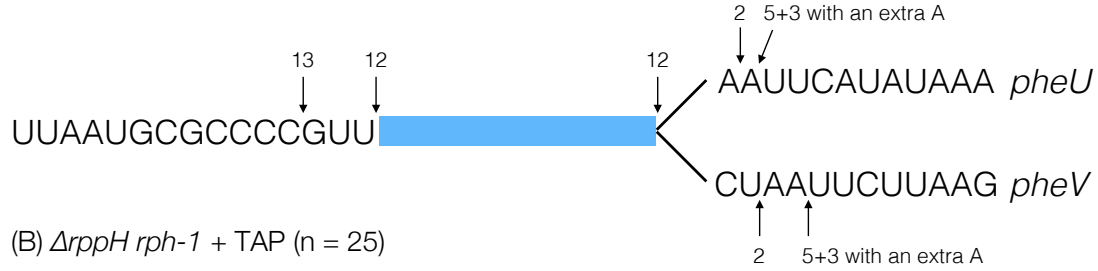


(B) *ΔrppH rph-1* + TAP (n = 25)

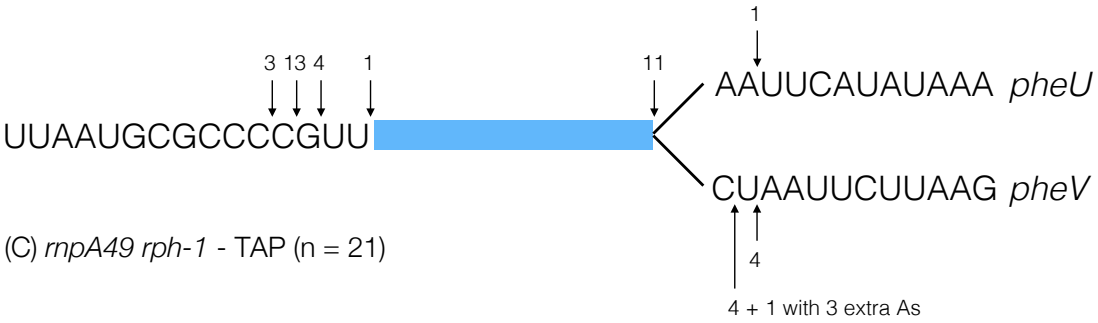


(C) *rnpA49 rph-1* - TAP (n = 21)

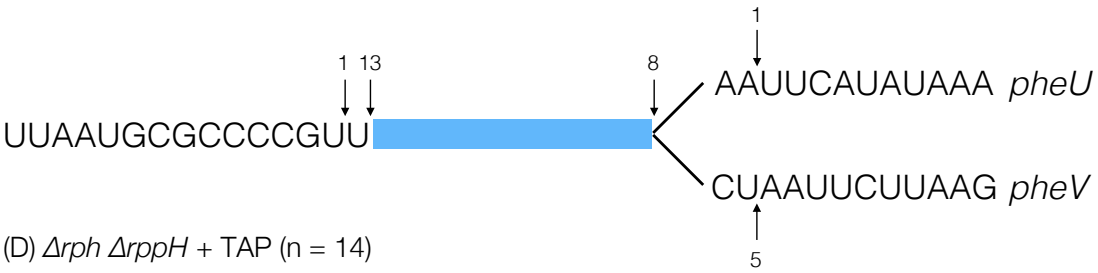


(D) *Δrph ΔrppH* + TAP (n = 14)

Figure 9. Processing of the *ileX* monocistronic operon in the *rph-1, rph*$^{+}$*, Δrph, ΔrppH,* and *rnpA49* mutant backgrounds.

Northern analysis was conducted as described in Materials and Methods. (A) Schematic of the *phe* transcripts. Numbers (nt) indicate the size of the 5′-leader of tRNA$^{ile}$. Downward arrow labeled "P" indicates RNase P cleavage. The diagram is not drawn to scale. (B) Northern analysis of the *ileX* transcript with the use of the *ile* oligonucleotide probe, indicated by the black bar in (A), hybridizes to the mature sequence of the *ileX* transcript. Processing intermediates of the transcript are indicated on the right-hand side of the northern blot.


(A)
P
2–3 nt
5’
ileX
3’

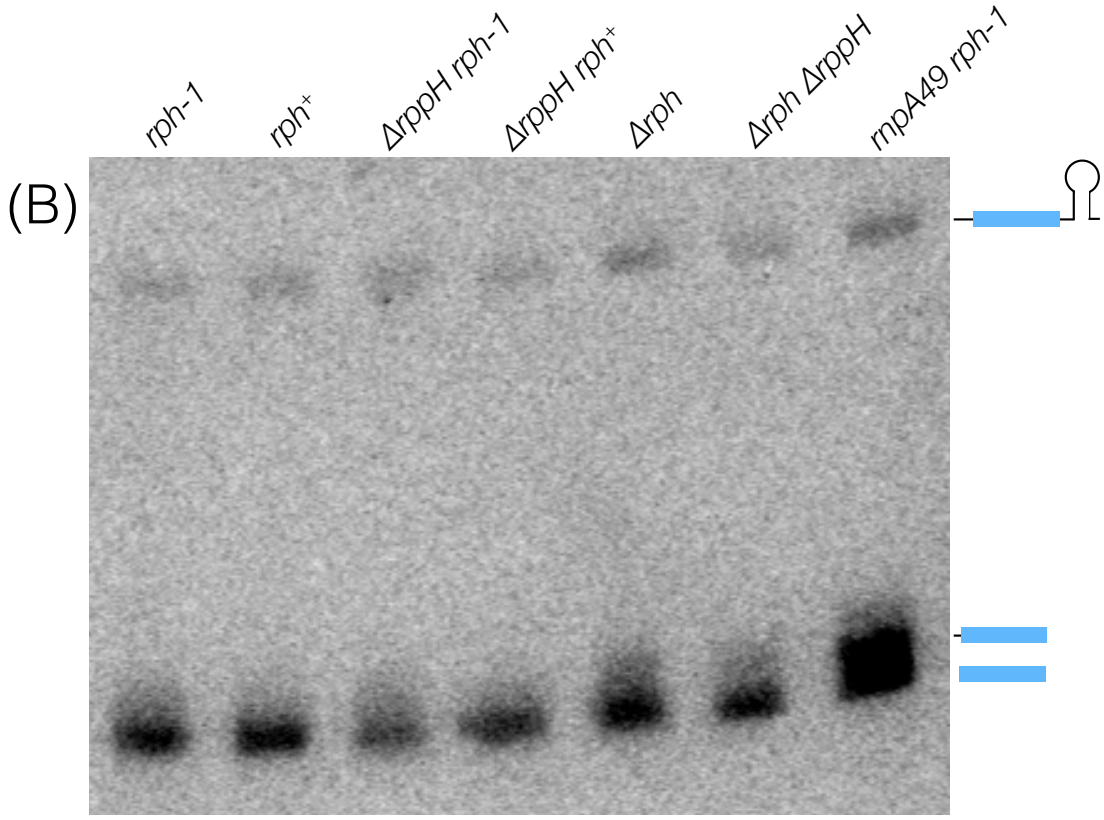
(B)
rph-1
rph+
ΔrppH rph-1
ΔrppH rph+
Δrph
Δrph ΔrppH
rnpA49 rph-1

Figure 10. Analysis of the 5′- and 3′-termini of *ileX* monocistronic operon in various mutant backgrounds.

RNA self-ligation and RT-PCR was conducted as described in Materials and Methods. Data is presented as described in Fig. 8. (A) Ligation products of *ileX* in the *rph-1* background with TAP. (B) Ligation products of *ileX* in the *Δrpph rph-1* background with TAP. (C) Ligation products of *ileX* in the *rnpA49 rph-1* background without TAP. (D) Ligation products of *ileX* in the *Δrph* background with TAP. (E) Ligation products of *ileX* in the *Δrpph Δrph* background with TAP.

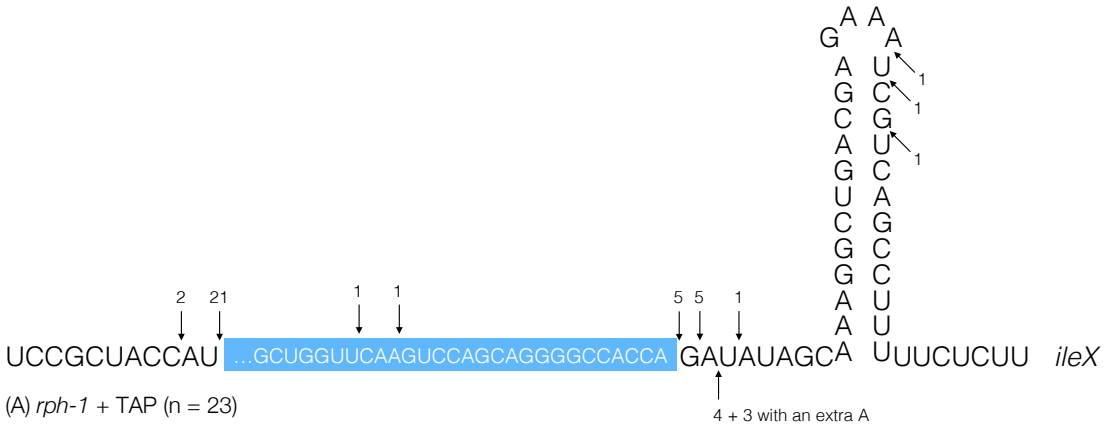


(A) *rph-1* + TAP (n = 23)

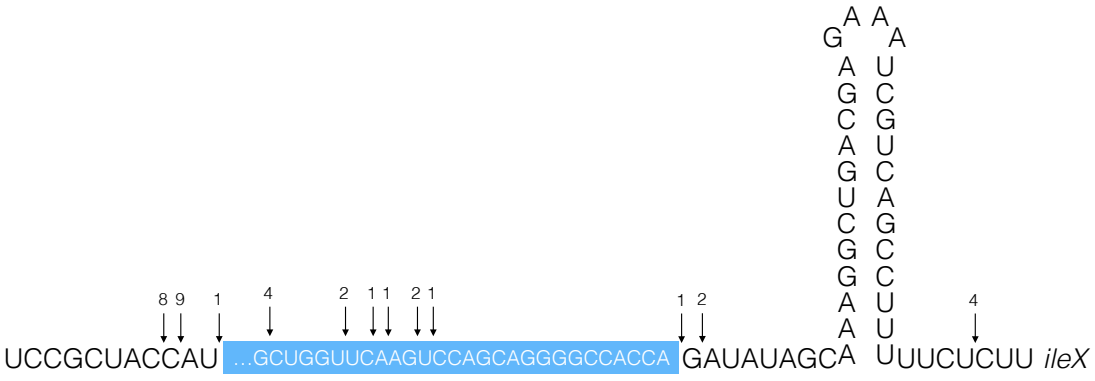


(B) *ΔrppH rph-1* + TAP (n = 21)

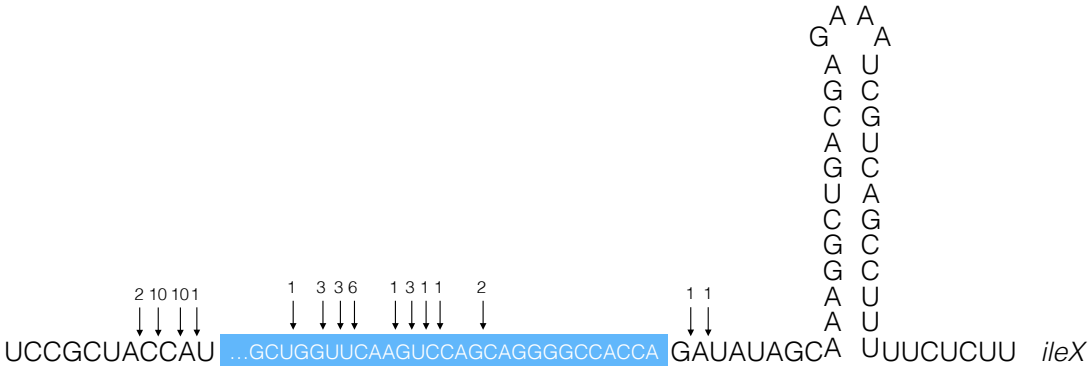


(C) *rnpA49 rph-1* + TAP (n = 23)

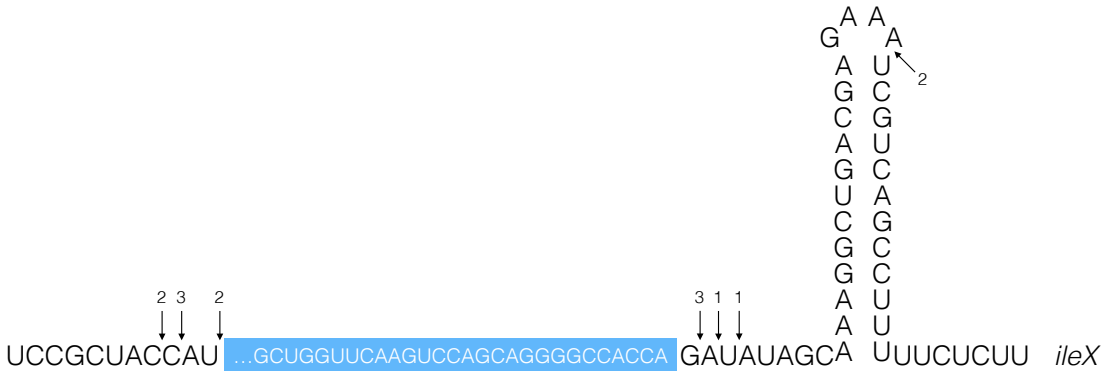


(D) *Δrph* + TAP (n = 7)

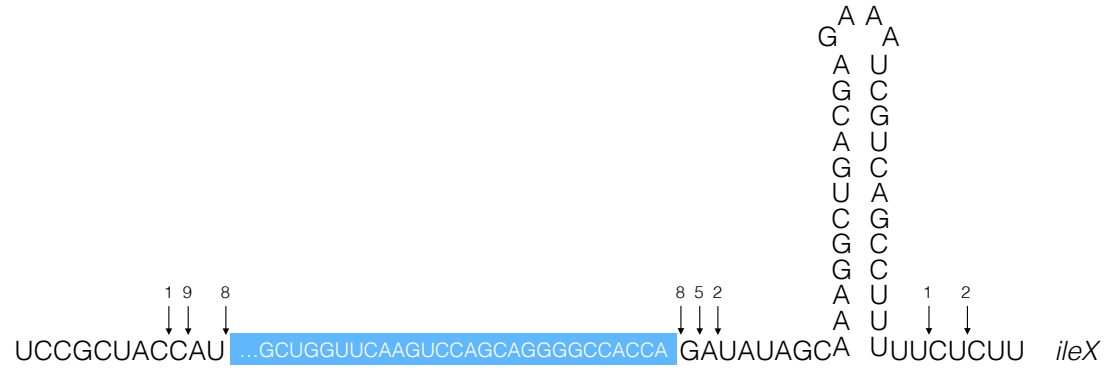


(E) *Δrph ΔrppH* + TAP (n = 18)

Figure 11. Immunoprecipitation analysis of *rph*$^{+}$ and *rppHΔ754 rph-1* strains. Immunoprecipitation was conducted as described in Material and Methods. Conditions for each strain used are listed above each lane. Proteins probed for are located in the lower left-hand corner of each blot. Arrows pointing to a band indicate the presence of RNase PH, Rph-1 truncation, or RppH. Approximate protein size is listed on the right-hand side of each blot. RNase PH migrates to ~31 kDa, Rph-1 truncation migrates to ~28 kDa, and RppH migrates to ~ 38 kDa.

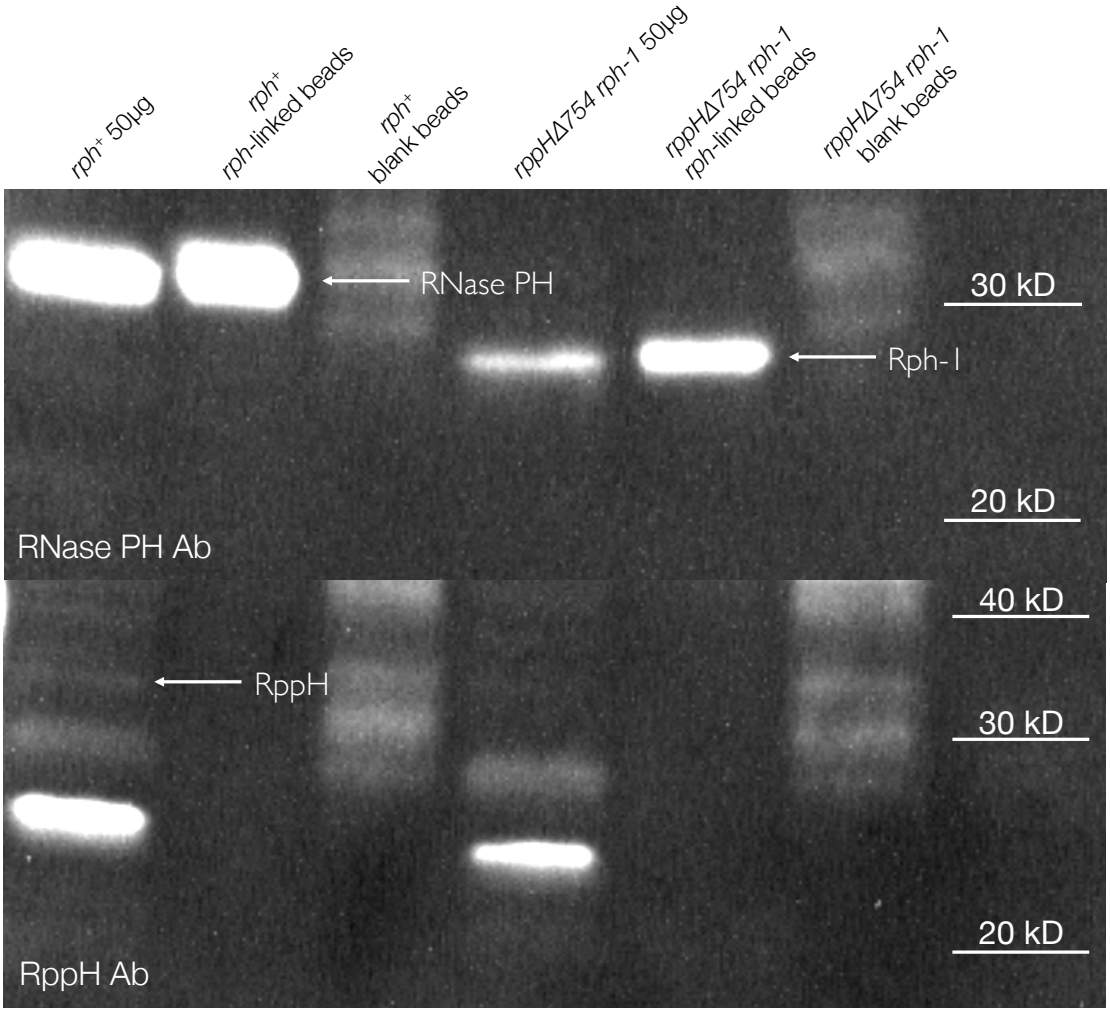
rph+ 50µg
rph+ rph-linked beads
rph+ blank beads
rppHΔ754 rph-1 50µg
rppHΔ754 rph-1 rph-linked beads
rppHΔ754 rph-1 blank beads
RNase PH
Rph-1
30 kD
20 kD
RNase PH Ab
40 kD
RppH
30 kD
20 kD
RppH Ab

Figure 12. Western blotting analysis for the presence of RNase PH or Rph-1 truncated protein.

Western blotting analysis was conducted as described in Materials and Methods. Strains used and total protein loading amounts are listed above each lane. Approximate protein size is listed on the right-hand side of each blot. RNase PH migrates to ~31 kDa, and the Rph-1 truncation migrates to ~28 kDa.

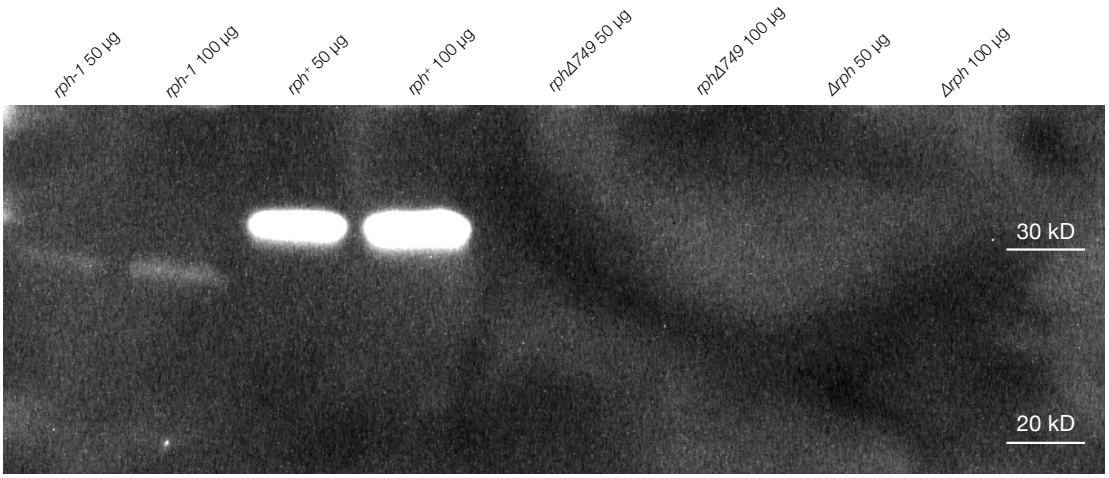
rph-1 50 µg
rph-1 100 µg
rph+ 50 µg
rph+ 100 µg
rphΔ749 50 µg
rphΔ749 100 µg
Δrph 50 µg
Δrph 100 µg
30 kD
20 kD

Figure 13. Western blot analysis of Rph-1 truncation overexpression in the *rph-1*, *ΔrppH rph-1, Δrph*, *ΔrppH Δrph* strains.

Western analysis was conducted as described in Materials and Methods. Strains used and total protein loading amounts are listed above each lane. Approximate protein size is listed on the left-hand side of each blot. The Rph-1 truncation migrates to ~28 kDa.

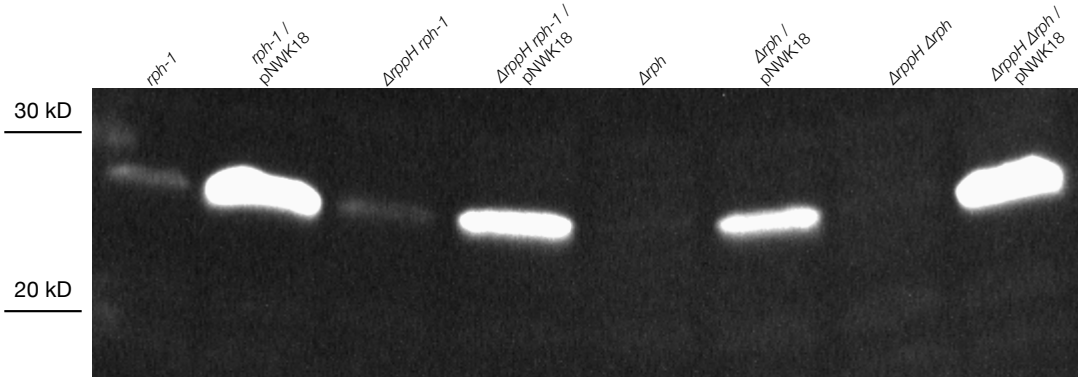
rph-1
rph-1 / pNWK18
ΔrppH rph-1
ΔrppH rph-1 / pNWK18
Δrph
Δrph / pNWK18
ΔrppH Δrph
ΔrppH Δrph / pNWK18
30 kD
20 kD

# CHAPTER 3

# ANALYSIS OF *ESCHERICHIA COLI* RPPH ACTIVITY *IN VIVO* USING TILING MICROARRAYS[1]

[1]Wiese, N.S., Bowden, K.E., Mohanty, B.K., and Kushner, S.R. To be submitted to *PLOS Genetics*.

**ABSTRACT**

RppH is known to be the “decapping” enzyme in *Escherichia coli* and its activity has been implicated in initiation of mRNA decay, tRNA maturation of certain tRNA precursors, polyphosphate regulation, and invasiveness of *E. coli* in brain tissue. To get a clearer understanding of its role in these complicated processes, microarray analysis was previously conducted, but with limited scope. Here, through the use of high density tiling microarrays, we have utilized a complete RppH deletion and analyzed its effect on all genes across the entire genome of *E. coli* at a 20 nucleotide resolution. Through this analysis it was evident that RppH regulates the entire flagellar gene regulatory network. Furthermore, strains with a *ΔrppH rph-1* background exhibits hypermotility and rescues motility defects in a known non-motile background. Interestingly, the effect on motility is only observed in the absence of the 3′→5′ exoribonuclease RNase PH, or in the presence of the truncated Rph-1 protein.

## INTRODUCTION

*rppH*, formerly *ygdP*, encodes RNA pyrophosphohydrolase in *Escherichia coli* and has been shown to facilitate mRNA decay by removal of a 5′-pyrophosphate from 5′-terminus of primary mRNA transcripts (1). These findings have been bolstered by several studies showing the requirement of a 5′-monophosphated RNA substrate for RNase E, an essential endoribonuclease that is involved in mRNA decay and the 3′-terminal maturation of several tRNAs (1-4). Along with helping to regulate the decay of various mRNAs, RppH has also been linked to the invasiveness of *E. coli* in human brain microvascular endothelial cells and the regulation of the *E. coli* general secretory (Sec) pathway (5-7). Seeing that RppH has substrate specificities for molecules other than 5′-triphosphate RNA caps, which include diadenosine *tetra*-, *penta*-, and *hexa*-phosphates, obtaining a clearer, more comprehensive picture of the role RppH plays in cellular RNA metabolism is of utmost importance (6).

With the identification that *rppH* encoded an RNA pyrophosphohydrolase activity, Deana et al. (1) carried out an analysis of all *E. coli* ORFs using JW2798 a strain deleted for *rppH* but containing the 6–8 copy number plasmid pPlacRppH-E53A, which had a mutant RppH protein under the control of the *lac* promoter. This mutant form of the RppH protein contains a substitution at an essential active-site residue and renders the protein nonfunctional, but it is unclear whether this altered protein is capable of RNA-binding, thereby protecting some transcripts from endonucleolytic decay (1). In their mutant they

observed increased steady-state levels for a significant number of ORFs (1). However, their analysis did not include non-translated RNAs (1).

Recently, our laboratory has developed a high-density tiling microarray for *E. coli* that provides 20 nt resolution across the entire genome (8). In addition, with current advances in RNA isolation, particularly the RNA*snap*™ method, it is now possible to have a more accurate depiction of the intracellular RNA pool, unlike other isolation methods, which either enrich or deplete certain size classes of RNA (9). Lastly, transcriptome analysis of a true chromosomal deletion of RppH has yet to be characterized.

Accordingly, we performed a tiling array analysis of MG1693 (*rph-1*) versus SK4390 (*ΔrppH rph-1*) as well as SK10153 ($rph^+$) versus SK4426 (*ΔrppH* $rph^+$) grown into mid-exponential phase. We show here that far fewer transcripts are affected by deletion of RppH than previously seen (1). In comparing the tiling microarrays to previously reported results, the *ΔrppH rph-1* array showed 98 transcripts were affected, and in the *ΔrppH* $rph^+$ array, 108 transcripts were affected. These data contrast with earlier results using an RppH inactive protein in which 382 gene transcripts were reported to show increased steady-state levels (1).

More importantly, we provide evidence that RppH regulates flagellar operon transcription. We show that *flhDC*, the transcript encoding the master regulator of flagellar transcription in *E. coli*, is much more abundant in a *ΔrppH rph-1* background. Previous studies have shown that transcription of *flhDC* is regulated in a cell-cycle dependent manner, with an increase of its transcription

observed immediately following cell division (10). So far only the RNA-binding protein CsrA has been shown to regulate the stability of the *flhDC* mRNA (11).

Once translated into protein, FlhDC activates transcription of class II genes in the flagellar gene regulatory network, which include genes that encode the flagellar protein apparatus, basal body, hook, and the alternative sigma factor $\sigma^{28}$ (12-16). $\sigma^{28}$ then activates transcription of class III genes in the flagellar gene regulatory network, specifically *fliC* which encodes flagellin, the protein that forms the filament of bacterial flagella, and the anti-sigma $\sigma^{28}$ factor, FlgM (17-19). Our data indicate that hypermotility is a result of the stabilization of the *flhDC* transcript. This is the first evidence that RppH regulates motility and may provide more insight into mechanisms in which RppH regulates other cellular pathways (6,7).

## MATERIALS AND METHODS

### Bacterial strains

The *E. coli* strains used in this study were all derived from MG1693 (*rph-1 thyA715*) (*E. coli* Genetic Stock Center, Yale University). This strain contains no RNase PH activity and shows reduced expression of *pyrE* due to the single nucleotide frameshift in the *rph* gene (20). True wild type strain, SK10153 (*thyA715*), contains a functional RNase PH protein (21). For this study, a P1 lysate grown on JW2798 (Keio Collection, Japan) was used to transduce MG1693 and SK10153 to construct SK4390 (*ΔrppH rph-1*) and SK4426 (*ΔrppH*

*rph*$^{+}$). A P1 lysate grown on JW0048 (Keio Collection, Japan) was used to transduce MG1693 to construct SK4417 (*ΔapaH rph-1*). To construct SK4420 (*ΔrppH ΔapaH rph-1*), the kanamycin cassette in SK4390 was removed with the use of Flp recombinase, as previously described (22-24), with the following exceptions. The SK4390 cells were made electrocompetent and transformed with pCP20, the plasmid carrying the FLP recombinase. Once the kanamycin cassette was confirmed to be absent, these cells were transduced with the P1 lysate grown on JW0048 to construct the *ΔrppH ΔapaH rph-1* triple mutant strain. SK10751 was constructed by transducing P1 lysate grown on JW3618 (*Δrph::kan* Keio Collection, Japan) into MG1693 (*rph-1 thyA715*). Plasmid pCP20 was then transformed into the cell in order to remove the kanamycin resistance cassette as previously described (23). SK10752 was constructed by transduction using a P1 lysate grown on JW2798 (*ΔrppH::kan*) Keio Collection, Japan) into SK10751.

**Growth of bacterial strains and isolation of total RNA**

Bacterial strains were grown with shaking in at 37°C in Luria broth supplemented with thymine (50 μg/mL) and kanamycin (25 μg/mL) (when *ΔrppH* was present) until a cell density of 50 Klett units above background (No. 42 green filter) was reached. RNA was extracted using the RNA*snap*™ method as described by Stead et al. (9). RNA was further treated with the DNA-free kit™ (Ambion) to remove contaminating DNA, and further quantified on a NanoDrop™ (Thermo Scientific) apparatus. 500 ng of each RNA sample were run on a 1%

Agarose-Tris-acetate-EDTA gel and visualized with ethidium bromide to ensure accurate quantities and satisfactory quality for further analysis.

**Construction of the *E. coli* tiling microarray & analysis**

The tiling microarray and subsequent analysis was conducted as previously described by Stead et al. (8).

**Northern analysis**

RNA isolation for Northern analysis employed the RNA*snap*™ method as described by Stead et al. (9), while Northern analysis itself was performed as described by O'Hara et al. (25).

**Motility assays**

Motility was tested using motility agar plates as described by (26), with the following changes. Initially, 0.35% agar plates were supplemented with 1% thymine and 25 μg/mL kanamycin (when required). For time course motility assays, M9 agar plates were used, supplemented with 1% thymine, 0.1% glucose, 0.1% thiamine, 1 mM $MgSO_4$, and 0.2 mM $CaCl_2$ to ensure that all strains grew with comparable generation times.

## RESULTS

### Analysis of the *E. coli* transcriptome in the absence of RppH

Through the use of tiling microarrays, we compared the transcriptomes of MG1693 (*rph-1*) to SK4390 *(ΔrppH rph-1*), as well as SK10153 (*rph*$^+$) to SK4426 (*ΔrppH rph*$^+$*)* using the RNA*snap*™ RNA isolation method as described by Stead et al. (9). The RNA*snap*™ method RNA showed 98 transcripts affected in the *ΔrppH rph-1* mutant background, 82 showing increased steady-state levels and 16 showing decreased steady-state levels (Tables 1 & 2). In the *ΔrppH rph*$^+$ mutant background 108 transcripts were affected, 61 showing increased steady-state levels and 47 showing decreased steady-state levels (Tables 1 & 2). In comparison, Deana et al. reported changes for 382 transcripts (1).

### Analysis of transcripts involved in the flagellar gene regulatory network

We then analyzed specific transcripts in order to determine if RppH had an effect on any major cell process. Through this analysis we discovered that 48% (39/82) of genes with increased steady-state levels in the *ΔrppH rph-1* mutant background belonged to the flagellar gene regulatory network (Table 1). Interestingly all of these transcripts showed an increase in abundance in the absence of RppH in an *rph-1* background whereas, in an *rph*$^+$ background none of these transcripts showed any fold-change from wild type (Table 1, Fig. 1). The transcript of *flhDC,* the flagellar gene regulatory pathway master regulator in *E. coli*, showed a 1.42-fold increase in the *Δrpph rph-1* mutant compared to wild

type, (Fig. 1A). The transcripts of the class II genes in the regulatory pathway were similarly stabilized.

Class II genes are known to form the basal body, the flagellar protein export apparatus, the hook and hook associated proteins, along with $\sigma^{28}$ and the anti-$\sigma^{28}$ factor [for review see (27-29)]. The transcript *flhBAE* encodes 3 of the 6 integral membrane components of the flagellar export apparatus (27-29). This transcript exhibited a 1.48-fold increase in the *ΔrppH rph-1* mutant when compared to wild type (Fig. 1A). The *flgBCDEFGHIJKL* transcript encodes the proteins that make up the flagellar rod (FlgB, FlgC, FlgF, FlgG), the hook-capping protein (FlgD), the hook protein (FlgE), 2 class III hook-associated proteins (FlgK, FlgL), the rod cap (FlgJ), the P-ring (FlgI), and the L-ring (FlgH) (27-29). This entire transcript showed a 1.52-fold increase in the *ΔrppH rph-1* mutant when compared to the wild type control (Table 1, Fig. 1B).

The transcript *fliAZY* encodes $\sigma^{28}$ and two novel genes thought to regulate $\sigma^{28}$ activity (27-30). *fliA* and *fliZ* showed a 1.71-fold increase in the *ΔrppH rph-1* mutant when compared to wild type, while the increase of *fliY* was not significant enough to be calculated using the parameters set for our analysis (Table 1, Fig. 1C). The transcript *fliE* encodes the last of the five proteins, FliE, that make up the flagellar rod, and exhibited a 1.59-fold increase in abundance in the *ΔrppH rph-1* mutant when compared to wild type (Table 1, Fig. 1C).

The polycistronic transcript *fliFGHIJK* encodes FliF, the MS ring of the flagellar basal body, FliG, one of the three components of the flagellar motor's "switch complex", soluble components of the flagellar export system (FliH, FliI,

and FliJ), and the hook-length control protein, FliK (31-35). This transcript showed an overall 1.40-fold increase in abundance in the *ΔrppH rph-1* mutant when compared to wild type (Table 1, Fig. 1C). The polycistronic transcript *fliLMNOPQR* encodes motor/switch proteins and integral membrane proteins of the flagellar export apparatus and shows an overall 1.48-fold increase in the *ΔrppH rph-1* mutant when compared to wild type (Table 1, Fig. 1C) (29). The transcript *flgAMN* encodes the FlgA, the chaperone of FlgI, while FlgM and FlgN are class III proteins, where FlgM binds to $\sigma^{28}$ to help in its regulation while FlgN acts as a chaperone of hook-binding proteins (36-39). *flgA* showed a 1.58-fold increase in the *ΔrppH rph-1* mutant when compared to wild type (Table 1, Fig. 1B), while *flgM* and *flgN* only showed a 1.51-fold increase in abundance in the *ΔrppH rph-1* mutant when compared to wild-type control (Table 1, Fig. 1B).

Class III genes in the flagellar gene regulatory pathway were also analyzed. These genes encode proteins that make up the filament, the cap, flagellins and hook associated proteins (27-29). *fliC* encodes flagellin, the protein subunit that forms the flagellar filament, and shows a 1.73-fold increase in abundance in the *ΔrppH rph-1* mutant when compared to wild type (Table 1, Fig. 1C) (27-29). The transcript *motAB cheAW* encodes the proteins that form the flagellar stator (MotA and MotB), the non-rotating part of the motor, and proteins involved in chemotaxis (CheA and CheW) (29). *motA* showed a 1.42-fold and *cheAW* showed a 1.41-fold increase in abundance in the *ΔrppH rph-1* mutant when compared to wild type (Table 1, Fig. 1A). Lastly, the transcript that encodes Tar, Tap, CheR, CheB, CheY, and CheZ, all involved in chemotaxis,

had varying abundance patterns (27-29). The *tap* and *tar* RNA levels showed a 1.37-fold increase in *ΔrppH rph-1* mutant when compared to wild type (Table 1, Fig. 1A).

**RppH affects the abundance of *flhDC*, the major regulator of the flagellar gene regulatory pathway**

To validate the array results and confirm that the *flhDC* transcript was stabilized in the *ΔrppH rph-1* background, northern analysis was conducted to observe steady-state levels of *flhDC*. It should be noted that due to the fact that *flhDC* is the master regulator of the flagellar gene regulatory pathway, changes in the stability of its mRNA could in turn up-regulate all downstream genes in the pathway if the change in mRNA stability resulted in increased levels of the master regulator protein. Thus, our focus here was to understand the effect RppH specifically had on the *flhDC* transcript. Northern analysis results showed *flhDC* was approximately 25.2-times more abundant in the *ΔrppH rph-1* mutant background as compared to wild type (Fig. 2C, Lanes 1 & 2). It is important to note that in the wild-type background, this transcript was barely present (Fig. 2C, Lane 1).

**Array validation through northern analysis of selected transcripts**

We also analyzed specific transcripts through northern analysis that were effected in either array that were not related to the flagellar gene regulatory network in order to better correlate the changes observed on the arrays with *in vivo* alterations in the steady state-level of specific mRNAs. For instance the

*yeiP* mRNA, which encodes an NAD-dependent predicted dehydrogenase, was reported as being 5.9 times more abundant in a previous array employing an in active RppH protein (1). Our array data showed increased abundance of the *yeiP* mRNA in both SK4390 (*ΔrppH rph-1*) (1.50-fold) and SK4426 (*ΔrppH rph*$^{+}$) (1.51-fold) versus the appropriate control strain (Fig. 3A & B). When northern analysis was used to verify the abundance of the *yeiP* mRNA in wild type, SK4390 (*ΔrppH rph-1*), and SK4426 (*ΔrppH rph*$^{+}$) strains, there were 29.5-fold and 19.3-fold increases in the full-length *yeiP* mRNA, respectively (Fig. 3C).

The small regulatory RNA *csrB*, is responsible for binding to the CsrA protein (40), which inhibits CsrA activity (41). CsrA is responsible for numerous biological functions in *E. coli* including, but not limited to glycogen biosynthesis, gluconeogenesis, glycolysis, and biofilm dynamics (42,43). Most interestingly however, is that CsrA is integral in posttranscriptional activation of the *flhDC* flagellar regulatory genes (44). Our array showed an increased abundance of the *csrB* RNA in SK4426 (*ΔrppH rph*$^{+}$) (1.2-fold), but no change in SK4390 (*ΔrppH rph-1*) (Fig. 4A & B). Northern analysis showed that *csrB* RNA was 1.7-fold more abundant in SK4426 but only 1.1-fold more abundant in SK4390 (Fig. 4C).

The *lpp* mRNA, which encodes a murein lipoprotein, is one of the most abundant proteins in *E. coli* and is necessary for the stabilization of the bacterial cell envelope (45,46). Array analysis showed a significant increase in abundance of the *lpp* mRNA in both SK4390 (*ΔrppH rph-1*) and SK4426 (*ΔrppH rph*$^{+}$), at 1.1-fold (Fig. 5A & B). Northern analysis of *lpp* confirmed the array data,

showing that there is 2.2-fold more *lpp* in SK4390 (*ΔrppH rph-1*) and SK4426 (*ΔrppH rph*$^{+}$) than in their wild-type controls (Fig. 5C).

Lastly, we analyzed the *ompF* mRNA, which encodes the outer membrane porin F protein and is produced as a monocistronic transcript (47,48). The array data showed that in SK4390 (*ΔrppH rph-1*) the mRNA is 1.4-fold more abundant than in its wild-type counterpart, whereas in SK4426 (*ΔrppH rph*$^{+}$) the mRNA is less abundant with a fold change of -1.5 compared to its wild-type counterpart (Fig. 6A & B). Northern analysis of *ompF* again confirmed the array data, showing that there was 20-fold more *ompF* in SK4390 (*ΔrppH rph-1*) and 2.0-fold less *ompF* in SK4426 (*ΔrppH rph*$^{+}$) than in their wild type counterparts (Fig. 6C).

**The *ΔrppH* mutation restores motility to the non-motile *ΔapaH* mutant strain**

With microarray and northern data supporting the idea that inactivation of RppH stabilizes the master regulator and downstream classes of genes in the flagellar gene regulatory network, we determined if the changes in mRNA levels resulted in altered cellular motility. The *ΔrppH* chromosomal deletion was transduced into a *ΔapaH* mutant background. ApaH is a known tetraphosphate pyrophosphohydrolase that has substrate specificity for similar diadenosine polyphosphates as RppH in the cell, but cleaves them symmetrically unlike asymmetrical cleavages by RppH (49-51). The *ΔapaH* mutant background causes an accumulation of AppppA and leads to decreased transcription of

genes in the flagellar regulatory network, thereby rendering the cells non-motile (26). We were interested in determining if the *ΔrppH* mutation restored motility to the non-motile *ΔapaH* mutant. Through the use of motility assays that measure the circumference of a migration halo on 0.35% agar plates, we observed that the *ΔrppH rph-1* strain had the highest motility, with an average halo circumference of 2.44 cm (SD 0.09) (Fig. 7). The *ΔapaH* mutant background was much less motile than the wild-type strain, migrating an average of 0.3 cm (SD 0.07) and 0.74 cm (SD 0.19) over 24 hours, respectively (Fig. 7). As hypothesized, the *ΔrppH* mutation restored motility to the *ΔapaH* mutant at levels far above the *rph-1* control, with migration averaging 1.72 cm (SD 0.19) over 24 hours (Fig. 7).

**The effect on motility by RppH is dependent upon RNase PH**

With microarray and northern analysis data supporting inactivation of RppH in an *rph-1* background stabilizes *flhDC*, we examined whether or not this would have an effect on cellular motility. Surprisingly, no significant changes in motility were observed when comparing the *rph*-1 strain to the *rph*$^+$ strain over a 48-hour period (Fig. 8). However, when comparing motility in these backgrounds that contained the *ΔrppH* mutation, the data were drastically different. The *ΔrppH rph-1* strain was the most motile after every time period tested through 48 hours. In contrast, the *ΔrppH rph*$^+$ strain showed comparable motility to both the *rph-1* and *rph*$^+$ strains (Fig. 8). After also observing that the effect of RppH on RNase P activity was dependent on the presence or absence of the

truncated Rph-1 protein (see Chapter 2), we wanted to investigate what effect a *Δrph* mutation may also have on motility. Surprisingly, the *Δrph* and *ΔrppH Δrph* strains were nearly as motile as a *ΔrppH rph*$^+$ strain (Fig. 8). These data clearly indicated that *ΔrppH* has some role in altering cellular motility, but only in the presence of an *rph-1* allele.

## DISCUSSION

Our study set out to get a more precise picture as to the effects of RppH on the *E. coli* transcriptome through the analysis of a chromosomal deletion of RppH by high-density tiling microarrays. Our data indicate that, when compared to the previous array data, which analyzed a non-functional RppH derivative, only 21% or 16% of the reported transcripts were seen to increase in abundance with a chromosomal deletion of RppH in an *rph-1* or an *rph*$^+$ strain, respectively (82/382 and 61/382) (Table 2). Additionally when comparing the individual arrays for similar transcripts that were either higher or lower in abundance, the results were even more disparate. When comparing the array conducted by Deana et al. (1) to the *ΔrppH rph-1* array and the *ΔrppH rph*$^+$ array there were only nine and twenty five transcripts that are higher in abundance in both arrays, respectively (Table 3). Interestingly when comparing the *ΔrppH rph-1* and the *ΔrppH rph*$^+$ array to each other only eight transcripts were similarly more abundant and only five transcripts are similarly less abundant (Table 3). These results suggest that completely eliminating the protein from the cell of RppH has a very different effect on the transcriptome than having a non-functional form

present in high abundance. Even though decapping activity is abolished in the RppH derivative used in the previous array (1), this form of RppH may still be functional on other substrates it has specificity for, such as the polyphosphates which do not structurally resemble 5′-mRNA caps (6,51). This in itself can change the profile of the transcriptome, either directly or indirectly. Alternatively, this derivative could also still exhibit RNA binding, resulting in non-functional RppH proteins bound to RNA substrates, which could stabilize a substrate by protecting against ribonucleolytic degradation. It is for these reasons our data reflect a more accurate depiction of how RppH affects the entire transcriptome.

Our data are the first to implicate RppH in the regulation of the flagellar gene regulatory network. We have shown that in the absence of RppH, all transcripts in this pathway increase in abundance by an average of 1.5 fold (Table 1, Fig. 1). Previous data have only implicated various environmental factors on transcription regulation of *flhDC*, such as pH levels, cAMP-CAP (carbon sources), quorum sensing, cell cycle, and the surface of adhesion (27). To date, only CsrA has been identified in regulating the message stability of *flhDC* (44). Interestingly, as shown in figure 4, *csrB* was shown to be higher in abundance in *ΔrppH rph*$^{+}$, but not in *ΔrppH rph-1*, and it is known that *csrB* inhibits activity of CsrA. Perhaps there is an indirect effect in the *ΔrppH rph*$^{+}$ background that decreases overall activation of *flhDC* from decreased activity of CsrA due to increased abundance in *csrB* RNA that can bind to CsrA. This observation is not apparent in SK4390, which could further explain why we notice increased motility in SK4390.

As for protein stability, the protease ClpXP is known to negatively regulate FlhDC (52,53). FliZ has been shown to positively regulate FlhDC, either by down regulating ClpXP expression, or by inducing transcription of the factor that directly stabilizes FlhDC (27,54-56). Lastly, FliT can also affect FlhDC activity by sequestering the protein and preventing it from activating transcription of class II genes in the regulatory network (54,57). Though extremely complicated, understanding regulation of the *flhDC* transcript is paramount for fully understanding the entire bacterial flagellar regulatory network. This study has provided new insights into understanding this exact regulation.

Through northern analysis, we have shown that the steady-state levels of the *flhDC* mRNA is up 25-fold, which would indicate higher levels than determined through high-density tiling microarray analysis (Fig. 2). This in itself can provide insight into the limitations of the tiling microarrays and support the need for validation for northern analysis. Seeing that the *ΔrppH rph-1* mutant showed hypermotility and complemented a non-motile *ΔapaH* strain, it would make sense that a 1.42-fold increase, as seen in the array data, would not be enough to cause this drastic change in motility (Table 1, Figs. 2 & 7). Therefore our northern data allow for a more exact validation of both the array data and the results seen in the motility assays.

As for motility, it is still unclear the mechanism that allows for hypermotility in the *ΔrppH rph-1* mutant background. Seeing that the *ΔrppH rph-1* mutant that was tested was not in a true wild-type background, we

wanted to see if the addition of a functional RNase PH would influence the effect RppH had on motility. Surprisingly, we were able to show that in the presence of RNase PH, the *ΔrppH* mutation does not have the same effect on motility (Fig. 8). It is possible that the activity of RNase PH, a 3′→5′ exoribonuclease, is influencing how the 5′-triphosphate is recognized by ribonucleases, thereby allowing the *flhDC* transcript to be degraded and restoring motility to wild-type levels. It is still unclear if and how this is occurring. More experimentation is needed to determine if *flhDC* is actually a substrate of RNase PH or if this is an indirect effect involving another aspect of *flhDC* regulation.

It is also unclear how hypermotility is occurring in the *ΔrppH rph-1* mutant background. Hypermotility can result from a number of factors: more flagella, longer flagella, faster rotation, increased cell division that results in more cells being flagellated. To date, the regulation of increased motility is not well understood. Filament growth is known to be independent of cell cycle while filament length is controlled in a more localized fashion at the base of each flagellum (58). Further, the number of filaments or flagellar basal bodies is dependent on cell cycle and can be increased by either increasing levels of FlhDC or $\sigma^{28}$ (28,59,60). A mutation in *flgM*, the anti-$\sigma^{28}$, showed a two- to three-fold increase in the number of flagellum in *S. enterica* serovar Typhimurium, while increasing the transcription of *flhDC* resulted in a transition from swimmers to swarmers and a two-fold increase in flagellum number in both *S. enterica* serovar Typhimurium and *E. coli* (28,61,62). These studies would indicate a feedback loop for class I and class II genes, allowing $\sigma^{28}$ to regulate *flhDC*

transcription. This would further increase the already abundant *flhDC*, therefore resulting in hypermotility. To determine what is actually occurring in the *ΔrppH rph-1* mutant background, it is important to determine which of these scenarios is actually occurring. Through the use of fluorescent microscopy, one can determine the number and length of flagella or the number of cells that are flagellated in the *ΔrppH rph-1* mutant background. Thus far, we hypothesize that it is a combination of all these scenarios.

Although this is an extremely complicated pathway, it is important to understand how it is being regulated. Seeing that the flagellar protein export apparatus is a type III secretion system, this study can provide answers to how *rppH* is involved in suppressing hybrid jamming in the general secretory (Sec) pathway, which may result in the presence of more export apparatus' to overcome the jamming (7,34). Further studies need to be conducted to determine how the polyphosphates that RppH has specificity for are involved in the hypermotility effect seen in our study, whether directly or indirectly. Levels of $Ap_4A$, $Ap_5A$, and $Ap_6A$ need to be measured to see how much RppH actually influences these levels, especially in the presence and absence of ApaH. One could determine how these polyphosphates regulate motility by manipulating the intracellular populations and seeing their effects on motility. Only time will tell how this intricate pathway of motility regulation is working in the cell. Our study paves the way for narrowing the search and better understanding all the key players in the flagellar gene regulatory network.

**ACKNOWLEDGEMENTS**

This work was supported in part by a grant from the National Institutes of Health (GM081544) to S.R.K.

**REFERENCES**

1. Deana, A., Celesnik, H. and Belasco, J.G. (2008) The bacterial enzyme RppH triggers messenger RNA degradation by 5' pyrophosphate removal. *Nature*, **451**, 355-358.
2. Celesnik, H., Deana, A. and Belasco, J.G. (2007) Initiation of RNA decay in *Escherichia coli* by 5' pyrophosphate removal. *Mol. Cell*, **27**, 79-90.
3. Jiang, X. and Belasco, J.G. (2004) Catalytic activation of multimeric RNase E and RNase G by 5'-monophosphorylated RNA. *Proc. Natl. Acad. Sci. USA*, **101**, 9211-9216.
4. Mackie, G.A. (1998) Ribonuclease E is a 5'-end-dependent endonuclease. *Nature*, **395**, 720-723.
5. Badger, J.L., Wass, C.A. and Kim, K.S. (2000) Identification of *Escherichia coli* K1 genes contributing to human brain microvascular endothelial cell invasion by differential fluorescence induction. *Mol. Microbiol.*, **36**, 174-182.
6. Bessman, M.J., Walsh, J.D., Dunn, C.A., Swaminathan, J., Weldon, J.E. and Shen, J. (2001) The gene *ygdP*, associated with the invasiveness of *Escherichia coli* K1, designates a Nudix hydrolase, Orf176, active on

adenosine (5')-pentaphospho-(5')-adenosine (Ap5A). *J. Biol. Chem.*, **276**, 37834-37838.

7. Hand, N.J. and Silhavy, T.J. (2003) Null mutations in a Nudix gene, *ygdP*, implicate an alarmone response in a novel suppression of hybrid jamming. *J. Bacteriol.*, **185**, 6530-6539.

8. Stead, M.B., Marshburn, S., Mohanty, B.K., Mitra, J., Pena Castillo, L., Ray, D., van Bakel, H., Hughes, T.R. and Kushner, S.R. (2011) Analysis of *Escherichia coli* RNase E and RNase III activity *in vivo* using tiling microarrays. *Nucleic Acids Res.*, **39**, 3188-3203.

9. Stead, M.B., Agrawal, A., Bowden, K.E., Nasir, R., Mohanty, B.K., Meagher, R.B. and Kushner, S.R. (2012) RNA*snap*: a rapid, quantitative and inexpensive, method for isolating total RNA from bacteria. *Nucleic Acids Res.*, **40**, e156.

10. Pruss, B.M. and Matsumura, P. (1997) Cell cycle regulation of flagellar genes. *J. Bacteriol.*, **179**, 5602-5604.

11. Wei, B.L., Brun-Zinkernagel, A.M., Simecka, J.W., Pruss, B.M., Babitzke, P. and Romeo, T. (2001) Positive regulation of motility and *flhDC* expression by the RNA-binding protein CsrA of *Escherichia coli*. *Mol. Microbiol.*, **40**, 245-256.

12. Claret, L. and Hughes, C. (2002) Interaction of the atypical prokaryotic transcription activator FlhD2C2 with early promoters of the flagellar gene hierarchy. *J. Mol. Biol.*, **321**, 185-199.

13. Frye, J., Karlinsey, J.E., Felise, H.R., Marzolf, B., Dowidar, N., McClelland, M. and Hughes, K.T. (2006) Identification of new flagellar genes of Salmonella enterica serovar Typhimurium. *J. Bacteriol.*, **188**, 2233-2243.

14. Gillen, K.L. and Hughes, K.T. (1993) Transcription from two promoters and autoregulation contribute to the control of expression of the *Salmonella typhimurium* flagellar regulatory gene *flgM*. *J. Bacteriol.*, **175**, 7006-7015.

15. Liu, X. and Matsumura, P. (1994) The FlhD/FlhC complex, a transcriptional activator of the *Escherichia coli* flagellar class II operons. *J. Bacteriol.*, **176**, 7345-7351.

16. Pruss, B.M., Liu, X., Hendrickson, W. and Matsumura, P. (2001) FlhD/FlhC-regulated promoters analyzed by gene array and *lacZ* gene fusions. *FEMS Microbiol. Lett.*, **197**, 91-97.

17. Ohnishi, K., Kutsukake, K., Suzuki, H. and Iino, T. (1990) Gene *fliA* encodes an alternative sigma factor specific for flagellar operons in *Salmonella typhimurium*. *Molecular Genetics and Genomics*, **221**, 139-147.

18. Kutsukake, K., Ohya, Y. and Iino, T. (1990) Transcriptional analysis of the flagellar regulon of *Salmonella typhimurium*. *J. Bacteriol.*, **172**, 741-747.

19. Hughes, K.T., Gillen, K.L., Semon, M.J. and Karlinsey, J.E. (1993) Sensing structural intermediates in bacterial flagellar assembly by export of a negative regulator. *Science*, **262**, 1277-1280.

20. Jensen, K.G. (1993) The *Escherichia coli* K-12 "wild types" W3110 and MG1655 have an *rph* frameshift mutation that leads to pyrimidine starvation due to low *pyrE* expression levels. *J. Bacteriol.*, **175**, 3401-3407.

21. Mohanty, B.K., Maples, V.F. and Kushner, S.R. (2012) Polyadenylation helps regulate functional tRNA levels in *Escherichia coli*. *Nucleic Acids Res.*, **40**, 4589-4603.

22. Baba, T., Ara, T., Hasegawa, M., Takai, Y., Okumura, Y., Baba, M., Datsenko, K.A., Tomita, M., Wanner, B.L. and Mori, H. (2006) Construction of *Escherichia coli* K-12 in-frame, single-gene knockout mutants: the Keio collection. *Mol. Syst. Biol.*, **2**, 2006 0008.

23. Cherepanov, P.P. and Wackernagel, W. (1995) Gene disruption in *Escherichia coli*: TcR and KmR cassettes with the option of Flp-catalyzed excision of the antibiotic-resistance determinant. *Gene*, **158**, 9-14.

24. Datsenko, K.A. and Wanner, B.A. (2000) One-step inactivation of chromosomal genes in *Escherichia coli* K-12 using PCR products. *Proc. Natl. Acad. Sci. USA*, **97**, 6640-6645.

25. O'Hara, E.B., Chekanova, J.A., Ingle, C.A., Kushner, Z.R., Peters, E. and Kushner, S.R. (1995) Polyadenylylation helps regulate mRNA decay in *Escherichia coli*. *Proc. Natl. Acad. Sci. USA*, **92**, 1807-1811.

26. Farr, S.B., Arnosti, D.N., Chamberlin, M.J. and Ames, B.N. (1989) An *apaH* mutation causes AppppA to accumulate and affects motility and

catabolite repression in *Escherichia coli*. *Proc. Natl. Acad. Sci. USA*, **86**, 5010-5014.

27. Smith, T.G. and Hoover, T.R. (2009) Deciphering bacterial flagellar gene regulatory networks in the genomic era. *Adv. Appl. Microbiol.*, **67**, 257-295.

28. Chilcott, G.S. and Hughes, K.T. (2000) Coupling of flagellar gene expression to flagellar assembly in Salmonella enterica serovar typhimurium and *Escherichia coli*. *Microbiol. Mol. Biol. Rev.*, **64**, 694-708.

29. Apel, D. and Surette, M.G. (2008) Bringing order to a complex molecular machine: the assembly of the bacterial flagella. *Biochim. Biophys. Acta*, **1778**, 1851-1858.

30. Mytelka, D.S. and Chamberlin, M.J. (1996) *Escherichia coli fliAZY* operon. *J. Bacteriol.*, **178**, 24-34.

31. Ueno, T., Oosawa, K. and Aizawa, S. (1992) M ring, S ring and proximal rod of the flagellar basal body of *Salmonella typhimurium* are composed of subunits of a single protein, FliF. *J. Mol. Biol.*, **227**, 672-677.

32. Minamino, T., Gonzalez-Pedrajo, B., Yamaguchi, K., Aizawa, S.I. and Macnab, R.M. (1999) FliK, the protein responsible for flagellar hook length control in Salmonella, is exported during hook assembly. *Mol. Microbiol.*, **34**, 295-304.

33. Minamino, T. and MacNab, R.M. (2000) FliH, a soluble component of the type III flagellar export apparatus of Salmonella, forms a complex with FliI and inhibits its ATPase activity. *Mol. Microbiol.*, **37**, 1494-1503.

34. Minamino, T. and Macnab, R.M. (1999) Components of the Salmonella flagellar export apparatus and classification of export substrates. *J. Bacteriol.*, **181**, 1388-1394.

35. Kubori, T., Sukhan, A., Aizawa, S.I. and Galan, J.E. (2000) Molecular characterization and assembly of the needle complex of the *Salmonella typhimurium* type III protein secretion system. *Proc. Natl. Acad. Sci. USA*, **97**, 10225-10230.

36. Macnab, R.M. (2003) How bacteria assemble flagella. *Annu. Rev. Microbiol.*, **57**, 77-100.

37. Nambu, T. and Kutsukake, K. (2000) The *Salmonella* FlgA protein, a putativeve periplasmic chaperone essential for flagellar P ring formation. *Microbiol.*, **146 ( Pt 5)**, 1171-1178.

38. Fraser, G.M., Bennett, J.C. and Hughes, C. (1999) Substrate-specific binding of hook-associated proteins by FlgN and FliT, putative chaperones for flagellum assembly. *Mol. Microbiol.*, **32**, 569-580.

39. Daughdrill, G.W., Chadsey, M.S., Karlinsey, J.E., Hughes, K.T. and Dahlquist, F.W. (1997) The C-terminal half of the anti-sigma factor, FlgM, becomes structured when bound to its target, sigma 28. *Nat. Struct. Biol.*, **4**, 285-291.

40. Liu, M.Y., Gui, G., Wei, B., Preston, J.F., 3rd, Oakford, L., Yuksel, U., Giedroc, D.P. and Romeo, T. (1997) The RNA molecule CsrB binds to the global regulatory protein CsrA and antagonizes its activity in *Escherichia coli*. *J. Biol. Chem.*, **272**, 17502-17510.

41. Weilbacher, T., Suzuki, K., Dubey, A.K., Wang, X., Gudapaty, S., Morozov, I., Baker, C.S., Georgellis, D., Babitzke, P. and Romeo, T. (2003) A novel sRNA component of the carbon storage regulatory system of *Escherichia coli*. *Mol. Microbiol.*, **48**, 657-670.

42. Sabnis, N.A., Yang, H. and Romeo, T. (1995) Pleiotrophic regulation of central carbohydrate metabolism in *Escherichia coli* via the gene *csrA*. *J. Biol. Chem.*, **270**, 29096-29104.

43. Jackson, D.W., Suzuki, K., Oakford, L., Simecka, J.W., Hart, M.E. and Romeo, T. (2002) Biofilm formation and dispersal under the influence of the global regulator CsrA of *Escherichia coli*. *J. Bacteriol.*, **184**, 290-301.

44. Wei, B.L., Brun-Zinkernagel, A.M., Simecka, J.W., Prub, B.M., Babitzke, P. and Romeo, T. (2001) Positive regulation of motility and *flhDC* expression by the RNA-binding protein CsrA of *Escherichia coli*. *Mol. Microbiol.*, **40**, 245-256.

45. Hirashima, A., Wang, S. and Inouye, M. (1974) Cell-free synthesis of a specific lipoprotein of the *Escherichia coli* outer membrane directed by purified messenger RNA. *Proc. Natl. Acad. Sci. USA*, **71**, 4149-4153.

46. Braun, V. and Rehn, K. (1969) Chemical characterization, spatial distribution and function of a lipoprotein (murein-lipoprotein) of the *E. coli* cell wall. The specific effect of trypsin on the membrane structure. *Eur. J. Biochem.*, **10**, 426-438.

47. Cowan, S.W., Schirmer, T., Rummel, G., Steiert, M., Ghosh, R., Pauptit, R.A., Jansonius, J.N. and Rosenbusch, J.P. (1992) Crystal structures explain functional properties of two *E. coli* porins. *Nature*, **358**, 727-733.

48. Mitchell, J.E., Zheng, D., Busby, S.J. and Minchin, S.D. (2003) Identification and analysis of 'extended -10' promoters in *Escherichia coli*. *Nucleic Acids Res.*, **31**, 4689-4695.

49. Mechulam, Y., Fromant, M., Mellot, P., Plateau, P., Blanchin-Roland, S., Fayat, G. and Blanquet, S. (1985) Molecular cloning of the *Escherichia coli* gene for diadenosine 5',5'''-P1,P4-tetraphosphate pyrophosphohydrolase. *J. Bacteriol.*, **164**, 63-69.

50. Plateau, P., Fromant, M. and Blanquet, S. (1987) Heat shock and hydrogen peroxide responses of *Escherichia coli* are not changed by dinucleoside tetraphosphate hydrolase overproduction. *J. Bacteriol.*, **169**, 3817-3820.

51. Guranowski, A. (2000) Specific and nonspecific enzymes involved in the catabolism of mononucleoside and dinucleoside polyphosphates. *Pharmacol. Ther.*, **87**, 117-139.

52. Claret, L. and Hughes, C. (2000) Functions of the subunits in the FlhD(2)C(2) transcriptional master regulator of bacterial flagellum biogenesis and swarming. *J. Mol. Biol.*, **303**, 467-478.

53. Tomoyasu, T., Takaya, A., Isogai, E. and Yamamoto, T. (2003) Turnover of FlhD and FlhC, master regulator proteins for *Salmonella* flagellum biogenesis, by the ATP-dependent ClpXP protease. *Mol. Microbiol.*, **48**, 443-452.

54. Kutsukake, K., Ikebe, T. and Yamamoto, S. (1999) Two novel regulatory genes, fliT and fliZ, in the flagellar regulon of *Salmonella*. *Genes Genet. Syst.*, **74**, 287-292.

55. Lanois, A., Jubelin, G. and Givaudan, A. (2008) FliZ, a flagellar regulator, is at the crossroads between motility, haemolysin expression and virulence in the insect pathogenic bacterium *Xenorhabdus*. *Mol. Microbiol.*, **68**, 516-533.

56. Saini, S., Brown, J.D., Aldridge, P.D. and Rao, C.V. (2008) FliZ Is a posttranslational activator of FlhD4C2-dependent flagellar gene expression. *J. Bacteriol.*, **190**, 4979-4988.

57. Yamamoto, S. and Kutsukake, K. (2006) FliT acts as an anti-FlhD2C2 factor in the transcriptional control of the flagellar regulon in Salmonella enterica serovar typhimurium. *J. Bacteriol.*, **188**, 6703-6708.

58. Aizawa, S.I. and Kubori, T. (1998) Bacterial flagellation and cell division. *Genes Cells*, **3**, 625-634.

59. Kutsukake, K. (1997) Autogenous and global control of the flagellar master operon, *flhD*, in *Salmonella typhimurium*. *Molecular Genetics and Genomics*, **254**, 440-448.

60. Yanagihara, S., Iyoda, S., Ohnishi, K., Iino, T. and Kutsukake, K. (1999) Structure and transcriptional control of the flagellar master operon of *Salmonella typhimurium*. *Genes Genet. Syst.*, **74**, 105-111.

61. Harshey, R.M. and Matsuyama, T. (1994) Dimorphic transition in *Escherichia coli* and *Salmonella typhimurium*: surface-induced differentiation into hyperflagellate swarmer cells. *Proc. Natl. Acad. Sci. USA*, **91**, 8631-8635.

62. Kutsukake, K. and Iino, T. (1994) Role of the FliA-FlgM regulatory system on the transcriptional control of the flagellar regulon and flagellar formation in *Salmonella typhimurium*. *J. Bacteriol.*, **176**, 3598-3605.

63. Nicol, J.W., Helt, G.A., Blanchard, S.G., Jr., Raja, A. and Loraine, A.E. (2009) The Integrated Genome Browser: free software for distribution and exploration of genome-scale datasets. *Bioinformatics*, **25**, 2730-2731.

Table 1. Comparison of *ΔrppH rph-1* and *ΔrppH rph*$^{+}$ array results to previously reported microarray data.

Fold increases calculated as described in Stead et *al*. (8)[1] and Deana et *al*. (1)[2]. Negative values indicate a decrease in overall abundance in the respective mutant compared to wild type, while positive values indicate an increase in overall abundance in the respective mutant compared to wild type. No value indicates no fold change reported.

| Gene | *ΔrppH rph-1* Array Fold-Change[1] | *ΔrppH rph*$^{+}$ Array Fold-Change[1] | Deana et al. Array Fold-Change[2] |
|---|---|---|---|
| *alaE* | 1.47 | – | – |
| *aspA* | – | -1.37 | – |
| *bfr* | – | 1.71 | – |
| *bglA* | – | 1.37 | 2.46 |
| *bsmA* | -1.56 | – | – |
| *carA* | -1.54 | -1.52 | – |
| *carB* | -1.54 | -1.52 | – |
| *cheA* | 1.41 | – | – |
| *cheW* | 1.41 | – | – |
| *cirA* | – | -1.67 | – |
| *clpB* | 1.63 | 1.55 | 1.30 |
| *cspB* | – | -1.96 | – |
| *cspG* | – | -1.35 | – |
| *cysQ* | – | 1.64 | 3.96 |
| *dctA* | – | -1.69 | – |
| *deoA* | -1.39 | – | 1.52 |

| Gene | *ΔrppH rph-1* Array Fold-Change[1] | *ΔrppH rph*⁺ Array Fold-Change[1] | Deana et al. Array Fold-Change[2] |
|---|---|---|---|
| *deoC* | -1.39 | – | 2.22 |
| *dhaK* | – | 1.38 | – |
| *dhaL* | – | 1.38 | – |
| *dhaM* | – | 1.38 | – |
| *dnaJ* | 1.56 | – | – |
| *dnaK* | 1.56 | 1.62 | 1.80 |
| *dps* | – | 1.81 | – |
| *dsdA* | 1.28 | 1.65 | – |
| *dsdX* | 1.47 | 1.65 | – |
| *emrE* | 1.41 | – | – |
| *entA* | – | -1.67 | – |
| *entB* | – | -1.41 | – |
| *entC* | – | -1.43 | – |
| *entE* | – | -1.54 | – |
| *entF* | – | -1.56 | – |
| *entS* | – | -1.64 | – |
| *fepA* | – | -1.47 | – |
| *fepG* | – | -1.39 | – |
| *fhuA* | – | -1.39 | – |
| *fhuB* | – | -1.37 | – |
| *fhuC* | – | -1.37 | – |
| *fimA* | 1.46 | – | 1.67 |
| *fimB* | 1.38 | – | – |
| *fimC* | 1.46 | – | – |
| *fimD* | 1.62 | – | – |
| *fimI* | 1.46 | – | 1.55 |

| Gene | *ΔrppH rph-1* Array Fold-Change[1] | *ΔrppH rph*$^{+}$ Array Fold-Change[1] | Deana et al. Array Fold-Change[2] |
|---|---|---|---|
| *flgA* | 1.58 | – | – |
| *flgB* | 1.52 | – | – |
| *flgC* | 1.52 | – | – |
| *flgD* | 1.52 | – | – |
| *flgE* | 1.52 | – | – |
| *flgF* | 1.52 | – | – |
| *flgG* | 1.52 | – | – |
| *flgH* | 1.52 | – | – |
| *flgI* | 1.52 | – | – |
| *flgJ* | 1.52 | – | – |
| *flgK* | 1.55 | – | – |
| *flgL* | 1.52 | – | – |
| *flgM* | 1.51 | – | – |
| *flgN* | 1.51 | – | – |
| *flhA* | 1.48 | – | – |
| *flhB* | 1.48 | – | – |
| *flhC* | 1.42 | – | – |
| *flhD* | 1.42 | – | – |
| *flhE* | 1.72 | – | – |
| *fliA* | 1.71 | – | – |
| *fliC* | 1.73 | – | – |
| *fliE* | 1.59 | – | – |
| *fliF* | 1.48 | – | – |
| *fliG* | 1.48 | – | – |
| *fliH* | 1.48 | – | – |
| *fliI* | 1.48 | – | – |

| Gene | *ΔrppH rph-1* Array Fold-Change[1] | *ΔrppH rph*$^{+}$ Array Fold-Change[1] | Deana et al. Array Fold-Change[2] |
|---|---|---|---|
| *fliJ* | 1.37 | – | – |
| *fliK* | 1.37 | – | – |
| *fliL* | 1.48 | – | – |
| *fliM* | 1.48 | – | – |
| *fliN* | 1.48 | – | – |
| *fliO* | 1.48 | – | – |
| *fliP* | 1.48 | – | – |
| *fliQ* | 1.48 | – | – |
| *fliR* | 1.48 | – | – |
| *fliY* | – | 1.42 | 2.16 |
| *fliZ* | 1.71 | – | – |
| *flu* | – | -1.82 | 10.16 |
| *fruB* | – | 1.37 | – |
| *ftnA* | – | 1.42 | – |
| *galU* | – | 1.47 | 1.26 |
| *glk* | – | 1.48 | 4.40 |
| *glpA* | – | -1.35 | – |
| *glpB* | – | -1.52 | – |
| *glpF* | – | -1.35 | – |
| *glpQ* | – | -1.52 | – |
| *glpT* | – | -1.52 | – |
| *gpmM* | – | 1.43 | – |
| *groL* | 1.58 | – | – |
| *groS* | 1.58 | – | – |
| *hdhA* | – | 1.46 | – |
| *hsdR* | -1.35 | – | – |

| Gene | *ΔrppH rph-1* Array Fold-Change[1] | *ΔrppH rph*$^{+}$ Array Fold-Change[1] | Deana et al. Array Fold-Change[2] |
|---|---|---|---|
| *hslU* | 1.43 | – | – |
| *hslV* | 1.43 | – | – |
| *htpG* | 1.61 | 1.56 | 2.00 |
| *ibpA* | 1.35 | – | – |
| *ibpB* | 1.35 | – | – |
| *iclR* | – | -1.39 | – |
| *insL* | 1.56 | – | – |
| *isrC* | – | -1.82 | 55.34 |
| *lamB* | – | -1.43 | 2.75 |
| *lldR* | – | -1.33 | – |
| *lrhA* | -1.35 | – | – |
| *lysU* | – | 1.50 | – |
| *mak* | – | 1.41 | – |
| *malF* | – | -1.49 | 2.52 |
| *malK* | – | -1.43 | – |
| *malM* | – | -1.43 | 2.22 |
| *malT* | – | -1.45 | – |
| *manA* | – | 1.54 | 3.76 |
| *mdtI* | – | -1.33 | – |
| *mdtL* | -1.47 | – | – |
| *mglC* | – | -1.54 | – |
| *mgsA* | – | 1.47 | 3.48 |
| *mhpC* | 1.56 | – | – |
| *mhpD* | 1.43 | – | – |
| *mhpE* | 1.49 | – | – |
| *mhpF* | 1.39 | – | – |

| Gene | *ΔrppH rph-1* Array Fold-Change[1] | *ΔrppH rph*⁺ Array Fold-Change[1] | Deana et al. Array Fold-Change[2] |
|---|---|---|---|
| *motA* | 1.42 | – | – |
| *nanA* | – | 1.47 | 3.84 |
| *nrdD* | – | -1.45 | – |
| *ompF* | 1.40 | -1.56 | – |
| *osmE* | – | 1.61 | – |
| *osmY* | – | 1.68 | 1.47 |
| *pgi* | – | 1.53 | 2.62 |
| *poxB* | – | 1.45 | – |
| *qorA* | – | 1.48 | – |
| *rbn* | – | 1.39 | – |
| *rcsA* | 1.83 | – | – |
| *ribC* | | 1.70 | – |
| *rplU* | 1.47 | – | – |
| *rppH* | -1.59 | -1.82 | – |
| *ryfD* | 1.63 | 1.55 | – |
| *sdhA* | – | -1.30 | – |
| *sdhB* | – | -1.30 | – |
| *sdhD* | – | -1.30 | – |
| *slyB* | – | 1.53 | 2.82 |
| *tabA* | 1.68 | – | – |
| *talA* | | 1.50 | – |
| *tap* | 1.37 | – | – |
| *tar* | 1.37 | – | – |
| *tdcA* | -1.69 | – | – |
| *tdcB* | -1.43 | – | – |
| *tdcC* | -1.43 | – | – |

| Gene | *ΔrppH rph-1* Array Fold-Change[1] | *ΔrppH rph*$^{+}$ Array Fold-Change[1] | Deana et al. Array Fold-Change[2] |
|---|---|---|---|
| *tdcD* | -1.67 | – | – |
| *thyA* | – | 1.55 | – |
| *tktB* | – | 1.45 | – |
| *tnaA* | -1.47 | -1.49 | 1.74 |
| *tnaB* | -1.47 | -1.69 | – |
| *tnaC* | -1.47 | – | – |
| *trxB* | 1.38 | 1.48 | 3.09 |
| *tsr* | 1.51 | – | – |
| *wrbA* | – | 1.48 | – |
| *yagU* | 1.38 | – | – |
| *yahK* | – | 1.35 | – |
| *yajQ* | – | 1.55 | 2.86 |
| *ybaY* | – | 1.60 | 2.40 |
| *ybbN* | – | 1.42 | 1.41 |
| *ybhB* | – | 1.52 | – |
| *ybhL* | – | 1.44 | 3.38 |
| *yccA* | – | 1.47 | 3.64 |
| *yccJ* | – | 1.48 | – |
| *yciU* | 1.42 | – | 2.54 |
| *ydbK* | – | 1.33 | 2.10 |
| *ydcL* | – | 1.47 | 1.46 |
| *ydfJ* | – | -1.96 | – |
| *yeaQ* | – | 1.80 | – |
| *yebF* | – | 1.36 | – |
| *yecR* | 1.49 | – | – |
| *yeeR* | – | -1.72 | 6.85 |

| Gene | *ΔrppH rph-1* Array Fold-Change[1] | *ΔrppH rph*$^{+}$ Array Fold-Change[1] | Deana et al. Array Fold-Change[2] |
|---|---|---|---|
| *yeeS* | – | -1.45 | – |
| *yeiP* | 1.56 | 1.61 | 5.93 |
| *ygaM* | – | 1.64 | 2.94 |
| *yggE* | – | 1.44 | – |
| *ygiW* | – | 1.62 | – |
| *yifE* | 1.53 | – | – |
| *yjbJ* | – | 1.46 | – |
| *yjcZ* | 1.28 | – | – |
| *yjdA* | 1.28 | – | – |
| *yjgL* | 1.70 | – | – |
| *yjhB* | 1.65 | – | 1.84 |
| *yjhC* | 1.39 | – | – |
| *yjiA* | – | 1.41 | – |
| *yjiX* | – | 1.96 | – |
| *yjiY* | – | 1.96 | – |
| *ymcE* | – | -1.35 | – |
| *yncE* | – | -1.39 | – |
| *yqhD* | – | 1.44 | 1.93 |
| *ytjA* | – | 1.68 | – |
| *zwf* | – | 1.39 | – |

Table 2. Summary of array data.

Rows state the number of genomic features that were either higher or lower in abundance in each array whereas columns describe the genotype of each array. N.R. indicates data were not reported.

| | Deana et al. Array | *ΔrppH rph-1* Array | *ΔrppH rph*$^+$ Array |
|---|---|---|---|
| **Up** | 382 | 82 | 61 |
| **Down** | N.R. | 16 | 47 |

Table 3. Comparison of common genomic features shared between each array. Rows state the number of common genomic features that were either higher or lower in abundance in each array. Rows indicate the array comparison and raw number of shared genomic features. N/A indicates data are not applicable because Deana et al. (1) did not report any transcripts that had lower steady-state levels.

| | **Deana et al. & *ΔrppH rph-1* Array** | **Deana et al. & *ΔrppH rph*⁺ Array** | ***ΔrppH rph-1* & *ΔrppH rph*⁺ Array** |
|---|---|---|---|
| **Up** | 9 | 25 | 8 |
| **Down** | N/A | N/A | 5 |

Figure 1. Microarray data for the flagellar gene regulatory network operons. Changes in the steady-state levels of the genes that are involved in the flagellar gene regulatory network. The image presented was obtained from a screen shot of the Integrated Genome Browser program (63). Gene names appear above or below the operons that encode them, which indicate their location in the genome relative to nucleotide coordinates, as displayed in the center of the graph. Objects above the genome coordinate line are on the forward strand, while objects below the coordinate line are on the reverse strand. Black arrows indicate the direction of transcription. The array data is displayed as vertical lines representing the $\log_2$ ratio of fluorescence between the mutant and wild-type strains. The horizontal line in the array data is equal to the $\log_2$ ratio of 0, with vertical lines above or below the baseline representing changes in the $\log_2$ ratio of greater or less than 0 for each probe. Vertical lines above the baseline indicate higher RNA abundance in the mutant compared to wild type, while lines below the baseline indicate lower RNA abundance in the mutant compared to wild type. (A) Master regulator *flhDC*; Class II genes: *flhEAB*; Class III genes: cheWAmotBA, tar, tap, cheZYBR; (B) Class II genes; (C) Class II genes: *fliAZY* $\sigma^{28}$; Class III gene: *fliC* flagellin

**1A.**

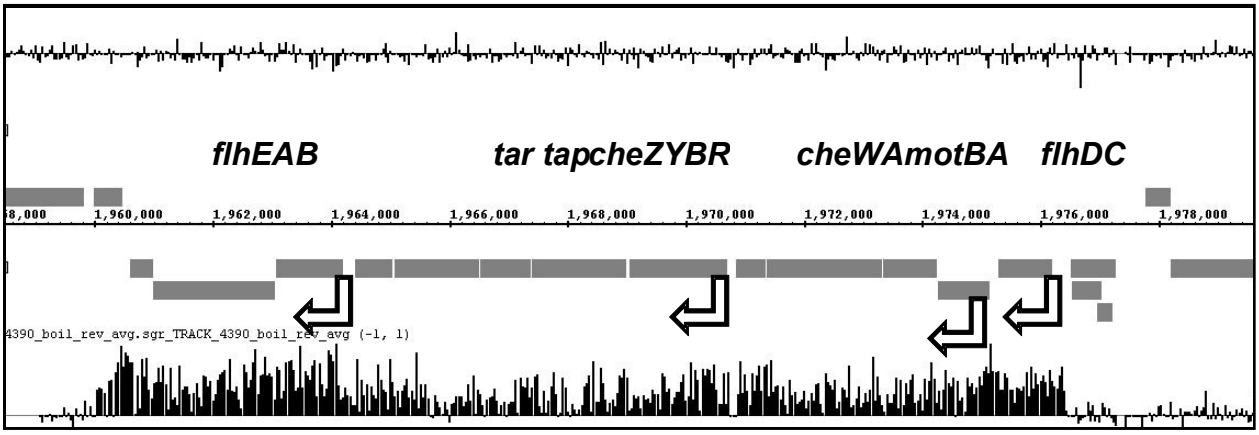
flhEAB
tar tapcheZYBR
cheWAmotBA
flhDC
1,960,000
1,962,000
1,964,000
1,966,000
1,968,000
1,970,000
1,972,000
1,974,000
1,976,000
1,978,000

**1B.**

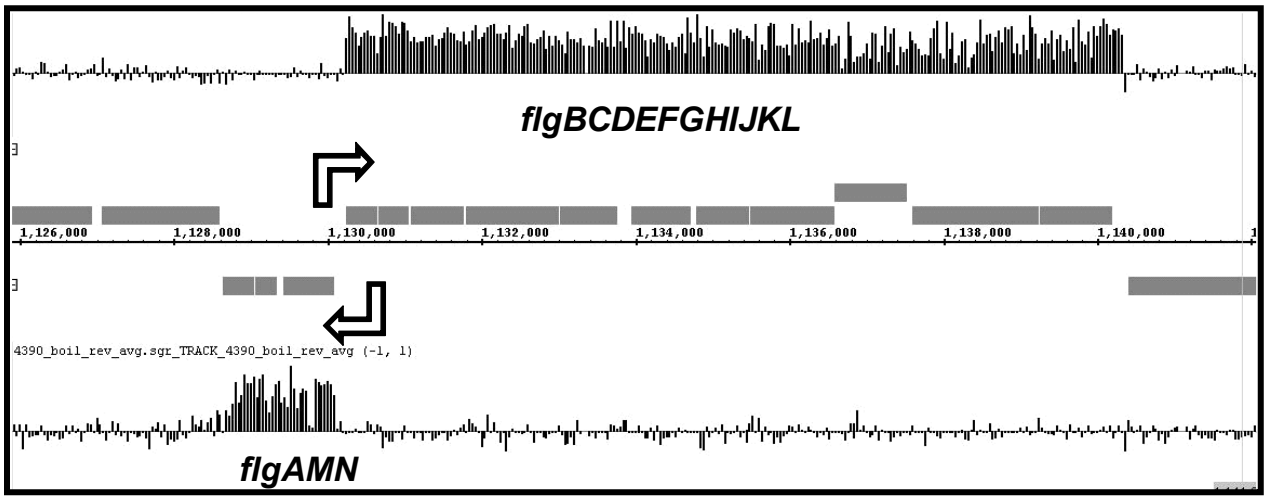
flgBCDEFGHIJKL
1,126,000
1,128,000
1,130,000
1,132,000
1,134,000
1,136,000
1,138,000
1,140,000
flgAMN

**1C.**

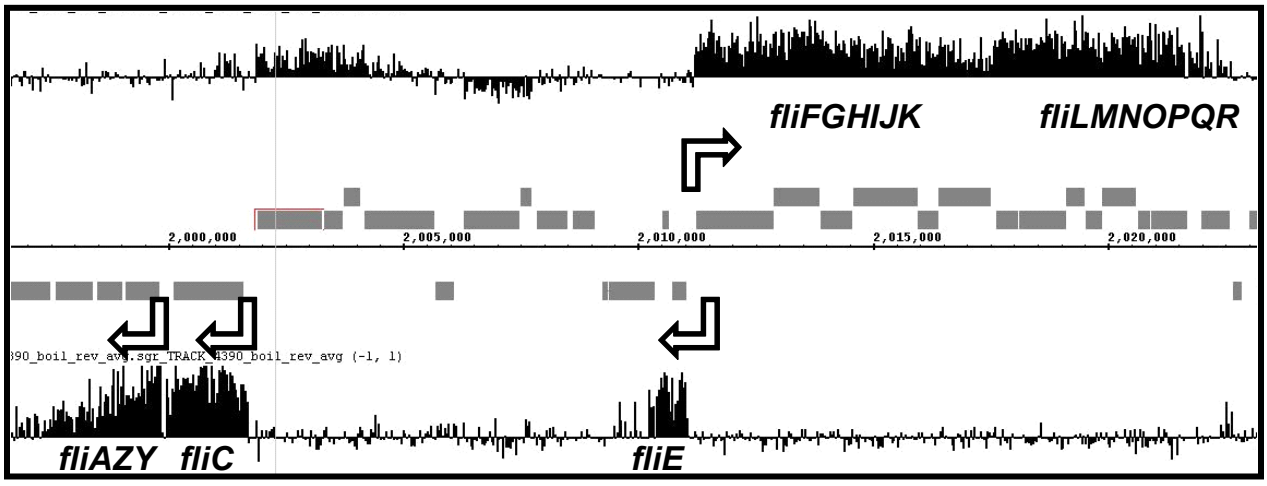
fliFGHIJK
fliLMNOPQR
2,000,000
2,005,000
2,010,000
2,015,000
2,020,000
fliAZY
fliC
fliE

Figure 2. Analysis of *flhDC*, the master regulator of the flagellar regulatory network in various mutant strains.

Northern analysis was conducted as described in Materials and Methods. (A) Microarray data for the *flhDC* operon in the *ΔrppH rph-1* strain. Data are presented as described in Fig. 1. (B) Microarray data for the *flhDC* operon in the *ΔrppH rph*$^{+}$ strain. Data are presented as described in Fig. 1. (C) Northern analysis of the *flhDC* RNA was conducted as described in Materials and Methods. Relative quantities of total signal as compared to the *rph-1* control are indicated below the image. Ribonucleotide size estimates are indicated to the right of the image.

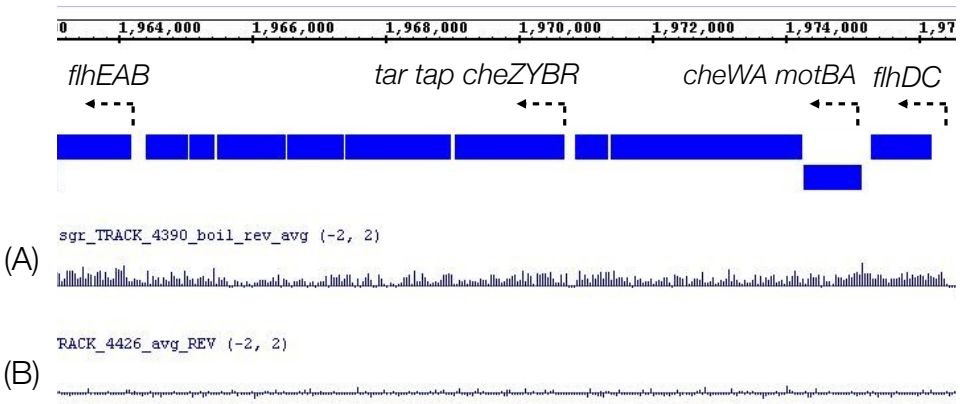
0
1,964,000
1,966,000
1,968,000
1,970,000
1,972,000
1,974,000
1,97
flhEAB
tar tap cheZYBR
cheWA motBA
flhDC
sgr_TRACK_4390_boil_rev_avg (-2, 2)
RACK_4426_avg_REV (-2, 2)

(A)

(B)

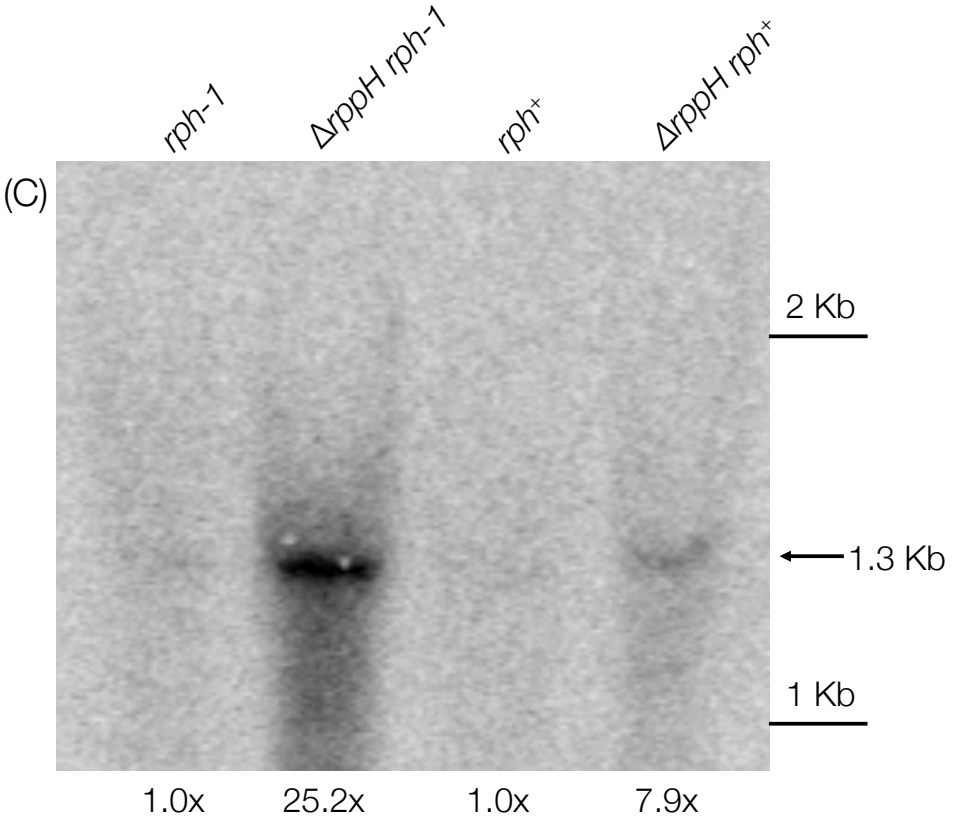
rph-1
ΔrppH rph-1
rph+
ΔrppH rph+
2 Kb
1.3 Kb
1 Kb
1.0x
25.2x
1.0x
7.9x

(C)

Figure 3. Analysis of *yeiP*, a small regulatory RNA in various mutant strains. Northern analysis was conducted as described in Materials and Methods. (A) Microarray data for the *yeiP* RNA in the *ΔrppH rph-1* strain. Data are presented as described in Fig. 1 (B) Microarray data for the *yeiP* RNA in the *ΔrppH rph*$^{+}$ strain. Data are presented as described in Fig. 1 (C) Northern analysis of the *yeiP* RNA was conducted as described in Materials and Methods. Relative quantities of total signal as compared to wild type are indicated below the image. Ribonucleotide size estimates are indicated to the right of the image.

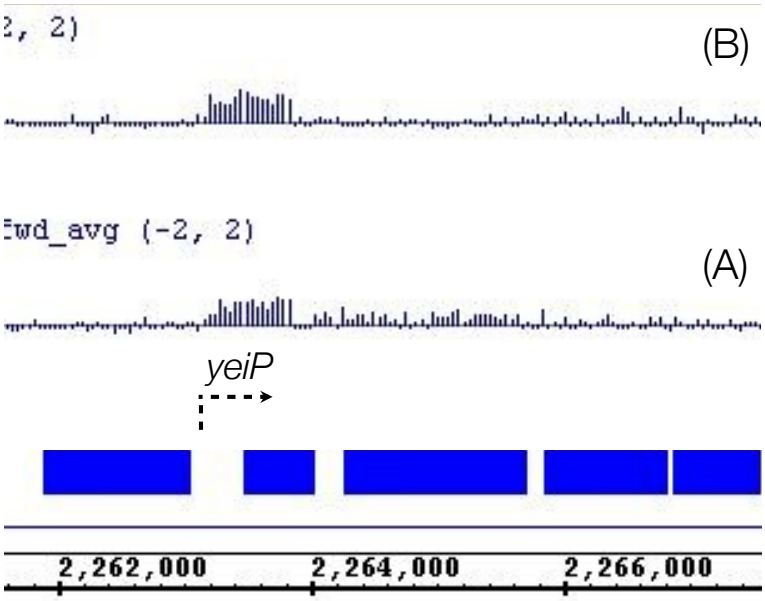
2, 2)
(B)
fwd_avg (-2, 2)
(A)
yeiP
2,262,000
2,264,000
2,266,000

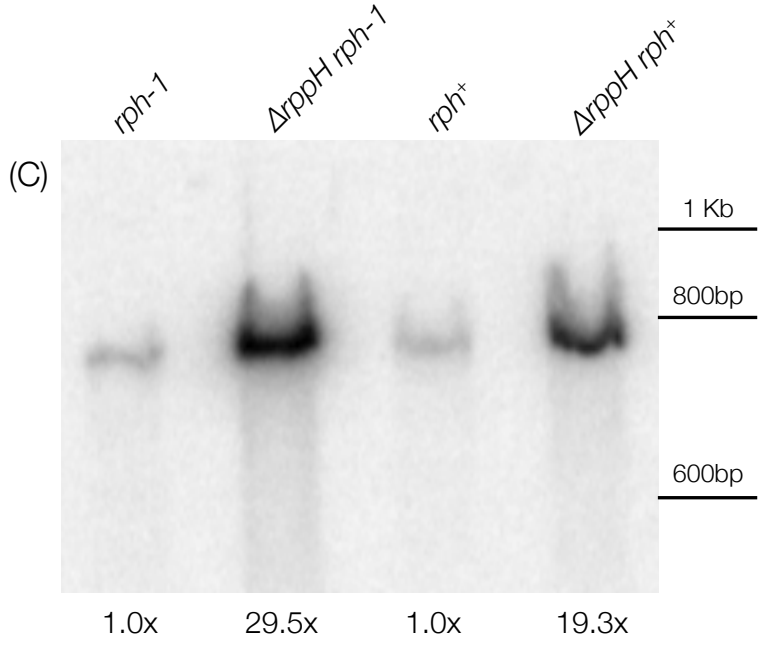
(C)
rph-1
ΔrppH rph-1
rph+
ΔrppH rph+
1 Kb
800bp
600bp
1.0x
29.5x
1.0x
19.3x

Figure 4. Analysis of *csrB*, a small regulatory RNA in various mutant strains. Northern analysis was conducted as described in Materials and Methods. (A) Microarray data for the *csrB* RNA in the *ΔrppH rph-1* strain. Data are presented as described in Fig. 1 (B) Microarray data for the *csrB* RNA in the *ΔrppH rph*$^{+}$ strain. Data are presented as described in Fig. 1 (C) Northern analysis of the *csrB* RNA was conducted as described in Materials and Methods. Relative quantities of total signal as compared to wild type are indicated below the image. Ribonucleotide size estimates are indicated to the right of the image.

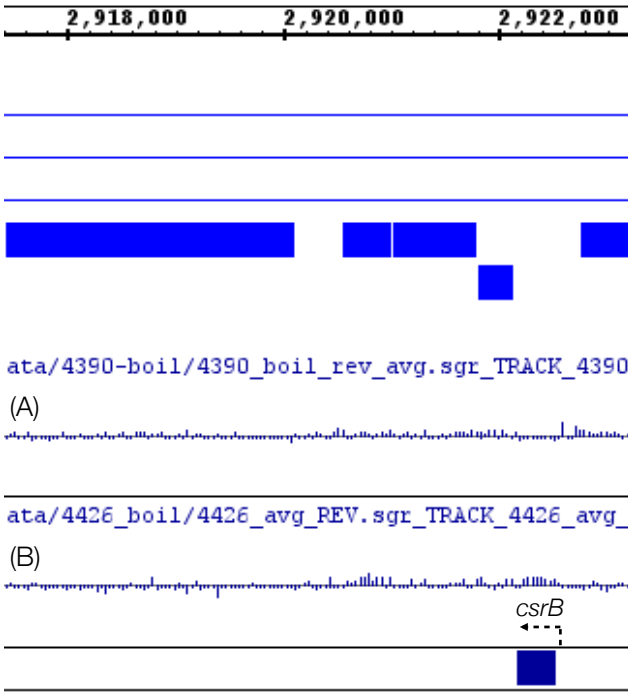
2,918,000
2,920,000
2,922,000
ata/4390-boil/4390_boil_rev_avg.sgr_TRACK_4390
(A)
ata/4426_boil/4426_avg_REV.sgr_TRACK_4426_avg_
(B)
csrB

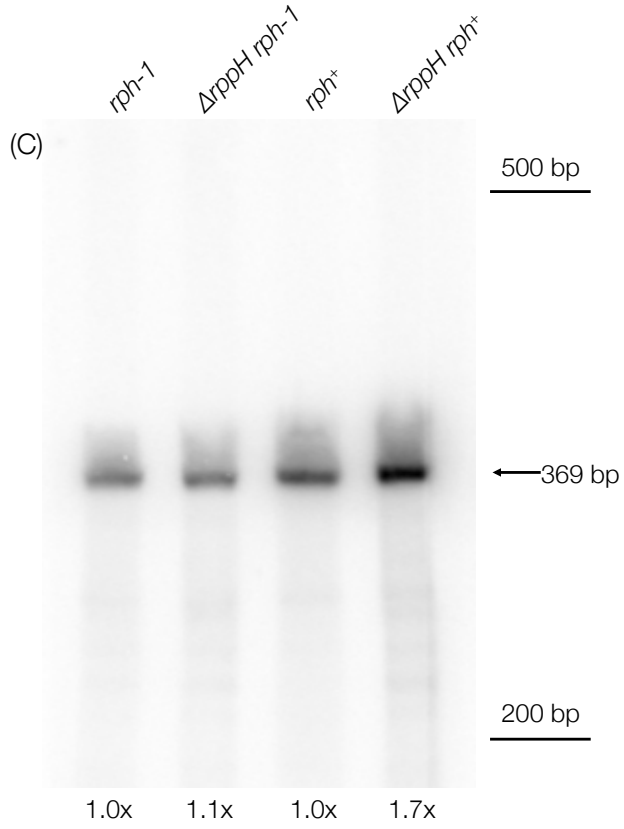
rph-1
ΔrppH rph-1
rph+
ΔrppH rph+
(C)
500 bp
369 bp
200 bp
1.0x
1.1x
1.0x
1.7x

Figure 5. Analysis of *lpp*, a major lipoprotein in various mutant strains. Northern analysis was conducted as described in Materials and Methods. (A) Microarray data for the *lpp* RNA in the *ΔrppH rph-1* strain. Data are presented as described in Fig. 1 (B) Microarray data for the *lpp* RNA in the *ΔrppH rph*$^{+}$ strain. Data are presented as described in Fig. 1 (C) Northern analysis of the *lpp* RNA was conducted as described in Materials and Methods. Relative quantities of total signal as compared to wild type are indicated below the image. Ribonucleotide size estimates are indicated to the right of the image.

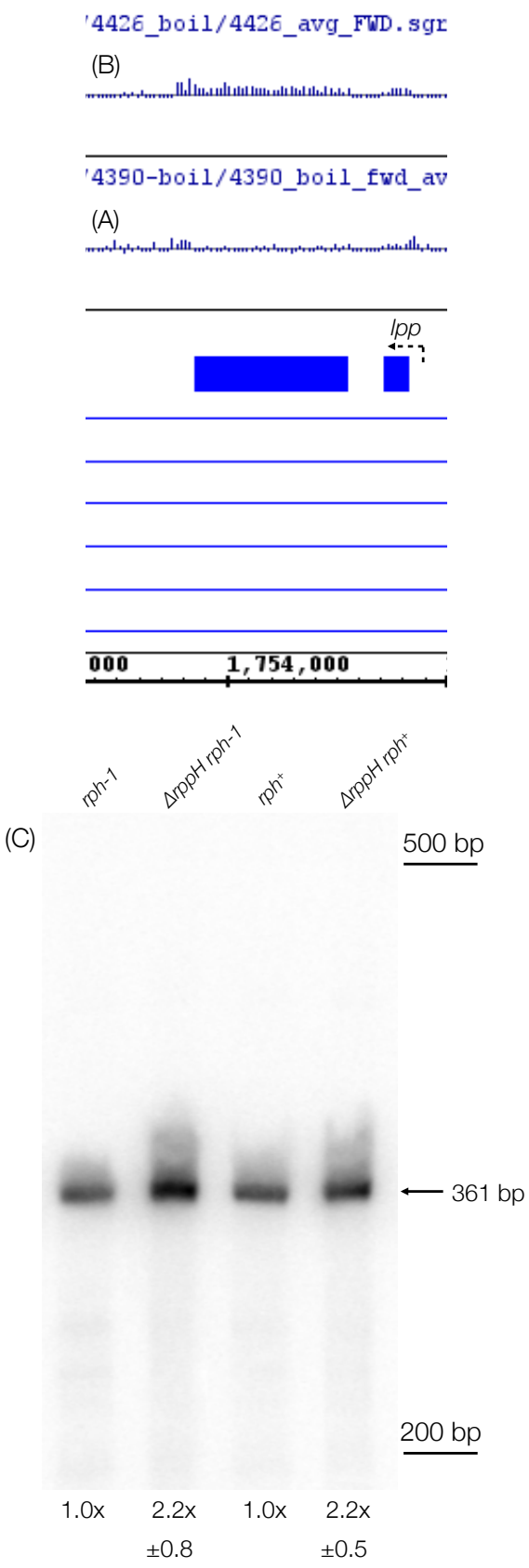
'4426_boil/4426_avg_FWD.sgr
(B)
'4390-boil/4390_boil_fwd_av
(A)
lpp
000
1,754,000
rph-1
ΔrppH rph-1
rph+
ΔrppH rph+
(C)
500 bp
361 bp
200 bp
1.0x
2.2x
±0.8
1.0x
2.2x
±0.5

Figure 6. Analysis of *ompF*, an outer membrane protein in various mutant strains.

Northern analysis was conducted as described in Materials and Methods. (A) Microarray data for the *ompF* RNA in the *ΔrppH rph-1* strain. Data are presented as described in Fig. 1 (B) Microarray data for the *ompF* RNA in the *ΔrppH rph*$^{+}$ strain. Data are presented as described in Fig. 1 (C) Northern analysis of the *ompF* RNA was conducted as described in Materials and Methods. Relative quantities of total signal as compared to wild type are indicated below the image. Ribonucleotide size estimates are indicated to the right of the image.

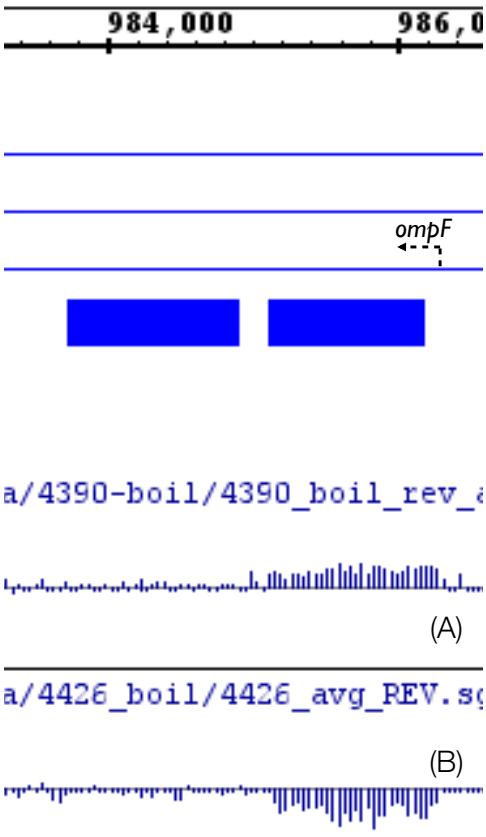
984,000
986,0
ompF
a/4390-boil/4390_boil_rev_
(A)
a/4426_boil/4426_avg_REV.s
(B)

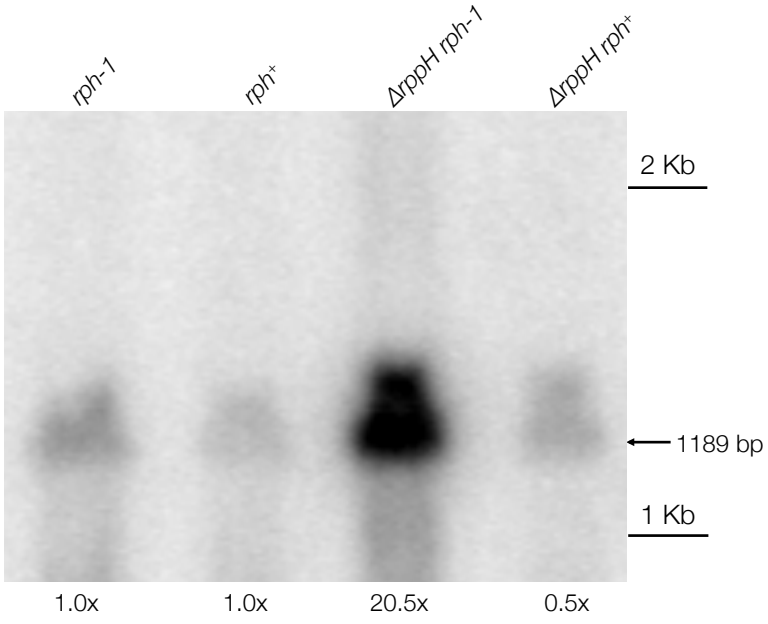
rph-1
rph+
ΔrppH rph-1
ΔrppH rph+
2 Kb
1189 bp
1 Kb
1.0x
1.0x
20.5x
0.5x

Figure 7. Motility analysis of *ΔrppH* and *ΔapaH* mutant strains after 24 hours. Motility analysis was conducted as described in Materials and Methods. Each strain examined is indicated below the graph. Growth was calculated by measuring the circumference of the halo that was seen around the original stab site after plates were left to grow for 24 hours. Bars indicate average halo circumference, brackets indicate values of standard deviation.

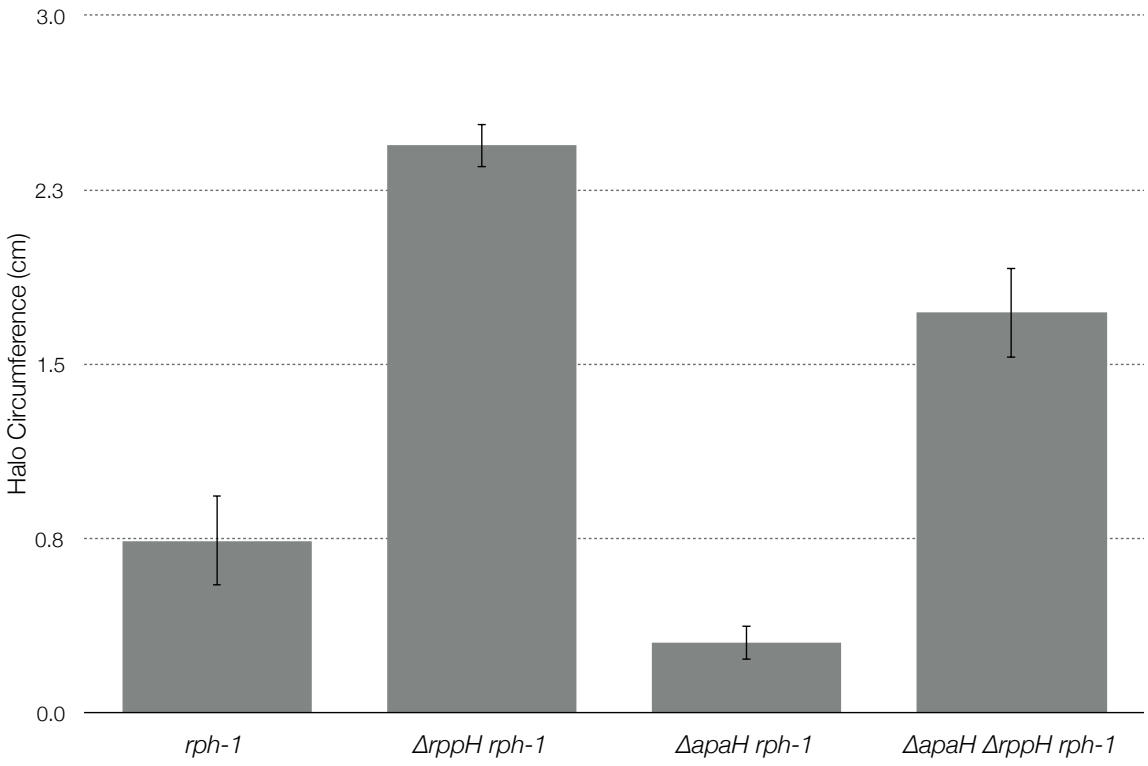
3.0
2.3
1.5
0.8
0.0
Halo Circumference (cm)
rph-1
ΔrppH rph-1
ΔapaH rph-1
ΔapaH ΔrppH rph-1

Figure 8. Motility assays in various mutant strains over 48 hours.

Motility analysis was conducted as described in Materials and Methods. Each strain examined is indicated below the graph. Growth was calculated by measuring the circumference of the halo that was seen around the original stab site normalized to the *rph*-1 strain after plates were left to grow for 24 and 48 hours. Bars indicate average normalized growth, and brackets indicate values of standard deviation.

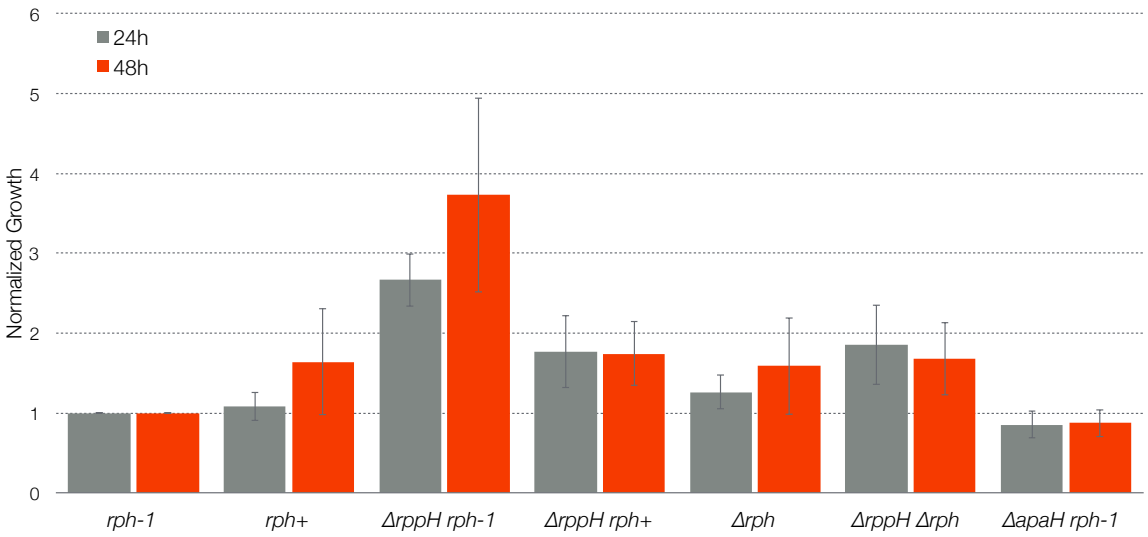
24h
48h
Normalized Growth
0
1
2
3
4
5
6
rph-1
rph+
ΔrppH rph-1
ΔrppH rph+
Δrph
ΔrppH Δrph
ΔapaH rph-1

# CHAPTER 4

# CELL VIABILITY OF AN ORN DELETION STRAIN IN *ESCHERICHIA COLI* IS DEPENDENT ON OTHER EXORIBONUCLEASES[1]

---

[1]Wiese, N.S., Mohanty, B.K., and Kushner, S.R. To be submitted to *Nucleic Acids Research*.

**ABSTRACT**

Oligoribonuclease has long been considered to be the “finishing enzyme” in mRNA decay in *Escherichia coli*. It has also been hypothesized to be essential for cell viability. In order to obtain a better understanding as to whether or not Orn is essential for cell viability and the role it plays in connection with other exoribonucleases, a complete *orn* deletion was constructed and its effects on the physiology of *E. coli* were analyzed. Through this analysis we have discovered that an *orn* deletion on its own does not alter cell viability, but rather its deletion in conjunction with other exoribonucleases such as RNase T or PNPase cause a cessation of growth. Furthermore, we have discovered that the currently annotated transcription start site for *orn* is incorrect and that the promoter is much further upstream than previously thought. This discovery could have further implications for research into the potential regulation of *orn*.

## INTRODUCTION

Messenger RNA (mRNA) degradation plays an essential role in gene expression in both prokaryotic and eukaryotic organisms by helping to control the steady-state level of transcripts, thereby allowing a cell to quickly adapt to its ever-changing metabolic and physiologic environments. In *Escherichia coli*, mRNA decay involves multiple pathways utilizing a series of endo- and exo-ribonucleases (RNases) (1-3). Initiation of mRNA decay begins with endonucleolytic cleavages from RNase E (4), RNase III, and to a lesser degree RNase G (5), followed by exoribonucleases selectively cleaving in the 3′→5′ direction releasing mononucleotides as the end product and thereby allowing synthesis of new transcripts (3).

The main enzymes responsible for exonucleolytic cleavage in the mRNA decay pathway are polynucleotide phosphorylase (PNPase) and RNase II. While these enzymes degrade the vast majority of mRNA decay intermediates generated by RNase E, III, and G. These primary exoribonucleases yield terminal digestion products known as nanoRNAs that are between 2 and 7 nucleotides in length (6-8). Because of the accumulation of these nanoRNAs due to incomplete processing by RNase II and PNPase, *E. coli* contains an enzyme known as oligoribonuclease (Orn).

Orn is a small, 20.7-kDa protein, that belongs to the DEDD family of exoribonucleases (9). Other enzymes in this family include the exoribonucleases RNase D and RNase T, the proofreading domains of numerous DNA polymerases, and DNA exonucleases (9). The enzyme is found in many

organisms ranging from bacteria to humans, and is highly conserved, with the degree of identity of any oligoribonuclease from any organism ranging from 40–50%, suggesting a critical conserved function (10-13) However, no Orn-like protein has been identified in Archaea, Cyanobacteria, or the α-Proteobacteria (13).

*E. coli* Orn is unique from the other known exoribonucleases because of its ability to degrade the nanoRNAs left over by PNPase and RNase II and has been reported as an essential enzyme, unlike in other organisms (11,14,15). Ghosh et al. (14) utilized a deletion of *orn* in the presence of a temperature-sensitive Orn covering plasmid. However, upon shifting to the non-permissive temperature, they reported the presence of micro-colonies that could be rescued when shifted back to the permissive temperature (14). These observations led us to hypothesize that either *orn* may not be truly essential for cell viability in *E. coli* or that there existed a back up mechanism of nanoRNA degradation.

Here we have characterized a *Δorn* mutant strain containing an arabinose-inducible *orn*$^{+}$ covering plasmid constructed in our laboratory. We show that under repressed conditions, no noticeable Orn can be detected by current western blotting techniques, yet the *Δorn* strain is still viable. We further show that the regulation of the *orn* gene may be more intricate than originally anticipated by determining the true transcription start site and identifying the putative promoter sequence. Lastly, we observed that *Δorn Δrnt* and *Δorn Δpnp*

mutants are inviable, providing proof that cell viability of a *Δorn* mutant is dependent on the presence of either RNase T or PNPase.

## MATERIALS AND METHODS

### Bacterial strains

All the *E. coli* strains used in this study were derived from MG1693 (*rph-1 thyA715*) (*E. coli* Genetic Stock Center, Yale University) and are listed in Table 1. SK1698 was constructed by transformation of pKD46 into MG1693. Construction of SK10153 (*rph*$^+$ *thyA715*) has been previously described (16). SK10705 was constructed by utilizing the Lambda-Red recombineering method, as previously described (17) with the following modifications. Overlapping PCR (polymerase chain reaction) was used to create a fragment containing an apramycin resistance cassette flanked by 500 bp and 197 bp of upstream and downstream homology to *orn*, respectively. This linear DNA fragment was then electroporated into SK10706 and was allowed to recover overnight in Luria broth. Samples were then plated onto Luria agar plates supplemented with apramycin (100 μg/mL) and incubated at 37ºC. Resultant colonies were then tested for the presence of *Δorn::apr.*

SK10706 was constructed by transformation of pKD46 and pNWK2 into SK1698. A P1 lysate grown on SK10705 (*Δorn rph-1)* was used to transduce SK10716 (*rph-1*/pNWK6), SK10719 (*rph-1* /pNWK5), and SK10727 (*rph*$^+$ /pNWK6) to generate SK10723 (*Δorn rph-1*/pNWK6), SK10730 (*Δorn rph-1*/pNWK5), and SK10742 (*Δorn rph*$^+$/pNWK6), respectively. SK10740 was

constructed by displacing pNWK6 from SK10736 (*Δorn rph-1* /pNWK6, pNWK11). P1 lysate grown from CMA201, JW1793, JW5741, SK2595, and SK10019 was used to transduce SK10723 to construct SK5984, SK5978, SK5988, SK6002, and SK5992 as well as transduce SK10742 to construct SK5986, SK5980, SK5990, SK6004, and SK5994 respectively. A P1 lysate grown on JW1644 was used to transduce SK10742 to construct SK5962. A P1 lysate grown on JW3618 was used to transduce SK10723 to construct SK5964.

**Plasmid constructions**

Plasmid pNWK2 is a 30–50 copy plasmid with a ColE1 origin of DNA replication expressing *orn* under the control of the *lac* promoter. A PCR fragment containing the *orn* coding sequence was generated using Phusion® High-Fidelity DNA Polymerase (NEB) and cloned into pBMK32 via the BglII/EcoRI restriction sites to construct pNWK2.

Plasmid pNWK5 is a derivative of pSBK29, a low-copy vector containing the pSC101 origin of DNA replication (6–8 copies/cell). A PCR fragment containing the AraC regulatory and pBAD regions from pKD46, the *orn* coding sequence, and the *rrnB* terminator from *E. coli* was generated employing an overlapping PCR technique using Phusion® High-Fidelity DNA Polymerase (NEB) and cloned into pSBK29 via the KpnI/SacII restriction sites to construct pNWK5.

Plasmid pNWK6 is a derivative of pVMK94, a single-copy vector containing the mini-F origin of DNA replication (1 copy/cell). The overlapping

PCR fragment from pNWK5 was cloned via the KpnI/SacII restriction sites into pVMK94 to construct pNWK6.

Plasmid pNWK11 is a derivative of pSBK29, a low-copy vector containing the pSC101 origin of DNA replication (6–8 copies/cell). A PCR fragment containing 100 bp upstream and downstream of the *orn* coding sequence including the *orn* coding sequence was generated using Phusion® High-Fidelity DNA Polymerase (NEB) and cloned into pSBK29 via the KpnI/SacII restriction sites to construct pNWK11.

All the plasmid constructions were confirmed by DNA sequencing of the cloned fragments (Eurofins MWG Operon). In addition, western blotting analysis was used to confirm that induction by isopropyl-β-D-1-thiosgalactopyranoside (IPTG) of plasmid pNWK2 was successful as well as induction and repression by arabinose and glucose, respectively, was successful of plasmids pNWK5 and pNWK6. Plasmid transformations were carried out as previously described (18)

**Growth of bacterial strains**

Bacterial strains were grown in one of three conditions. To induce expression of Orn, all strains were grown at 37ºC with shaking in Luria broth supplemented with thymine (50 μg/mL), arabinose (100 μM), and when appropriate antibiotics apramycin (100 μg/mL), ampicillin (50 μg/mL), chloramphenicol (20 μg/mL), kanamycin (25 μg/mL) in order to maintain selective pressure of mutant genotypes.

To repress expression of Orn, all strains were grown at 37ºC with shaking in Luria broth supplemented with thymine (50 μg/mL), glucose (30 μM), and when appropriate antibiotics apramycin (100 μg/mL), ampicillin (50 μg/mL), chloramphenicol (20 μg/mL), kanamycin (25 μg/mL) in order to maintain selective pressure of mutant genotypes.

To not have any induction of Orn production, all strains were grown at 37ºC with shaking in Luria broth supplemented with thymine (50 μg/mL) and when appropriate antibiotics apramycin (100 μg/mL), ampicillin (50 μg/mL), chloramphenicol (20 μg/mL), kanamycin (25 μg/mL) in order to maintain selective pressure of mutant genotypes.

**Growth curves**

Bacterial strains were grown overnight at either 30ºC or 37ºC with shaking at 225 rpm in Luria broth supplemented with thymine (50 μg/mL) and when appropriate apramycin (100 μg/mL), ampicillin (50 μg/mL), chloramphenicol (20 μg/mL), kanamycin (25 μg/mL), arabinose (100 μM), and/or glucose (30mM). The following morning cells were spun down, washed with fresh Luria broth (with no supplements), and then subcultured into fresh Luria broth (thymine and antibiotic concentrations listed above) with either arabinose (150 μM) or glucose (30 mM) until they reached a cell density of approximately 1 x $10^8$/mL (50 Klett units above background, No. 42 green filter). Cell densities were recorded every 30 minutes and cultures were diluted with pre-warmed growth medium as needed to maintain the cultures in exponential phase (50–90 Klett units above

background). The resultant Klett values were adjusted to reflect the appropriate dilution factors. Cells were harvested at 50–70 Klett units above background, when appropriate, for further biological assays.

**Plate growth assays**

To determine how both temperature and expression of Orn from the constructed covering plasmids affected growth, various *orn* mutant strains were grown on Luria agar plates supplemented with either arabinose (1 mM) to induce protein expression, glucose (30mM) to repress protein expression, or neither as a control and incubated at 16ºC, 30ºC, 37ºC, or 44ºC for up to 7 days. All plate growth assays were replicated in triplicate and images of the growth on the plates were taken for record.

**Isolation of total protein and western blotting analysis**

Strains were grown at 37°C with shaking at 255 rpm to Klett 80 above background in Luria broth supplemented with thymine (50 µg/mL) antibiotic and inducer/repressor, where appropriate. Isolation of total protein was performed as described by Ow et al. (19,20). Protein concentrations were determined by the Bio-Rad protein assay with bovine serum albumin as the standard. Protein samples (10–150 µg for Orn) were electrophoresed in a 12% SDS-polyacrylamide gel and transferred to PVDF membranes (Immobilon TM-P; Millipore) using a Bio-Rad Mini-Protean 3 electrophoretic apparatus. The membranes were probed with Orn antibody (1:10,000 dilution) using the ECL

Plus™ Western Blotting Detection Kit (GE Healthcare) per manufacturer instructions. The Orn MAP antibody was raised against Orn-specific peptides by GenScript USA Inc, NJ.

**Primer extension analysis**

Total RNA was isolated from various exponentially growing strains as previously described (21) under the growth conditions described above. RNA was further treated to a phenol/chloroform extraction followed by sodium acetate precipitation in order to remove any contaminants that could affect downstream application such as RT-PCR cloning, primer extensions, or sequencing experiments. RNA was quantified on a NanoDrop™ 2000c (Thermo Scientific) apparatus. Five hundred nanogram of each RNA sample were run on a 1% Agarose-Tris-acetate-EDTA gel and visualized with ethidium bromide to ensure satisfactory quality for further analysis.

Primer extension analysis of the various mRNA transcripts was carried out as previously described (22). The sequences were analyzed on a 6% PAGE containing 8 M urea.

**RESULTS**

**Verification of Δ*orn* strain**

The original mutagenesis conducted to interrupt chromosomal *orn* involved CF881 (*recB xthA rna rph-1*), and required the presence of an *orn* covering plasmid (14). Our belief was that because *Δorn* was obtained in a non wild-type

genetic background, that the absence of either *recB* or *xthA* could have had some effect on the phenotype observed with the *Δorn* mutant. Therefore, we set out to obtain a *Δorn* in a clean genetic background and characterize the resultant strain.

Initial attempts utilizing the Hamilton method (23) were largely unsuccessful due to inefficiencies in recombination events between the chromosome and the plasmid containing the flanking regions to *orn*. We subsequently decided to use the Lambda-Red recombineering method to obtain a chromosomal deletion of *orn* (17). A linear DNA fragment containing an apramycin resistant cassette ($Apr^R$) flanked by 500 bp of upstream homology and 197 base pairs of downstream homology to chromosomal *orn* was transformed (Fig. 1A) into strain SK10706 (*rph-1*/pKD46, pNWK2) and selected for apramycin resistance after allowing to outgrow in non-selective media overnight. The resultant transformants were then screened for the loss of ampicillin resistance conferred by pKD46. The isolates were further screened by PCR analysis for presence of *Δorn::apr* in the chromosome (data not shown). Chromosomal DNA from three transformants that showed *Δorn::apr* through PCR screening was subjected to Southern blot analysis using probes specific for *orn* as well as the $Apr^R$ cassette (Fig. 1A). When probing for *orn,* none of the three transformants yielded a band on the Southern blot as compared to wild type and control plasmid, pNWK3, which contained the template fragment used for linear transformation (Fig. 1B, Lanes 1–5). When probing for the $Apr^R$ cassette, no band was present in the control as expected, and a band was

present in the pNWK3 control lane as well as in each transformant lane (Fig. 1B, Lanes 6–10). These data conclusively showed that all three transformants contained *Δorn::apr* in a clean genetic background and was kept for characterization.

Initially, the covering plasmid for the *Δorn::apr* strain had *orn* expressed under control of the *lac* promoter in a 30–50 copy number plasmid (pNWK2). Subsequent assays confirmed that this plasmid allowed for a basal level of *orn* expression in uninduced conditions (data not shown). Accordingly, an arabinose expression system was chosen because of its ability to more tightly control expression of genes of interest through the use of arabinose as an inducer and glucose as a repressor as well as its low level of basal expression (24). Plasmids pNWK5 and pNWK6 were constructed as described in Methods and Materials and were used for further characterization of the *Δorn::apr* mutant strain.

**Plate growth observations**

Following construction of both SK10723 (*Δorn rph-1*/pNWK6) and SK10730 (*Δorn rph-1*/pNWK5) these strains were grown on Luria agar plates at varying temperatures with either arabinose added to the media to induce protein expression, glucose added to the media to repress protein expression, or no addition to the media to observe basal protein expression from the *orn* covering plasmids. The goal was to analyze how expression of *orn* from the covering

plasmids would affect the growth properties in the *Δorn* strain and to see if the covering plasmids would completely complement *Δorn*.

Numerous strains were grown at 16ºC for 7 days. The *rph-1* wild-type strain grew as expected as compared to a known cold-sensitive *pnpΔ683 rph-1* strain, where no growth was observed after 7 days on all plates (Fig. 2A, Sections 1 & 5). When comparing the *Δorn::apr* strains containing either pNWK5 or pNWK6 in induced and repressed expression conditions, there was a noticeable difference. In both strains when either plasmid was induced there is a slight amount of growth as compared to the *rph-1* control (Fig. 2A, Sections 1, 3 & 4). However, in both strains when either plasmid was repressed there was no growth as compared to the *rph-1* control (Fig. 2A, Sections 1, 3 & 4). These data suggested that the *Δorn* mutant resulted in a cold-sensitive phenotype similar to the *pnpΔ683 rph-1* strain.

When growing the various strains at 30ºC, a different growth phenotype was observed. The *rph-1* strain displayed normal growth after 24 hours (Fig. 2B, Section 1). When analyzing the growth of SK10730 (*Δorn rph-1*/pNWK5), which contains the 6–8 copy covering plasmid, growth under induced and uninduced conditions, were similar (Fig. 2B, Section 4) yet still not comparable to wild-type growth (Fig. 2B, Section 1). Growth under repressed conditions yielded little growth with production of microcolonies (Fig. 2B, Section 4). Strain SK10723 (*Δorn rph-1*/pNWK6) contains the single-copy covering plasmid. When comparing growth at 30ºC after 24 hours under induced conditions, pNWK6 did not fully complement the *Δorn* deletion (Fig. 2B, Sections 1 & 3), but did allow

for tight control of Orn expression as evidenced in Figure 2B, Section 3, where there is no growth as compared to wild type (Fig. 2B, Section 1). These data suggest that neither covering plasmid offers full complementation to wild-type growth in induced conditions, but pNWK6 does offer better-controlled protein expression at this temperature than its 6–8 copy counterpart.

Lastly, growth at 37ºC for 24 hours was performed. When comparing SK10730 (*Δorn rph-1*/pNWK5), which contains the 6–8 copy covering plasmid, growth in all conditions was nearly identical to the *rph-1* control (Fig. 2C, Sections 1 & 4). These data suggest that when Orn production was induced, there was near 100% complementation compared to the *rph-1* control on plates. However, of interest was that when the production of Orn was actively repressed, there was still a nearly 100% complementation of growth, suggesting that either the plasmid was producing Orn when being repressed at low levels, and that only a small amount of Orn was necessary for complete complementation. This is unlikely however, since growth at 30ºC did not produce the same results at 37ºC in this particular strain. Another explanation could be that Orn expression is actively repressed, but another enzyme present in *E. coli* is acting, even inefficiently, in place of *orn,* allowing for growth to occur. When comparing growth of SK10723 (*Δorn rph-1* /pNWK6), which has the single-copy covering plasmid compared to the *rph*-1 control, there were more striking differences. When grown under induced conditions the single-copy covering plasmid still did not fully complement the *Δorn* mutation (Fig. 2C, Section 3). Growth in uninduced and repressed conditions is similar to one

another, and do differ substantially from that of wild-type growth (Fig. 2C, Sections 1 & 3). When Orn production was repressed there is little growth throughout the section and only microcolonies appear after 24 hours of incubation. With these observations, we concluded that the arabinose controlled expression plasmid was allowing for adequate regulation of *orn,* especially in the single-copy version, although why there was still not 100% complementation in induced conditions remained a question. In addition there exists a noticeable dependence on growth temperature as well as copy number of the covering plasmid for complementation of *Δorn.*

**Growth curve analysis in an *orn* single mutant**

Because SK10723 (*Δorn rph-1*/pNWK6) provided better control of *orn* regulation, subsequent assays were carried out in this strain. We followed the plate growth assays with growth curve analysis in liquid medium to see if the growth phenotypes at different temperatures and expression conditions would be similar. SK10723 (*Δorn rph-1*/pNWK6) was grown either in induced or repressed conditions overnight and then subcultured into either induced or repressed conditions where the growth curve was conducted as described in material and methods. For the growth curve conducted at 30ºC (Fig. 3), when comparing cells that were kept in inducing conditions overnight and throughout the growth curve to cells grown in induced conditions overnight and then switched to repressed conditions, there is no discernable difference in growth properties, providing evidence that Orn may be extremely stable in the cell and

can survive numerous round of cellular division. When cells were grown overnight in repressed conditions and then switched to induced conditions, there is a noticeable lag phase in growth, but starts to grow faster after 4 hours. When cells were in repressed conditions throughout, there was a noticeable growth deficiency as compared to cells in induced conditions throughout, with repressed cells struggling to reach above 100 Klett after 5 hours of growth.

When analyzing growth properties in liquid medium at 37ºC (Fig. 4), overall growth characteristics are similar to cells grown at 30ºC with two exceptions. First, all cells performed slightly better at 37ºC, reaching a final Klett measurement approximately 10-fold higher at 37ºC than at 30ºC. Second, when cells were grown overnight in repressed conditions and then switched to induced conditions, there was almost no apparent lag phase of growth as compared to the same growth conditions at 30ºC. These cells reached a final Klett measurement similar to cells grown in induced conditions throughout.

**Analysis of Orn levels in various mutant strains**

Both plate growth and growth curve analysis in our *Δorn* mutant were providing confounding results to those originally reported by Ghosh et al. (14). In their strain, growth at the non-permissive temperature was decreasing, yet in our system in repressed conditions growth continued at a steady pace albeit much slower than compared to both inducing conditions and wild type. However on plates there was still not 100% complementation in inducing conditions. These results made us hypothesize that with respect to Orn levels, that, either the

plasmids are still providing some basal expression of Orn even when being actively repressed, or that Orn may be extremely stable and that multiple cell divisions would be required to dilute out Orn levels to a point where a growth phenotype would be observable. We therefore conducted western analysis to determine what the levels of Orn look like in differing expression conditions.

After the growth curves at 30ºC and 37ºC, western analysis was performed on cell lysates. In every instance where the covering plasmid was being repressed, regardless of temperature, no detectable Orn levels were observed (Fig. 5A, Lanes 2, 4, 6 & 8). Conversely in every instance where the covering plasmid was induced Orn was detected (Fig. 5A, Lanes 1, 3, 5 & 7). These data were rather surprising given the observation from the growth curves in which cells were switched from induced to repressed expression conditions grew similarly to those in induced expression conditions the entire time. If Orn were extremely stable than perhaps cells that were originally grown under induced expression conditions and then switched to repressed conditions, some amount of Orn could be detected on the western blot, but this was not observed.

Because the previous western blot was loaded with crude extracts, we wanted to obtain a clearer picture of how much Orn was being produced from the covering plasmids as well as in wild-type strains. We therefore conducted western analysis on samples that had been quantified to compare samples better. An interesting observation in the western analysis was that in wild type a substantial amount of total protein was needed in order to detect Orn (150 µg),

and that expression of Orn did not change as a result of growth temperature (Fig. 5C, Lanes 1–3). We also compared the expression of Orn from pNWK5 & 6 in induced, repressed, and uninduced conditions. When comparing equal amounts of protein loaded, in induced conditions pNWK5 produced substantially more Orn than pNWK6 (Fig. 5B, Lanes 1 & 4). These results were expected given the difference in copy number of the individual plasmids (Table 2). When analyzing the Orn levels produced from both plasmids under repressed or uninduced expression conditions in the *Δorn* strain, results were also as expected. When the plasmids were actively repressed neither produced any detectable Orn (Fig. 5B, Lanes 2 & 5), and when grown in uninduced conditions no Orn could be detected as well (Fig. 5B, Lanes 3 & 6). Lastly, when comparing equal protein loading amounts (150 μg) in wild type to *Δorn*/pNWK6 in repressed conditions, Orn could be detected in wild type, but not in the mutant strain. These data show that Orn is not produced in substantial amounts in wild type, that both covering plasmids provide excellent control of expression, and that the results observed in the growth curves in which *Δorn* is still able to grow in repressed conditions is not a result of Orn being produced from the covering plasmid and must be a result of some other cellular function.

**The *orn* 5′-untranslated region allows for full complementation of *Δorn***

Since expression of Orn from either pNWK5 or pNWK6 did not provide 100% complementation either on plates or liquid medium, we hypothesized that regulation of *orn* expression from the covering plasmids could be different than

*orn* regulation from the chromosome. Therefore pNWK11 was constructed as described in Materials and Methods. This plasmid contains 100 base pairs of sequence upstream of the ATG start codon of *orn* and included any potential regulatory regions unlike that of pNWK5 and pNWK6, where expression of *orn* was under control of the p*BAD* promoter. If growth were restored to wild-type levels in a *Δorn* mutant in the presence of pNWK11, then that would suggest that regulation of *orn* expression does play a role in full complementation of *Δorn*. This was in fact the case as observed in plate growth analysis where growth equaled that of wild type (Fig. 2A, B & C; Sections 1 & 2). Growth curve analysis showed equal growth rates to that of the *rph-1* control (data not shown). Given the discrepancy observed of *Δorn* complementation from pNWK11 to pNWK5 & pNWK6 determination of the transcription start site was conducted. Initial investigation through EcoCyc reported that the transcription start site (TSS) was approximately 20 base pairs upstream of the ATG start codon of *orn* (Fig. 6A) (25). However, these results were never experimentally verified, so primer extension analysis was conducted. When comparing wild type to SK10740 (*Δorn rph-1* /pNWK11), it was evident that the TSS was indeed much longer than currently annotated through EcoCyc (Fig. 6C) (25). Our experimentally verified TSS was 43 base pairs upstream of the ATG start codon of *orn*, and has a potential -10 and -35 promoter region of 83% and 50% homology to the consensus sequence, respectively (Fig. 6B). These data showed that the 5′-untranslated region (UTR) is indeed longer than previously annotated, and that the UTR may provide essential regulation of *orn* that allows

for full complementation in a *Δorn* mutant. Investigation for identification of potential transcriptional regulators is currently being investigated to elucidate the role of the *orn* 5′-UTR.

**Growth curve analysis in a *Δorn Δrnt* double mutant**

To this point all the data suggested that there existed another enzyme that was providing a possible back up mechanism in a *Δorn* strain. Our next step, therefore, was to construct multiple mutant strains of all the known exoribonucleases in *E. coli* in conjunction with *Δorn* (26). Following the mutagenesis, the growth properties of the double deletion mutants would be characterized to see if there were any differences to a *Δorn* strain. Many of the double deletion strains grew similarly to the *Δorn* single mutant, suggesting that the deleted exoribonucleases did not provide a backup mechanism for the *Δorn* mutant (Table 3). There were two double deletion combinations that when grown in differing protein expression conditions, did have a growth phenotype different from that of the *Δorn* single mutant (Table 3). Specifically when PNPase or RNase T were deleted in the *Δorn* single mutant, regardless of growth temperature, when these strains were grown in either uninduced or repressed Orn expression conditions, they were inviable. Growth only occurred under inducing Orn expression conditions, indicating that at least one of the previously mentioned enzymes must be present in a *Δorn* mutant strain to remain viable.

Because of its similarity to *orn,* growth curve analysis of the *Δorn Δrnt* double mutant was conducted (13). The growth curve further corroborated the results observed on plates (Fig. 7). When grown under Orn inducing conditions the entire time, the *Δorn Δrnt* double mutant grew similar to the *Δorn* single mutant when grown under Orn repressing conditions. When the *Δorn Δrnt* double mutant was grown under Orn repressing conditions the entire time, there was no measurable increase in Klett, even after 5 hours. These data are the first to implicate RNase T as a backup enzyme for Orn. Further investigations into RNase T backup are currently being conducted.

**DISCUSSION**

Our study set out to obtain a clearer understanding of the physiological role that Orn plays in global regulation of transcription through its activity in the mRNA decay pathway. While original published work indicated that *orn* is essential for cell viability (14), we conclude through our work that it is not the sole exclusion of *orn* that causes a cessation of growth, but rather a combination of exoribonuclease deletions that cause cell inviability.

Work done by Ghosh et al. (14) showed that in their genetic background, in order to obtain *Δorn*, a covering plasmid maintaining production of Orn was needed. Our data confirmed their original finding. However, because our system did not require the use of a shift to a non-permissive temperature, we did not have to worry about potential effects from an elevated growth

temperature and were able to focus on characterization of *Δorn* under normal physiological temperatures.

Through growth curve and plate growth analysis in different growth conditions we were able to fully characterize the growth properties of *Δorn* (Figs. 2–4). Several interesting conclusions can be gleaned from these analyses. First, *Δorn* displays a temperature-dependent growth phenotype. When comparing growth of *Δorn* on plates in any growth condition, growth is better as temperature is increased (37ºC>30ºC>16ºC), and is always less than wild-type growth (Fig. 2). Growth curve analysis conducted at 30ºC and 37ºC supported the observations in the plate growth analysis (Figs. 3 & 4). These data suggest that the accumulation of nanoRNAs have a greater deleterious effect at lower temperatures, most likely due to increased stability of the oligoribonucleotides.

Through testing a single-copy and 6–8 copy inducible Orn expression plasmid, we also discovered that the growth phenotype was copy-number dependent. When production of Orn was induced, in every temperature and with increasing copy-number of the plasmid, we observed better growth when comparing the *Δorn* strains to each other. These data suggest that increased production of Orn, even in excess, is not deleterious to cellular growth.

Numerous explanations for the growth properties in our *Δorn* strain exist. For instance Goldman et al. (7,8) have shown that accumulation of nanoRNAs can prime transcription initiation at different locations and also incorporate nanoRNAs into new transcripts. If nanoRNA-mediated priming could produce transcripts that are 1–3 nucleotides longer than in wild type, this could effect

gene expression, such as inefficient translation of PyrC in *E. coli* (27). In a *Δorn* strain, accumulation of nanoRNAs would contain a 5′-monophosphate or a 5′-hydroxyl end. If a nanoRNA containing a 5′-monophosphate, instead of the traditional 5′-triphosphate, were to be incorporated into new transcripts, these could potentially become targets for RNase E mediated decay (28) that would have otherwise escaped degradation.

We also showed through detailed western blotting analysis that Orn is present in minute amounts within the cell, providing evidence that Orn is highly specific and can quickly process its nanoRNAs targets (Fig. 5C). Most interesting, however, was the observation that in growth conditions where production of Orn from the covering plasmid is repressed, no noticeable Orn can be detected, even when loading the western in excess of total protein. Two reasons can explain this observation. One, the covering plasmid is still producing Orn even when actively repressed but is under the limit of detection for the assay. In order to see if this could be the case, a more sensitive assay could be employed such as qPCR. Two, there exists a backup mechanism from another exoribonuclease present in the cell. Further experiments have provided excellent indications that this is the answer.

The data presented in Fig. 6 showed that the 5′-UTR of *orn* is 20 base pairs long, about 23 base pairs longer (43 base pairs total) than the currently annotated 5′-UTR in EcoCyc (25). Upon visual inspection of the region upstream to the 5′-UTR a rather clear putative promoter sequence can be identified. When this region, along with the *orn* coding sequenced was cloned

into a *Δorn* strain, 100% complementation of the deletion was observed, as shown in Fig. 2A, B & C Section 2. These data clearly demonstrate that the 5′-UTR plays a pivotal role in the regulation of *orn.* There exists the possibility of the presence of transcription factors that may bind and alter gene expression (29). Additionally, *orn* regulation may be controlled by another ribonuclease such as RNase II regulation by RNase E and PNPase mediated degradation (30), as well as PNPase regulation by RNase III (31). While the *orn* 5′-UTR is smaller than some other UTRs by comparison, the nucleotide makeup may allow for secondary structure formation that could help to block decay of the *orn* transcript.

Our data are also the first to implicate RNase T as a backup mechanism for Orn activity as it pertains to degradation of nanoRNAs exclusively within the mRNA decay pathway (Fig. 7). Previous to this study, RNase T was shown to be mainly involved with the processing of the 3′-end of tRNA precursors to their mature form (32). However, our data clearly show that in the absence of *orn* and *rnt* together, that strain is inviable. While data suggests that RNase T can act on oligoribonucleotides smaller than 6 residues, it does so inefficiently, this activity in a *Δorn* strain seems to be enough to maintain viability, and explains why even when no Orn is produced can the cell maintain homeostasis (33).

**ACKNOWLEDGEMENTS**

This work was supported in part by a grant from the National Institutes of Health (GM081544) to S.R.K.

## REFERENCES


1. Cannistraro, V.J. and Kennell, D. (1993) The 5' ends of RNA oligonucleotides in *Escherichia coli* and mRNA degradation. *Eur. J. Biochem.*, **213**, 285-293.
2. Carpousis, A.J., Luisi, B.F. and McDowall, K.J. (2009) Endonucleolytic initiation of mRNA decay in *Escherichia coli*. *Prog. Mol. Biol. Transl. Sci.*, **85**, 91-135.
3. Kushner, S.R. (2002) mRNA decay in *Escherichia coli* comes of age. *J. Bacteriol.*, **184**, 4658-4665; discussion 4657.
4. Mudd, E.A., Krisch, H.M. and Higgins, C.F. (1990) RNase E, an endoribonuclease, has a general role in the chemical decay of *Escherichia coli* mRNA: evidence that *rne* and *ams* are the same genetic locus. *Mol. Microbiol.*, **4**, 2127-2135.
5. Lee, K., Bernstein, J.A. and Cohen, S.N. (2002) RNase G complementation of *rne* null mutation identified functional interrelationships with RNase E in *Escherichia coli*. *Mol. Microbiol.*, **43**, 1445-1456.
6. Nickels, B.E. (2012) A new way to start: nanoRNA-mediated priming of transcription initiation. *Transcription*, **3**, 300-304.
7. Goldman, S.R., Sharp, J.S., Vvedenskaya, I.O., Livny, J., Dove, S.L. and Nickels, B.E. (2011) NanoRNAs prime transcription initiation *in vivo*. *Mol. Cell*, **42**, 817-825.

8. Nickels, B.E. and Dove, S.L. (2011) NanoRNAs: a class of small RNAs that can prime transcription initiation in bacteria. *J. Mol. Biol.*, **412**, 772-781.

9. Zuo, Y. and Deutscher, M.P. (2001) Exoribonuclease superfamilies: structural analysis and phylogenetic distribution. *Nucleic Acids Res.*, **29**, 1017-1026.

10. Koonin, E.V. (1997) A conserved ancient domain joins the growing superfamily of 3'-5' exonucleases. *Curr. Biol.*, **7**, R604-606.

11. Fang, M., Zeisberg, W.M., Condon, C., Ogryzko, V., Danchin, A. and Mechold, U. (2009) Degradation of nanoRNA is performed by multiple redundant RNases in *Bacillus subtilis*. *Nucleic Acids Res.*, **37**, 5114-5125.

12. Nguyen, L.H., Erzberger, J.P., Root, J. and Wilson, D.M., 3rd. (2000) The human homolog of *Escherichia coli* Orn degrades small single-stranded RNA and DNA oligomers. *J. Biol. Chem.*, **275**, 25900-25906.

13. Zhang, X., Zhu, L. and Deutscher, M.P. (1998) Oligoribonuclease is encoded by a highly conserved gene in the 3'-5' exonuclease superfamily. *J. Bacteriol.*, **180**, 2779-2781.

14. Ghosh, S. and Deutscher, M.P. (1999) Oligoribonuclease is an essential component of the mRNA decay pathway. *Proc. Natl. Acad. Sci. USA*, **96**, 4372-4377.

15. Yu, D. and Deutscher, M.P. (1995) Oligoribonuclease is distinct from the other known exoribonucleases of *Escherichia coli*. *J. Bacteriol.*, **177**, 4137-4139.

16. Mohanty, B.K., Maples, V.F. and Kushner, S.R. (2012) Polyadenylation helps regulate functional tRNA levels in *Escherichia coli*. *Nucleic Acids Res.*, **40**, 4589-4603.

17. Datsenko, K.A. and Wanner, B.A. (2000) One-step inactivation of chromosomal genes in *Escherichia coli* K-12 using PCR products. *Proc. Natl. Acad. Sci. USA*, **97**, 6640-6645.

18. Kushner, S.R. (1978) In Boyer, H. W. and Nicosia, S. (eds.), *Genetic Engineering*. Elsevier/North-Holland Biomedical Press, Amsterdam, pp. 17-23.

19. Ow, M.C., Liu, Q., Mohanty, B.K., Andrew, M.E., Maples, V.F. and Kushner, S.R. (2002) RNase E levels in *Escherichia coli* are controlled by a complex regulatory system that involves transcription of the *rne* gene from three promoters. *Mol. Microbiol.*, **43**, 159-171.

20. Ow, M.C., Liu, Q. and Kushner, S.R. (2000) Analysis of mRNA decay and rRNA processing in *Escherichia coli* in the absence of RNase E-based degradosome assembly. *Mol. Microbiol.*, **38**, 854-866.

21. Stead, M.B., Agrawal, A., Bowden, K.E., Nasir, R., Mohanty, B.K., Meagher, R.B. and Kushner, S.R. (2012) RNA*snap*: a rapid, quantitative

and inexpensive, method for isolating total RNA from bacteria. *Nucleic Acids Res.*, **40**, e156.

22. Mohanty, B.K. and Kushner, S.R. (2007) Ribonuclease P processes polycistronic tRNA transcripts in *Escherichia coli* independent of ribonuclease E. *Nucleic Acids Res.*, **35**, 7614-7625.

23. Hamilton, C.M., Aldea, M., Washburn, B.K., Babitzke, P. and Kushner, S.R. (1989) A new method for generating deletions and gene replacements in *Escherichia coli*. *J. Bacteriol.*, **171**, 4617-4622.

24. Guzman, L.M., Belin, D., Carson, M.J. and Beckwith, J. (1995) Tight regulation, modulation, and high-level expression by vectors containing the arabinose PBAD promoter. *J. Bacteriol.*, **177**, 4121-4130.

25. Keseler, I.M., Bonavides-Martinez, C., Collado-Vides, J., Gama-Castro, S., Gunsalus, R.P., Johnson, D.A., Krummenacker, M., Nolan, L.M., Paley, S., Paulsen, I.T. *et al.* (2009) EcoCyc: a comprehensive view of *Escherichia coli* biology. *Nucleic Acids Res.*, **37**, D464-470.

26. Andrade, J.M., Pobre, V., Silva, I.J., Domingues, S. and Arraiano, C.M. (2009) The role of 3'-5' exoribonucleases in RNA degradation. *Prog. Mol. Biol. Transl. Sci.*, **85**, 187-229.

27. Wilson, H.R., Archer, C.D., Liu, J.K. and Turnbough, C.L., Jr. (1992) Translational control of *pyrC* expression mediated by nucleotide-sensitive selection of transcriptional start sites in *Escherichia coli*. *J. Bacteriol.*, **174**, 514-524.

28. Mackie, G.A. (1998) Ribonuclease E is a 5'-end-dependent endonuclease. *Nature*, **395**, 720-723.

29. Mendoza-Vargas, A., Olvera, L., Olvera, M., Grande, R., Vega-Alvarado, L., Taboada, B., Jimenez-Jacinto, V., Salgado, H., Juarez, K., Contreras-Moreira, B. *et al.* (2009) Genome-wide identification of transcription start sites, promoters and transcription factor binding sites in *E. coli*. *PLoS One*, **4**, e7526.

30. Zilhao, R., Cairrao, R., Régnier, P. and Arraiano, C.M. (1996) PNPase modulates RNase II expression in *Escherichia coli*: Implications for mRNA decay and cell metabolism. *Mol. Microbiol.*, **20**, 1033-1042.

31. Robert-Le Meur, M. and Portier, C. (1992) *Escherichia coli* polynucleotide phosphorylase expression is autoregulated through an RNase III-dependent mechanism. *EMBO J.*, **11**, 2633-2641.

32. Deutscher, M.P., Marlor, C.W. and Zaniewski, R. (1985) RNase T is responsible for the end-turnover of tRNA in *Escherichia coli*. *Proc. Natl. Acad. Sci. USA*, **82**, 6427-6430.

33. Huang, S. and Deutscher, M.P. (1992) Sequence and transcriptional analysis of the *Escherichia coli rnt* gene encoding RNase T. *J. Biol. Chem.*, **267**, 25609-25613.

34. Piedade, J., Zilhao, R. and Arraiano, C.M. (1995) Construction and characterization of an absolute deletion of *Escherichia coli* ribonuclease II. *FEMS Microbiol. Lett.*, **127**, 187-193.

35. Perwez, T. and Kushner, S.R. (2006) RNase Z in *Escherichia coli* plays a significant role in mRNA decay. *Mol. Microbiol.*, **60**, 723-737.

36. Mohanty, B.K. and Kushner, S.R. (2003) Genomic analysis in *Escherichia coli* demonstrates differential roles for polynucleotide phosphorylase and RNase II in mRNA abundance and decay. *Mol. Microbiol.*, **50**, 645-658.

37. Mohanty, B.K. and Kushner, S.R. (1999) Analysis of the function of *Escherichia coli* poly(A) polymerase I in RNA metabolism. *Mol. Microbiol.*, **34**, 1094-1108.

38. Mohanty, B.K. and Kushner, S.R. (1999) Residual polyadenylation in poly(A) polymerase I (*pcnB*) mutants of *Escherichia coli* does not result from the activity encoded by the *f310* gene. *Mol. Microbiol.*, **34**, 1109-1119.

Table 1. Bacterial strains used in this work

| Strains | Genotype | Reference/Source |
|---|---|---|
| **MG1693** | *rph-1 thyA715* | *E. coli* Genetic Stock Center |
| **CMA201** | *Δrnb-201::Tn10 rph-1 thyA715* | (34) |
| **JW1644** | *Δrnt-730::kan, F-, Δ(araD-araB)567, ΔlacZ4787(::rrnB-3), λ-, rph-1, Δ(rhaD-rhaB)568, hsdR514* | *E. coli* Genetic Stock Center |
| **JW1793** | *Δrnd-729::kan, F-, Δ(araD-araB)567, ΔlacZ4787(::rrnB-3), λ-, rph-1, Δ(rhaD-rhaB)568, hsdR514* | *E. coli* Genetic Stock Center |
| **JW3618** | *Δrph-749::kan, F-, Δ(araD-araB)567, ΔlacZ4787(::rrnB-3), λ-, Δ(rhaD-rhaB)568, hsdR514* | *E. coli* Genetic Stock Center |
| **JW5741** | *Δrnr-729::kan, F-, Δ(araD-araB)567, ΔlacZ4787(::rrnB-3), λ-, rph-1, Δ(rhaD-rhaB)568, hsdR514* | *E. coli* Genetic Stock Center |
| **SK1698** | *rph-1 thyA715* / pKD46 | This study |
| **SK2595** | *rnzΔ500::kan rph-1 thyA715* | (35) |
| **SK5962** | *Δorn::apr rntΔ730::kan rph⁺ thyA715*/pNWK6 | This study |
| **SK5964** | *Δorn::apr rphΔ749::kan thyA715*/pNWK6 | This study |
| **SK5978** | *Δorn::apr rndΔ729::kan rph-1 thyA715* /pNWK6 | This study |
| **SK5980** | *Δorn::apr rndΔ729::kan rph⁺ thyA715*/pNWK6 | This study |
| **SK5984** | *Δorn::apr Δrnb::Tn10 rph-1 thyA715* /pNWK6 | This study |
| **SK5986** | *Δorn::apr Δrnb::Tn10 rph⁺ thyA715*/pNWK6 | This study |
| **SK5988** | *Δorn::apr rnrΔ729::kan rph-1 thyA715* /pNWK6 | This study |
| **SK5990** | *Δorn::apr rnrΔ729::kan rph⁺ thyA715*/pNWK6 | This study |
| **SK5992** | *Δorn::apr pnpΔ683::str/spc rph-1 thyA715* /pNWK6 | This study |
| **SK5994** | *Δorn::apr pnpΔ683::str/spc rph⁺ thyA715*/pNWK6 | This study |
| **SK6002** | *Δorn::apr rnzΔ500::kan rph-1 thyA715* /pNWK6 | This study |

| | | |
|---|---|---|
| **SK6004** | *Δorn::apr rnzΔ500::kan rph⁺ thyA715*/pNWK6 | This study |
| **SK10019** | *pnpΔ683::str/spc rph-1 thyA715* | (36) |
| **SK10153** | *rph⁺ thyA715* | (16) |
| **SK10705** | *Δorn::apr rph-1 thyA715* /pNWK2 | This study |
| **SK10706** | *rph-1 thyA715* /pKD46 pNWK2 | This study |
| **SK10716** | *rph-1 thyA715* /pNWK6 | This study |
| **SK10719** | *rph-1 thyA715* /pNWK5 | This study |
| **SK10723** | *Δorn::apr rph-1 thyA715* /pNWK6 | This study |
| **SK10727** | *rph⁺ thyA715* /pNWK6 | This study |
| **SK10730** | *Δorn::apr rph-1 thyA715* /pNWK5 | This study |
| **SK10736** | *Δorn::apr rph-1 thyA715* /pNWK6 pNWK11 | This study |
| **SK10740** | *Δorn::apr rph-1 thyA715* /pNWK11 | This study |
| **SK10742** | *Δorn::apr rph⁺ thyA715*/pNWK6 | This study |

Table 2. Plasmids used in this work.

| Plasmids | Genotype | Reference/Source |
|---|---|---|
| **pKD46** | oriR101, repA101, P*ara*BAD-*gam-bet-exo*, $Amp^R$ | (17) |
| **pBMK32** | pBR322 origin, *lacI*$^q$, $Cm^R$ | (37) |
| **pSBK29** | pSC101 origin, $Cm^R$ | (38) |
| **pVMK94** | miniF origin, $Amp^R$ | Maples & Kushner Unpublished Results |
| **pNWK2** | pBMK32, *orn*$^+$, $Cm^R$ | This study |
| **pNWK3** | pWSK29, $Amp^R$ with *orn* flanking regions | This study |
| **pNWK5** | pSBK29, *orn*$^+$, $Cm^R$ | This study |
| **pNWK6** | pVMK94, *orn*$^+$, $Amp^R$ | This study |
| **pNWK11** | pSBK29, *orn*$^+$, $Cm^R$ w/*orn* promoter | This study |

Figure 1. Southern analysis of *orn* deletion.

Southern analysis was performed as described in Materials and Methods. A) Diagrams of the probes designed for Southern analysis. Red arrows indicate the relative location of the primers used to generate Southern probe. Grey bars indicate the upstream and downstream regions to the gene of interest. Blue rectangle indicates the gene of interest for use in the Southern probes. Diagrams are not drawn to scale. B) Southern blot for verification of *Δorn::apr*. The red boxes indicate areas of interest on the blot for either the location of *orn* or $Apr^R$ cassette. Strains are indicated above each lane.

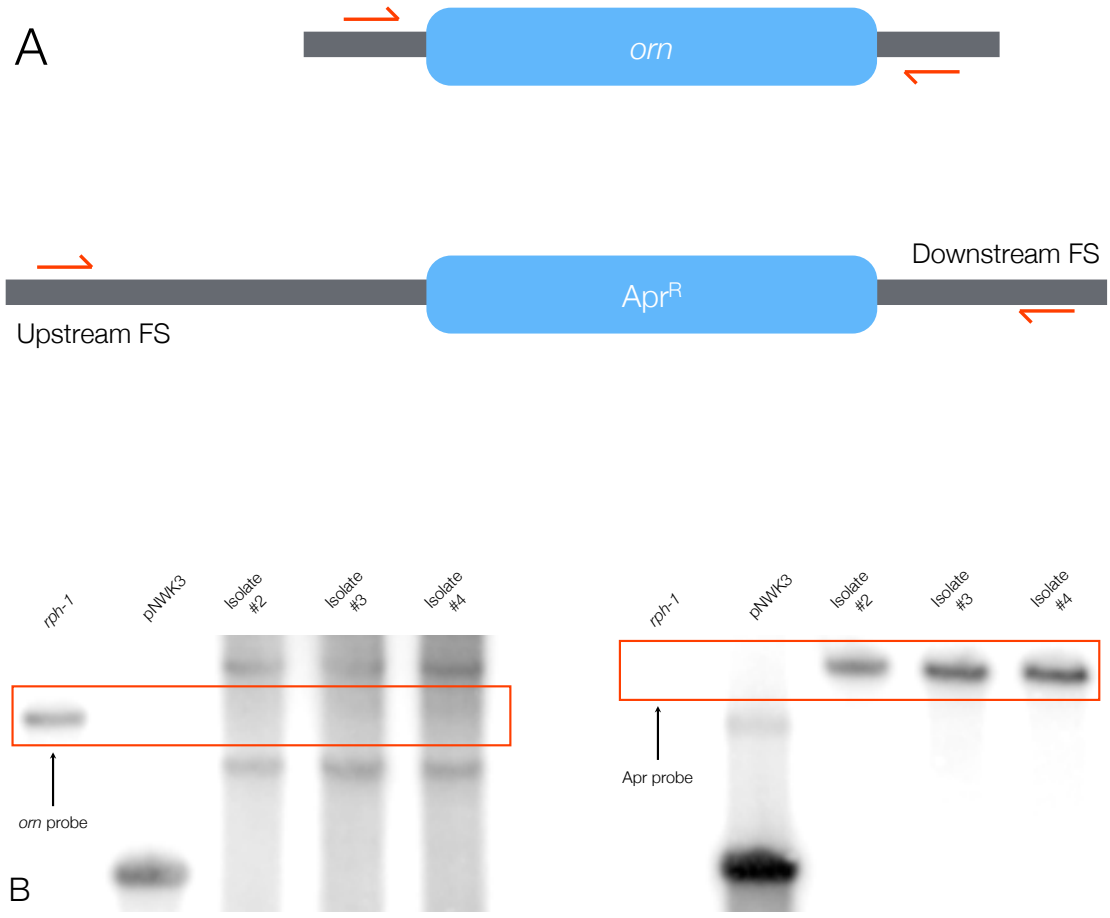
A
orn
Downstream FS
AprR
Upstream FS
rph-1
pNWK3
Isolate #2
Isolate #3
Isolate #4
orn probe
B
rph-1
pNWK3
Isolate #2
Isolate #3
Isolate #4
Apr probe

Figure 2. Plate growth assays of *Δorn* mutant strains.

Plates were treated and incubated as described in Materials and Methods. Table identifying strains grown is located below. Arrow pointing to each plate describes protein expression conditions. A) Plates incubated at 16ºC for one week. B) Plates grown at 30ºC for 24 hours. C) Plates grown at 37ºC for 24 hours.

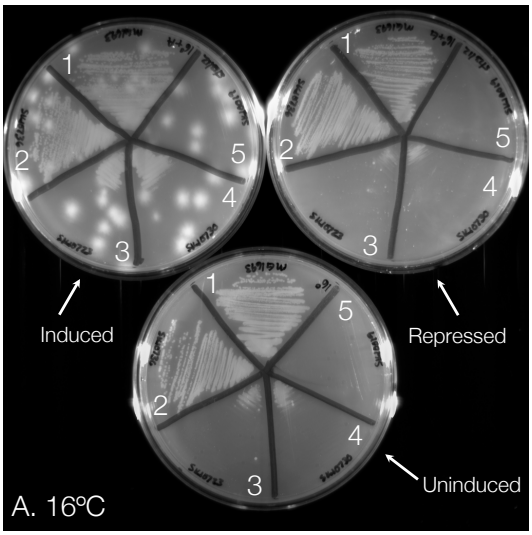


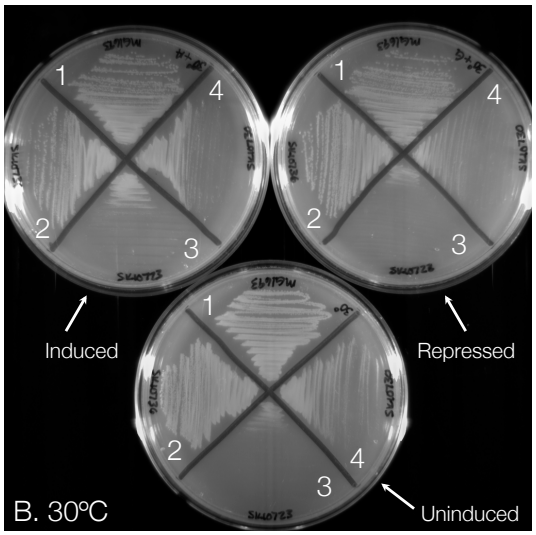


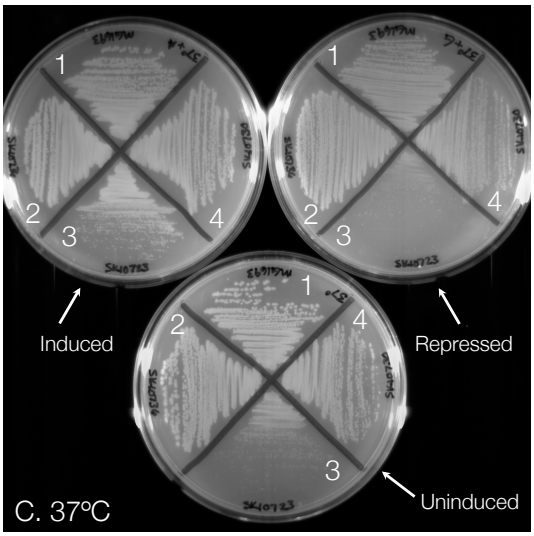


| | |
|---|---|
| 1 | *rph-1* |
| 2 | *Δorn rph-1, orn* promoter |
| 3 | *Δorn rph-1*, *orn*$^{+}$ single-copy |
| 4 | *Δorn rph-1*, *orn*$^{+}$ 6–8 copy |
| 5 | *Δpnp rph-1* |

Figure 3. Growth curve analysis of *Δorn* mutant strain at 30ºC.

Growth curves were conducted as described in Materials and Methods. Legend for each strain is located within the growth curve. IND = induced protein expression conditions. REP = repressed protein expression conditions.

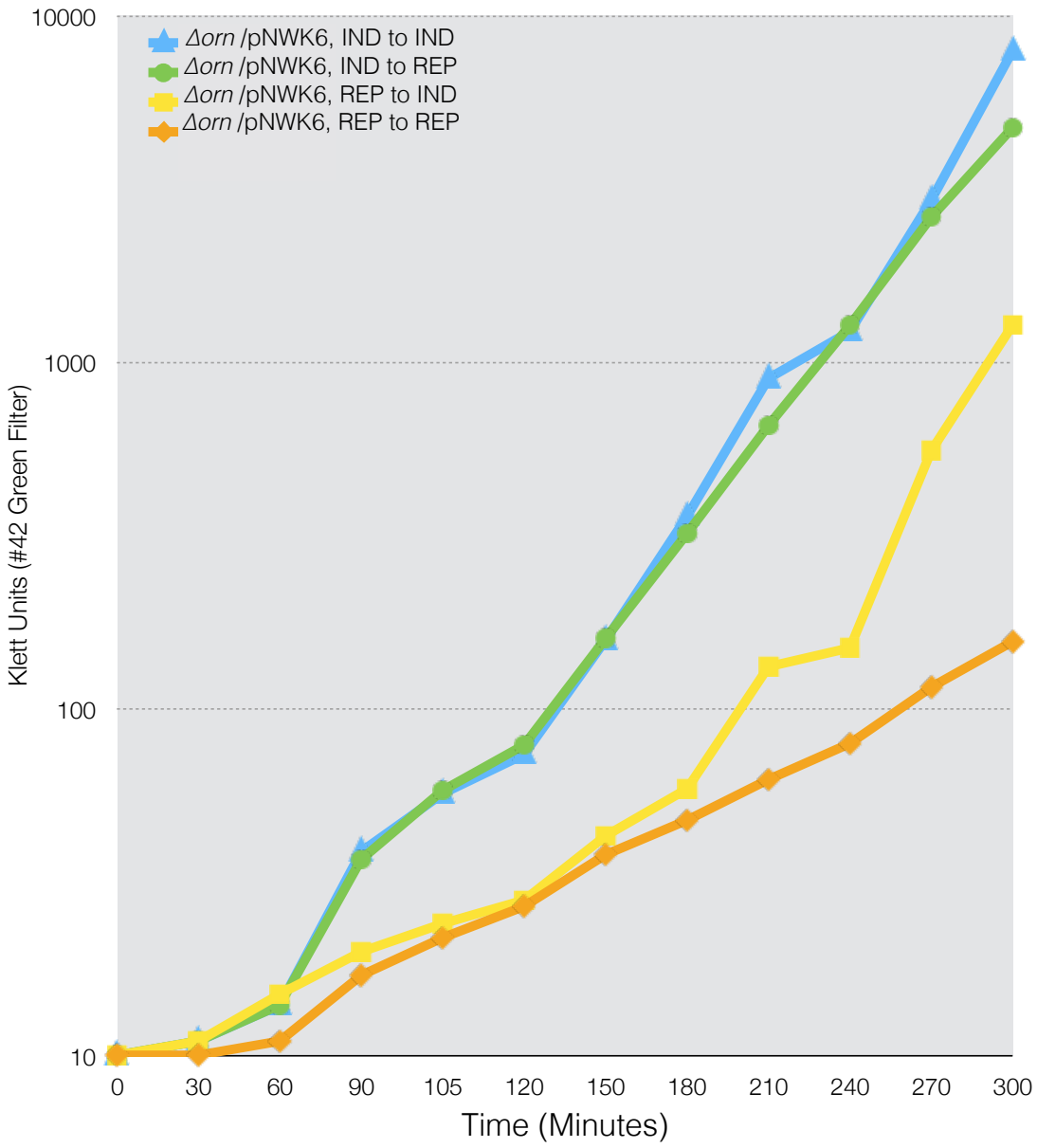
10000
1000
100
10
Klett Units (#42 Green Filter)
Δorn /pNWK6, IND to IND
Δorn /pNWK6, IND to REP
Δorn /pNWK6, REP to IND
Δorn /pNWK6, REP to REP
0
30
60
90
105
120
150
180
210
240
270
300
Time (Minutes)

Figure 4. Growth curve analysis of *Δorn* mutant strain at 37ºC.

Growth curves were conducted as described in Materials and Methods. Legend for each strain is located within the growth curve. IND = induced protein expression conditions. REP = repressed protein expression conditions.

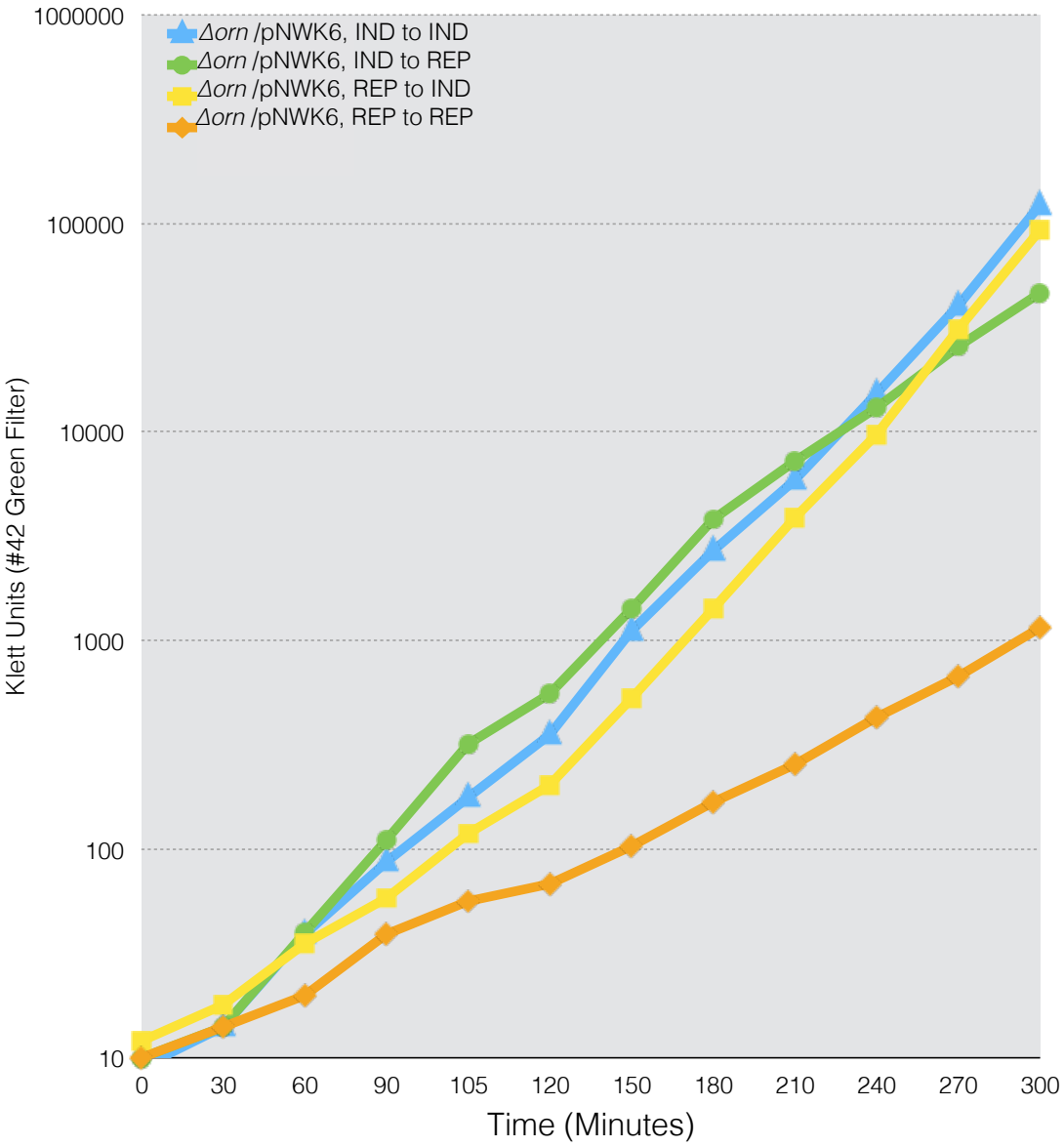
1000000
100000
10000
1000
100
10
Klett Units (#42 Green Filter)
Δorn /pNWK6, IND to IND
Δorn /pNWK6, IND to REP
Δorn /pNWK6, REP to IND
Δorn /pNWK6, REP to REP
0
30
60
90
105
120
150
180
210
240
270
300
Time (Minutes)

Figure 5. Western blotting analysis of *Δorn* mutant strains at 30ºC & 37ºC in various expression conditions.

Western blotting analysis was performed as described Materials and Methods. Protein size estimates are located to the right of each western blot. Orn migrates to ~21 kDa. IND = induced protein expression, REP = repressed protein expression, UND = uninduced protein expression. A) Western blot analysis of Orn levels taken from the growth curves conducted in Figures 3 & 4. Strain and growth conditions are located at the bottom of the blot. Changes in protein expression conditions are located above the sample lanes. B & C) Strain genotype listed above the sample lanes. Amount of total protein loaded in each lane located at the bottom of each sample lane.

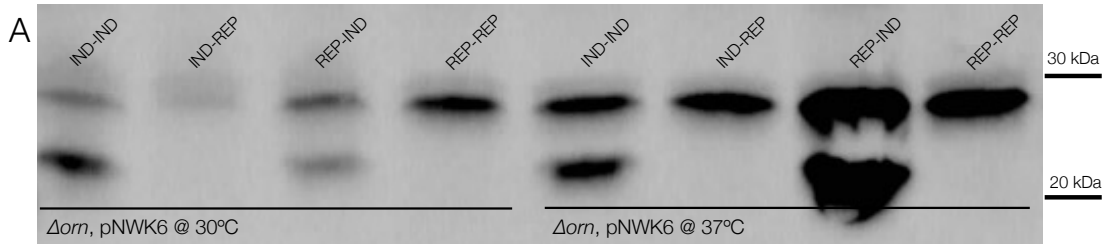
A
IND-IND
IND-REP
REP-IND
REP-REP
IND-IND
IND-REP
REP-IND
REP-REP
30 kDa
20 kDa
Δorn, pNWK6 @ 30ºC
Δorn, pNWK6 @ 37ºC

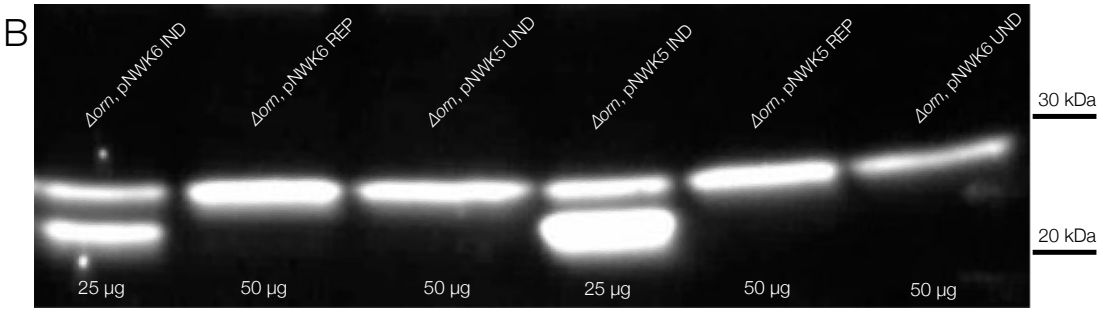
B
Δorn, pNWK6 IND
Δorn, pNWK6 REP
Δorn, pNWK5 UND
Δorn, pNWK5 IND
Δorn, pNWK5 REP
Δorn, pNWK6 UND
30 kDa
20 kDa
25 µg
50 µg
50 µg
25 µg
50 µg
50 µg

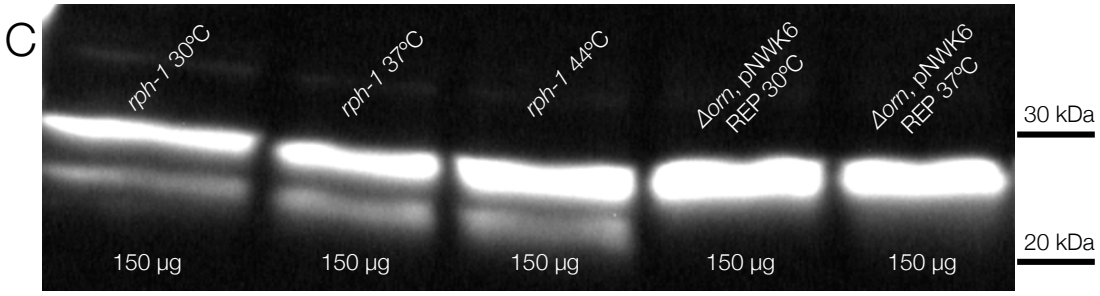
C
rph-1 30ºC
rph-1 37ºC
rph-1 44ºC
Δorn, pNWK6 REP 30ºC
Δorn, pNWK6 REP 37ºC
30 kDa
20 kDa
150 µg
150 µg
150 µg
150 µg
150 µg

Figure 6. Primer extension analysis of *Δorn* mutant.

Primer extension analysis was conducted as described in Materials and Methods. A) Black arrows indicate the transcription start sites of *orn* either through experimental analysis or through EcoCyc annotation. The expanded sequence is shown to the left of the figure. Strains and loading amounts are listed above each lane. B) Diagram of the 5'-UTR and putative promoter sequence as annotated in EcoCyc. White dashed arrow indicates the +1 site. Red indicates the -35 & -10 putative promoter regions, the transcription start site, and the *orn* start codon. C) Diagram of the 5'-UTR and putative promoter sequence as obtained through experimental analysis. White dashed arrow indicates the +1 site. Red indicates the -35 & -10 putative promoter regions, the transcription start site, and the *orn* start codon.

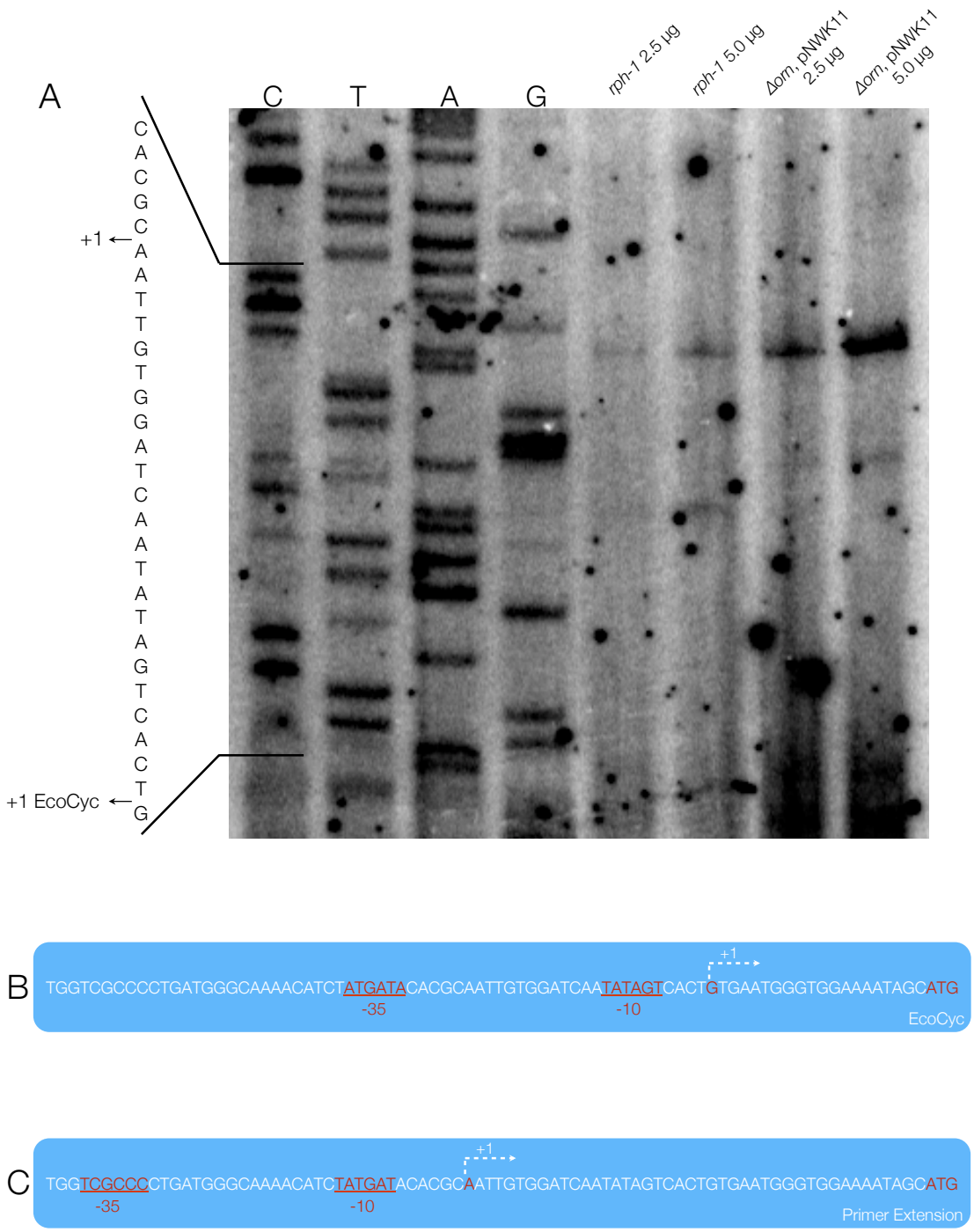
A
C
T
A
G
rph-1 2.5 µg
rph-1 5.0 µg
Δorn, pNWK11 2.5 µg
Δorn, pNWK11 5.0 µg
+1
+1 EcoCyc
CACGCAATTTGTGGATCAATTATAGTCACTG
B
TGGTCGCCCCTGATGGGCAAAACATCTATGATACACGCAATTGTGGATCAATATAGTCACTGTGAATGGGTGGAAAATAGCATG
-35
-10
+1
EcoCyc
C
TGGTCGCCCCTGATGGGCAAAACATCTATGATACACGCAATTGTGGATCAATATAGTCACTGTGAATGGGTGGAAAATAGCATG
-35
-10
+1
Primer Extension

Table 3. Growth properties of *Δorn* double mutant strains at 30ºC and 37ºC. Table legend is below.

| **Strain** | **30ºC UND/REP** | **30ºC IND** | **37ºC UND/REP** | **37ºC IND** |
|---|---|---|---|---|
| *Δorn rph-1*/pNWK6 | - | ± | ± | + |
| *Δorn rph*$^{+}$/pNWK6 | - | ± | ± | + |
| *Δorn rphΔ749*/pNWK6 | + | + | + | + |
| *Δorn rndΔ729 rph-1*/pNWK6 | ± | + | + | + |
| *Δorn rndΔ729 rph*$^{+}$/pNWK6 | ± | + | + | + |
| *Δorn Δrnb rph-1*/pNWK6 | + | + | + | + |
| *Δorn Δrnb rph*$^{+}$/pNWK6 | + | + | + | + |
| *Δorn rnrΔ729 rph*$^{+}$/pNWK6 | ± | + | ± | + |
| *Δorn rnzΔ500 rph-1*/pNWK6 | + | + | + | + |
| *Δorn rnzΔ500 rph*$^{+}$/pNWK6 | + | + | + | + |
| *Δorn rph-1*/pNWK6 | - | ± | ± | + |
| *Δorn rph*$^{+}$/pNWK6 | - | ± | ± | + |

| | | | | |
|---|---|---|---|---|
| *Δorn rntΔ730 rph*$^{+}$/pNWK6 | - - | ± | - - | + |
| *Δorn rnrΔ729 rph-1*/pNWK6 | - - | + | - - | + |
| *Δorn pnpΔ683 rph-1*/pNWK6 | - - | - - | - - | + |
| *Δorn pnpΔ683 rph*$^{+}$/pNWK6 | - - | + | - - | + |

| | |
|---|---|
| - - | No Growth |
| - | Microcolonies |
| ± | Little Growth |
| + | Near Wild Type Growth |
| ++ | Wild Type Growth |

Figure 7. Growth curve analysis of *Δorn* & *Δorn Δrnt* mutant strains at 37ºC. Growth curves were conducted as described in Materials and Methods. Legend for each strain is located within the growth curve. IND = induced protein expression conditions. REP = repressed protein expression conditions. Bars above and below each line indicate standard deviation.

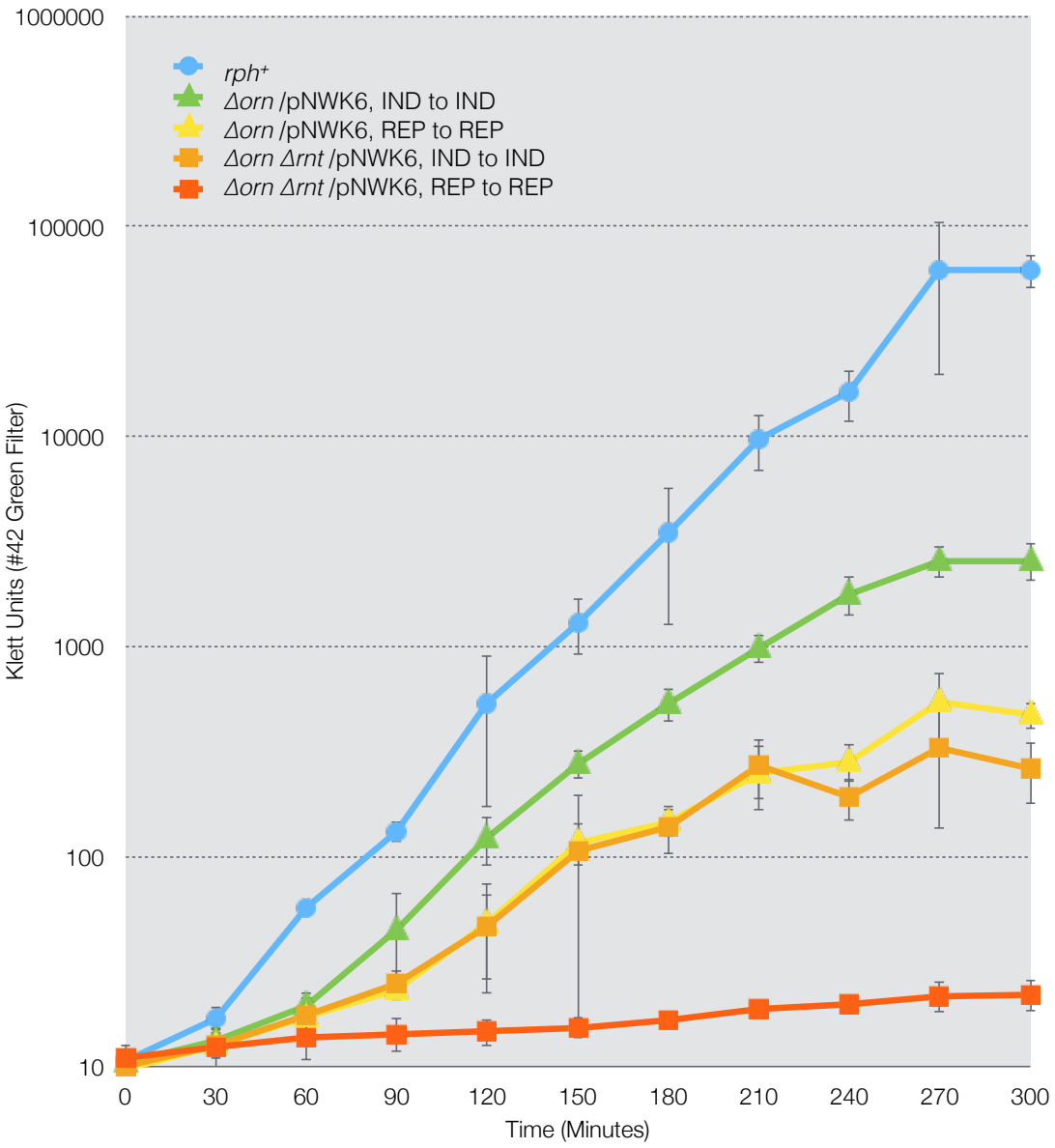
1000000
100000
10000
1000
100
10
Klett Units (#42 Green Filter)
rph+
Δorn /pNWK6, IND to IND
Δorn /pNWK6, REP to REP
Δorn Δrnt /pNWK6, IND to IND
Δorn Δrnt /pNWK6, REP to REP
0
30
60
90
120
150
180
210
240
270
300
Time (Minutes)

# CHAPTER 5

# CONCLUSIONS

Since the discovery of RNA pyrophosphohydrolase (RppH) and oligoribonuclease (Orn), it has become of interest to researchers in our field to further elucidate the roles of these enzymes in the cell (1,2). Evidence suggested that RppH could initiate RNase E mediated decay by removal of the 5′ pyrophosphate from primary transcripts (1), and little to no investigation into what role Orn played in *E. coli* beyond the degradation of 2–7 oligoribonucleotide species (nanoRNAs) had been conducted (3). My dissertation research has further explored the roles of RNA RppH and Orn in post-transcriptional regulation of gene expression in *Escherichia coli*.

Prior to our work, RppH was shown to act as an "activator" of mRNA degradation through the removal of the 5' pyrophosphate of RNA transcripts (1), but little was known about what role RppH could play in tRNA processing in *E. coli.* In Chapter 2, the role of RppH in tRNA maturation was examined. The work demonstrated that RppH is not required for RNase E mediated tRNA processing. This was surprising given the fact that RNase E was previously shown to be inhibited by the presence of a 5′-triphosphate. These data suggest that RNase E bypasses the 5′ terminus and cleaves internally to initiate

processing of tRNA precursors, similar to the was RNase E initiates mRNA decay (4).

Previous studies have shown that RNase P activity on tRNA precursors is determined by the phosphorylation status and length of the 5′-leader region (5); therefore, we desired to obtain a clearer understanding of this relationship as it pertains to RppH activity on the 5′ termini. We also show that RppH is required for the maturation of certain tRNA precursors, specifically primary tRNA transcripts with 5′ leaders less than 5 nucleotides in length. Removal of the 5′ triphosphate from *pheU, pheV*, and *ilex* tRNAs were required for RNase P to properly mature the 5′-end of the precursor tRNAs.

In Chapter 3, through the use of high-density tiling microarrays, we were able to further elucidate the role of RppH in regulating cellular motility in *E. coli*. In a *Δrpph rph-1* strain, we were able to show all genes involved in the flagellar biosysnthesis pathway to be significantly higher in abundance compared to wild type. These data were confirmed through motility assays confirming the hypothesis that increased motility is due to a stabilization of mRNAs involved in the flagellar biosynthesis pathway. We also show the ability of *Δrpph* to restore motility of *ΔapaH*, a known non-motile strain.

One interesting side effect of our work was identifying the presence of the Rph-1 truncated protein and its effects on numerous phenotypes. The canonical wild-type strain, MG1655, contains the *rph-1* deletion, which is naturally occurring (6). In Chapters 2 and 3 we show that its presence not only affects tRNA processing, but also motility. For instance, inefficient processing

of the *pheU* and *pheV* tRNAs in a *Δrpph rph-1* strain is abolished in both the *Δrpph rph*$^{+}$ and the *Δrpph Δrph* strain, suggesting an interplay between 5′ and 3′ processing of tRNA precursors. We ruled out that RppH and RNase PH interact, and show that overproduction of the Rph-1 truncation does not exacerbate the phenotype associated with *pheU* and *pheV* tRNA processing. We also showed that in a *Δrpph rph*$^{+}$ strain, that hypermotility was abolished. While the biochemical mechanisms for these observations are not clear yet, investigation into why this is occurring is important.

In Chapter 4, work also expanded the knowledge concerning degradation of nanoRNAs by Orn. Previous to our investigation, limited research had been conducted into *E. coli* nanRNA degradation. We analyzed the growth characteristics of a *Δorn*, and found that in cells depleted of Orn, the growth phenotype was temperature dependent. This could be explained by increased stability of nanoRNA molecules binding to substrates, which could cause transcriptional slippage, decreased stability of new transcripts, or decreased efficiency of translation (7). Further experiments to prove what exactly is causing the growth phenotypes will have to be conducted. Microarray analysis in a *Δorn* strain identifying down-regulated transcripts could identify potential targets of nanoRNA-mediated decay.

Most importantly in our work, we show that other exoribonucleases, specifically RNase T and PNPase, are able to serve as a backup mechanism for Orn activity and that loss of either of these enzymes along with Orn causes inviability in *E. coli*. These data are the first to implicate either RNase T or

PNPase in nanoRNA degradation. Given the knowledge that RNase T and Orn are closely related in sequence and structure (8), it would be interesting to investigate whether RNase T overexpression could complement a *Δorn*.

While certainly not complete, my dissertation covered three distinct areas, tRNA processing, transcriptome analysis, and oligoribonulease characterization, each aspect has helped to further the knowledge of post-transcriptional regulation in *Escherichia coli*. The data contained in this dissertation have demonstrated in increased role of RppH in tRNA processing as well as regulation of the flagellar biosynthesis network. While we don't understand all of the data yet, we show that the canonical wild type strain, MG1655, contains a naturally occurring point mutation in RNase PH, which has implications for numerous cellular processes. Lastly, while the work is still in a nascent phase, that RNase T and PNPase have potential roles in nanoRNA degradation. These findings will aid in the future work of the field, and demonstrate the import of post-transcriptional regulation in *Escherichia coli.*

**REFERENCES**

1. Deana, A., Celesnik, H. and Belasco, J.G. (2008) The bacterial enzyme RppH triggers messenger RNA degradation by 5' pyrophosphate removal. *Nature*, **451**, 355-358.
2. Ghosh, S. and Deutscher, M.P. (1999) Oligoribonuclease is an essential component of the mRNA decay pathway. *Proc. Natl. Acad. Sci. USA*, **96**, 4372-4377.

3. Datta, A.K. and Niyogi, K. (1975) A novel oligoribonuclease of *Escherichia coli*. II. Mechanism of action. *J. Biol. Chem.*, **250**, 7313-7319.

4. Baker, K.E. and Mackie, G.A. (2003) Ectopic RNase E sites promote bypass of 5'-end-dependent mRNA decay in *Escherichia coli*. *Mol. Microbiol.*, **47**, 75-88.

5. Koutmou, K.S., Zahler, N.H., Kurz, J.C., Campbell, F.E., Harris, M.E. and Fierke, C.A. (2010) Protein-precursor tRNA contact leads to sequence-specific recognition of 5' leaders by bacterial ribonuclease P. *J. Mol. Biol.*, **396**, 195-208.

6. Jensen, K.G. (1993) The *Escherichia coli* K-12 "wild types" W3110 and MG1655 have an *rph* frameshift mutation that leads to pyrimidine starvation due to low *pyrE* expression levels. *J. Bacteriol.*, **175**, 3401-3407.

7. Nickels, B.E. and Dove, S.L. (2011) NanoRNAs: a class of small RNAs that can prime transcription initiation in bacteria. *J. Mol. Biol.*, **412**, 772-781.

8. Zuo, Y. and Deutscher, M.P. (2001) Exoribonuclease superfamilies: structural analysis and phylogenetic distribution. *Nucleic Acids Res.*, **29**, 1017-1026.